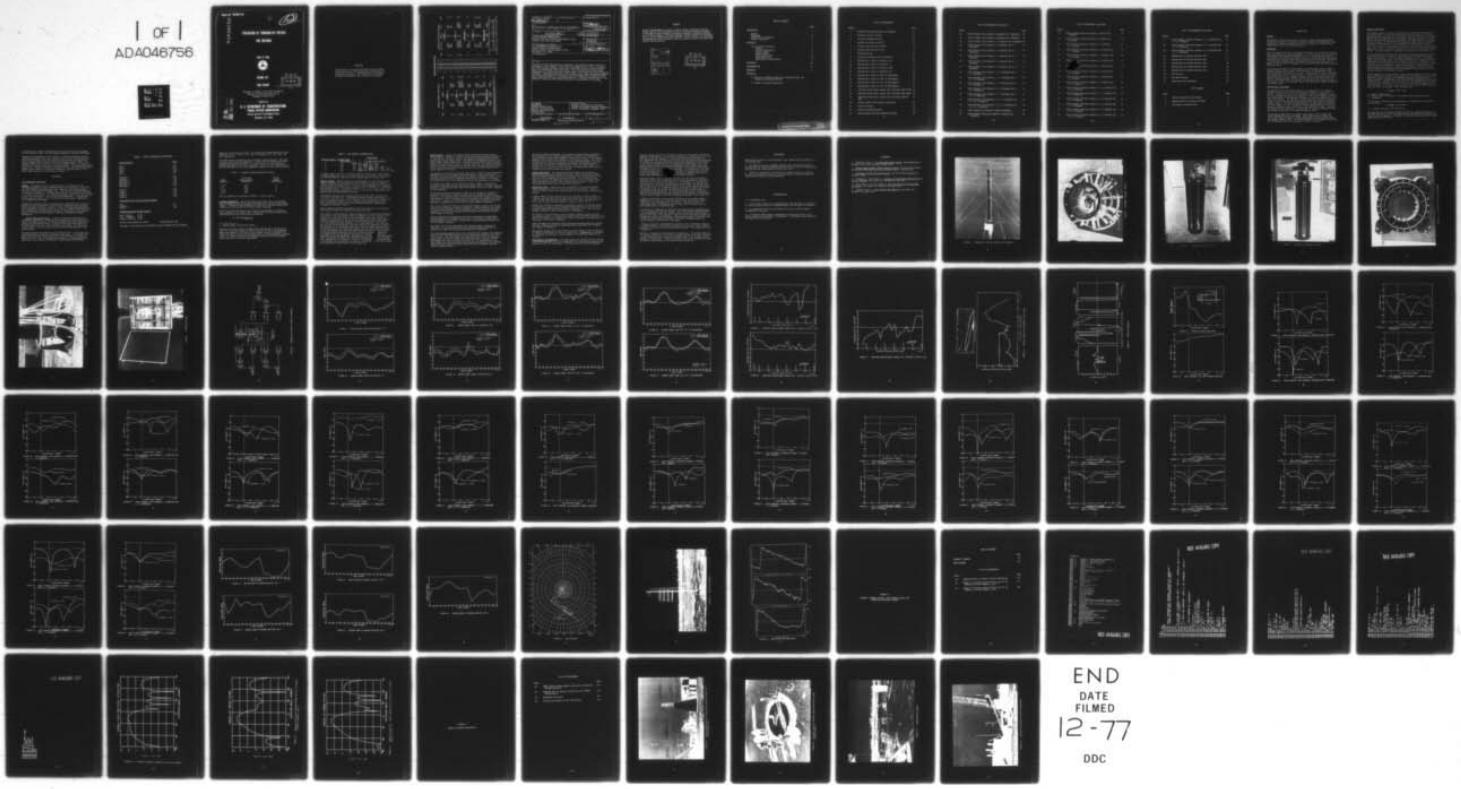
AD-A046 756 NATIONAL AVIATION FACILITIES EXPERIMENTAL CENTER ATL--ETC F/G 17/7
EVALUATION OF THOMSON/CSF FIVE-BAY VOR ANTENNA.(U)
OCT 77 J G DONG

UNCLASSIFIED FAA-NA-77-7 FAA/RD-77/82 NL

1 OF 1
AD A046756



END
DATE FILMED
12-77
DDC

Report No. FAA-RD-77-82

AD A046756

EVALUATION OF THOMSON/CSF FIVE-BAY VOR ANTENNA

James G. Dong



OCTOBER 1977

FINAL REPORT

DDC
RECEIVED
NOV 28 1977
D

Document is available to the public through the
National Technical Information Service
Springfield, Virginia 22151

AD No.
DDC FILE COPY

Prepared for

U. S. DEPARTMENT OF TRANSPORTATION
FEDERAL AVIATION ADMINISTRATION
Systems Research & Development Service
Washington, D.C. 20590

NOTICE

This document is disseminated under the sponsorship of the Department of Transportation in the interest of information exchange. The United States Government assumes no liability for its contents or use thereof.

METRIC CONVERSION FACTORS

Approximate Conversions to Metric Measures

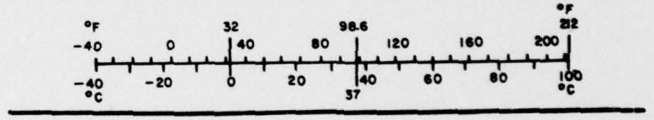
Symbol	When You Know	Multiply by	To Find	Symbol
		LENGTH		
in	inches	*2.5	centimeters	cm
ft	feet	30	centimeters	cm
yd	yards	0.9	meters	m
mi	miles	1.6	kilometers	km
		AREA		
in^2	square inches	6.5	square centimeters	cm^2
ft^2	square feet	0.09	square meters	m^2
yd^2	square yards	0.8	square meters	m^2
mi^2	square miles	2.6	square kilometers	km^2
	acres	0.4	hectares	ha
		MASS (weight)		
oz	ounces	28	grams	g
lb	pounds	0.45	kilograms	kg
	short tons (2000 lb)	0.9	*tonnes*	t
		VOLUME		
tsp	teaspoons	5	milliliters	ml
Tbsp	tablespoons	15	milliliters	ml
fl oz	fluid ounces	30	milliliters	ml
c	cups	0.24	liters	l
pt	pints	0.47	*liters*	l
qt	quarts	0.96	liters	l
gal	gallons	3.8	liters	l
ft^3	cubic feet	0.03	cubic meters	m^3
yd^3	cubic yards	0.76	cubic meters	m^3
		TEMPERATURE (exact)		
°F	Fahrenheit temperature	5/9 (after subtracting 32)	Celsius temperature	°C

*1 in = 2.54 (exactly). For other exact conversions and more detailed tables, see NBS Misc. Publ. 286, Units of Weights and Measures, Price $2.25, SD Catalog No. C13.10:286.



Approximate Conversions from Metric Measures

Symbol	When You Know	Multiply by	To Find	Symbol
		LENGTH		
mm	millimeters	0.04	inches	in
cm	centimeters	0.4	inches	in
m	meters	3.3	feet	ft
m	meters	1.1	yards	yd
km	kilometers	0.6	miles	mi
		AREA		
cm^2	square centimeters	0.16	square inches	in^2
m^2	square meters	1.2	square yards	yd^2
km^2	square kilometers	0.4	square miles	mi^2
ha	hectares (10,000 m^2)	2.5	acres	
		MASS (weight)		
g	grams	0.035	ounces	oz
kg	kilograms	2.2	pounds	lb
t	tonnes (1000 kg)	1.1	short tons	
		VOLUME		
ml	*milliliters*	0.03	fluid ounces	fl oz
l	liters	2.1	pints	pt
l	liters	1.06	quarts	qt
l	liters	0.26	gallons	gal
m^3	cubic meters	35	cubic feet	ft^3
m^3	cubic meters	1.3	cubic yards	yd^3
		TEMPERATURE (exact)		
°C	Celsius temperature	9/5 (then add 32)	Fahrenheit temperature	°F



Technical Report Documentation Page

1. Report No.	2. Government Accession No.	3. Recipient's Catalog No.
FAA-RD-77-82		

4. Title and Subtitle

EVALUATION OF THOMSON/CSF FIVE-BAY VOR ANTENNA

5. Report Date

Oct[illegible] 1977

6. Performing Organization Code

77p.

7. Author(s)

James G. Dong

8. Performing Organization Report No.

FAA-NA-77-7

9. Performing Organization Name and Address

Federal Aviation Administration
National Aviation Facilities Experimental Center
Atlantic City, New Jersey 08405

10. Work Unit No. (TRAIS)

11. Contract or Grant No.

041-305-800

13. Type of Report and Period Covered

Final rept.
Jan[illegible] - Nov[illegible] 1976,

12. Sponsoring Agency Name and Address

U.S. Department of Transportation
Federal Aviation Administration
Systems Research and Development Service
Washington, D.C. 20590

14. Sponsoring Agency Code

15. Supplementary Notes

16. Abstract

A stacked five-bay VOR antenna was evaluated at the National Aviation Facilities Experimental Center (NAFEC). The antenna was designed for use with a conventional very high frequency omnidirectional radio range (VOR) system to reduce multipath effects by diminishing ground reflections. Tests included airborne and ground measurements to assure operational compatibility of the antenna with FAA transmitting equipment. Measurements were made on the complete array, bays, and antenna elements. Test results indicated that the bearing error was marginal and the large sidelobes caused multipath reflection from nearby obstacles. A computer program used for the analysis of vertical plane radiation patterns in stacked arrays is included.

17. Key Words	18. Distribution Statement
VOR Antenna Multibay Stacked Array Reduced Site Reflections Computer Analysis/Display Coverage Nulls	Document is available to the public through the National Technical Information Service, Springfield, Virginia 22151

19. Security Classif. (of this report)	20. Security Classif. (of this page)	21. No. of Pages	22. Price
Unclassified	Unclassified	58	

Form DOT F 1700.7 (8-72) Reproduction of completed page authorized

240550

PREFACE

Special acknowledgement is given to John N. Warren, Surveillance Systems Branch, ANA-120, for developing the Fortran IV program enabling the analysis of free-space antenna patterns by changing parameters in multibay antennas, and to Frank W. Bassett, Sub-Program Manager, Systems Research and Development Service, Enroute Navigation Branch, ARD-330, for his assistance in converting the program into Basic language to enable the hands-on use of a Tektronix 4051 graphic computing system.

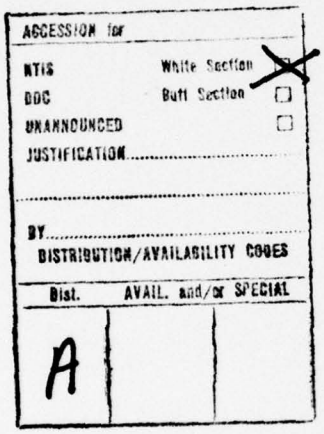




TABLE OF CONTENTS

	Page
INTRODUCTION	1
Purpose	1
Background	1
Description of Equipments	1
Theory of Operation	2
DISCUSSION	3
Test Procedure and Results	3
General	3
Airborne Measurements	5
Orbital Flights	6
Radial Flights	7
Ground Measurements	8
Obstruction Tests	8
Applicability Considerations	8
CONCLUSIONS	10
RECOMMENDATIONS	10
REFERENCES	11
APPENDICES	
A - Fortran IV Program Listing, Basic Program Listing, and Theoretical Free-Space Pattern	
B - Details of Antenna Installation	

PRECEDING PAGE BLANK-NOT FILMED

LIST OF ILLUSTRATIONS

Figure		Page
1	Thomson/CSF Five-Bay Antenna (with Radome)	12
2	Reference (Carrier) Antenna	13
3	Variable (Sideband) Antenna	14
4	Antenna Bay Assembly (Partial)	15
5	Rotation Ring and Guy Attachment	16
6	Antenna Stand with Swivel Base	17
7	Distribution Unit	18
8	Thomson-CSF Antenna (Partial Schematic)	19
9	Bearing Error, Orbit at Elevation 1.47°	20
10	Bearing Error, Orbit at Elevation 1.7°	20
11	Bearing Error, Orbit at Elevation 3.06°	21
12	Bearing Error, Orbit at Elevation 9.3°	21
13	Bearing Error, Orbit at 3.06° (3 wavelengths)	22
14	Bearing Error, Orbit at 3.06° (2 wavelengths)	22
15	Bearing Error, Orbit at 0.57° (3 wavelengths)	23
16	Bearing Error, Orbit at 0.57° (2 wavelengths)	23
17	Indicated Station Error, Radial 330°, Altitude 1,500 FT MSL	24
18	Indicated Station Error, Radial 220°, Altitude 6,500 FT MSL	24
19	Indicated Station Error, Radial 220°, Altitude 12,500 FT MSL	25
20	Vertical Plane Field Strength, 220° Radial	26
21	Cone of Confusion	27
22	Vertical Polarization Error	28
23	Field Strength, All Sine Elements Energized	28

LIST OF ILLUSTRATIONS (Continued)

Figure		Page
24	Field Strength, Sine Elements 1 Energized and 2 Energized	29
25	Field Strength, Sine Elements 3 Energized and 4 Energized	29
26	Field Strength, Sine Elements 1, 2 Energized and 5 Energized	30
27	Field Strength, Sine Elements 1, 3 Energized and 1, 4 Energized	30
28	Field Strength, Sine Elements 1, 5 Energized and 2, 3 Energized	31
29	Field Strength, Sine Elements 2, 4 Energized and 2, 5 Energized	31
30	Field Strength, Sine Elements 3, 4 Energized and 3, 5 Energized	32
31	Field Strength, Sine Elements 4, 5 Energized and 1, 2, 3 Energized	32
32	Field Strength, Sine Elements 1, 2, 4 Energized and 1, 2, 5 Energized	33
33	Field Strength, Sine Elements 1, 3, 4 Energized and 1, 3, 4, 5 Energized	33
34	Field Strength, Sine Elements 1, 4, 5 Energized and 2, 3, 4 Energized	34
35	Field Strength, Sine Elements 2, 3, 5 Energized and 2, 4, 5, Energized	34
36	Field Strength, Sine Elements 3, 4, 5 Energized and 1, 2, 3, 4 Energized	35
37	Field Strength, Sine Elements 1, 2, 3, 5 Energized and 1, 2, 4, 5 Energized	35
38	Field Strength, Sine Elements 1, 3, 4, 5 Energized and 2, 3, 4, 5 Energized	36
39	Field Strength, All Reference Elements Energized	36
40	Field Strength, References Elements 1 Disabled and 2 Disabled	37

LIST OF ILLUSTRATIONS (Continued)

Figure		Page
41	Field Strength, Reference Elements 3 Disabled and 4 Disabled	37
42	Field Strength, Reference Elements 5 Disabled and 6 Disabled	38
43	Field Strength, Reference Elements 1, 2 Disabled 1, 3 Disabled	38
44	Field Strength, Reference Elements 1, 4 Disabled and 1, 5 Disabled	39
45	Field Strength, Reference Elements 1, 6 Disabled and 2, 3 Disabled	39
46	Field Strength, Reference Elements 2, 4 Disabled and 2, 5 Disabled	40
47	Fi rength, Reference Elements 2, 6 Disabled and isabled	40
48	ield Strength, Reference Elements 3, 5 Disabled and 3, 6 Disabled	41
49	Field Strength, Reference Elements 4, 5 Disabled and 4, 6 Disabled	41
50	Field Strength, Reference Elements 5, 6 Disabled and 1, 5, 6 Disabled	42
51	Field Strength, Reference Elements 2, 5, 6 Disabled and 3, 5, 6 Disabled	42
52	Field Strength, Reference Elements 4, 5, 6 Disabled and 3, 4, 6 Disabled	43
53	Field Strength, Reference Elements 2, 4, 6 Disabled and 1, 4, 6 Disabled	43
54	Field Strength, Reference Elements 2, 3, 6 Disabled and 1, 3, 6 Disabled	44
55	Field Strength, Reference Elements 1, 2, 6 Disabled and 1, 4, 5 Disabled	44
56	Field Strength, Reference Elements 2, 4, 5 Disabled and 3, 4, 5, Disabled	45

LIST OF ILLUSTRATIONS (Continued)

Figure		Page
57	Field Strength, Reference Elements 1, 3, 5 Disabled and 2, 3, 5 Disabled	45
58	Field Strength, Reference Elements 1, 2, 5 Disabled and 1, 3, 4 Disabled	46
59	Field Strength, Reference Elements 2, 3, 4 Disabled and 1, 2, 3 Disabled	46
60	Bearing Error by Antenna Rotation, Bay 1	47
61	Bearing Error by Antenna Rotation, Bay 2	47
62	Bearing Error by Antenna Rotation, Bay 3	48
63	Bearing Error by Antenna Rotation, Bay 4	48
64	Bearing Error by Antenna Rotation, Bay 5	49
65	Wire Location	50
66	Wire Mesh Cylinder	51
67	Obstruction Test Recordings	52

LIST OF TABLES

Table		Page
1	Initial Installation Test Results	4
2	Quadrantal Error Correction (109 MHz)	5
3	Null Matrix of Antenna Pairs	6

INTRODUCTION

PURPOSE.

The purpose of this project was to evaluate the Thomson/CSF "high gradient" antenna for use with a conventional very high frequency omnidirectional radio range (VOR) to minimize propagation towards the ground, and thereby reduce siting effects due to multipath reflections.

BACKGROUND.

There is a need to provide a satisfactory performance at all VOR sites without major modifications to existing equipment. Use of a stacked array antenna with conventional VOR transmitting equipment that will satisfactorily lessen the susceptibility of course deterioration because of siting conditions may be more economical than employing more complex and expensive alternatives. Evaluation of a stacked loop antenna array is documented in Report No. FAA-RD-75-9 by Edward N. Lind entitled, "Development of a Stacked Five-Bay VOR Antenna System," dated June 1975.

A contract was awarded by Systems Research and Development Service (SRDS) to Thomson CSF/T-VT, Paris, France, under Department of Transportation (DOT) Contract FA75WA-3721, dated June 30, 1975, to lease with an option to purchase the cylinder type five-bay array antenna. The manufacturer claims the antenna system provides tilt to a narrower vertical beam with a broadside array resulting from antenna stacking, thereby avoiding course obstructions in the near field of the antenna below the horizon. In addition, they consider the use of the antenna system a more efficient method than employing a larger counterpoise or parasitic loops.

DESCRIPTION OF EQUIPMENTS.

The Thomson/CSF five-bay antenna (figure 1) is comprised of six reference antennas (figure 2) and five variable antennas (figure 3) in the array. In figure 4, a portion of the array is shown depicting the arrangement of parts for the individual antennas in the assembly. In the array assembly, two rotation rings (figure 5) are employed for guying the array and permit the rotation of the antenna. The four-meter antenna stand with a swivel-jointed base (figure 6) has a scale marked in degrees and retractable indexes to measure antenna rotation. All the individual antennas are terminated in a distribution unit (figure 7) which contains the energy feeding modules and circuitry. Antenna weather protection is provided by the cylindrical radome. Access to the antenna element adjustment is accomplished by removing a number of screws and sliding one portion of the radome through the other.

The five-bay antenna with a four-meter stand weighs 2,555.6 pounds (lbs) (1150 kilograms (kg)) with the radome. This figure does not include the obstruction light and Federal Aviation Administration (FAA) distance measuring equipment (DME) antenna. The maximum diameter of the antenna is 2.31 feet (ft) (0.700 meter (m)) and the height is 47.59 ft (14.42 m).

THEORY OF OPERATION.

The schematic diagram in figure 8 illustrates the electrical configuration of the antenna array. The reference antenna in the array (figure 2) has four quarter-circular bands made of tinned copper, which are concentric to a support drum and routed through insulating spreaders. Each quarter of the circular band has an adjustable disc at one end and an electrical terminal for energizing at the other. At the center of the drum is a connecting box containing the balun with the two-wire line terminations and an adjustable coil with a brass core. Distribution of uniform currents is possible by the quarter section. Each section is energized by the two-wire line with appropriate polarity. Adjustment of the disc capacitors allows uniform field distribution around the circle. The input impedance is adjusted to 50 ohms by the adjustable coil.

In the variable antenna (figure 3), four vertical tubes are devised to avoid undesirable vertical polarization and provide a sine and cosine radiation pattern configuration. The basic radiating element consists of two parallel tubes fed by a coaxial cable. The center conductor of the coaxial cable is connected to one of the tubes and the shield to the other. Operation of the system could be considered as a very long loop where vertical currents cancel each other and the horizontal currents add (implying a concentration of currents at the base extremities). However, the designer's tests have demonstrated that the horizontal pattern is independent of the length of the tubes and the quality of the terminal contacts.

Another approach to the explanation of the variable antenna operation is based on the diffraction pattern of two cylinders. In this approach, the excitation modes are computed allowing for mechanical parameters and polarization of incident fields. Systematically, the results of this computation show that the system acts as a capacitor if the electric field is perpendicular to the axes of the cylinders (TE mode), or as an inductor if the field is parallel to the axes (TM mode). In the first case, it can be shown that the diffraction pattern is, at the first order, in the following form:

$$\sin \left(\frac{2\pi D}{\lambda} \cos \theta\right), \text{ with:}$$

D - distance between axes
θ - azimuth angle with respect to the normal plane containing the axes
λ - wavelength.

If D is small, compared with the wavelength, the expression of the pattern can be written:

$$J_1 \left(\frac{2\pi D}{\lambda}\right) \cos \theta, \text{ where:}$$

J_1 - a Bessel function of the first order.

The condition for energizing eliminates the TM even components (currents in the same direction) so that the system radiates practically a sinusoidal lobe with no vertical component. Consequently, the nulls are defined by the system geometry and no other factor.

By adjusting the cylinder tube lengths, the vertical pattern can be shaped and the reactance tuned. The tube length is adjusted to one-half wavelength.

Because of good quadrature of the patterns, it has been possible to build a complete antenna with four tubes. Opposite slots are fed in phase with the same signal providing a sine and cosine pattern uncoupled from each other. Correct feeding phase is obtained within the frequency range of 108 to 118 megahertz (MHz) by the position of the tube excitation point. The tubes are fed in pairs through a balanced divide-by-two network. The power divider splits signals into a number of equiphase, equiamplitude parts and provides isolation between output terminals with matched impedances. Detailed theory of the power divider operation is described in reference 1.

DISCUSSION

TEST PROCEDURES AND RESULTS.

GENERAL. The antenna tests were accomplished at the National Aviation Facilities Experimental Center (NAFEC) utilizing the experimental collocated very high frequency omnidirectional radio range and an ultrahighfrequency tactical air navigation aid (VORTAC) site. The four-meter stand was employed in mounting the antenna atop building 196 which has a standard VOR counterpoise 52 ft (15.8 m) in diameter. The VOR ground equipment used in the test included: a type TV-12 transmitter, a type CA-1761 carrier modulator, a type CA-1768 carrier modulator driver, and a type FA-5226 station monitor. Operational site frequency was 109.0 MHz.

Assembly and initial testing on the antenna was accomplished with a contract engineer from the manufacturer to assure proper installation and operation before the NAFEC test phase. References 2 and 3 provided technical guidance and standardized procedures during the test phase. Airborne and ground tests were accomplished to measure bearing accuracy, polarization, field strength gradient, and antenna effectiveness in reducing scalloping from nearby obstructions.

Initial Installation Tests. To assure satisfactory installation and operation of the antenna, initial tests were completed jointly with the contractor and NAFEC personnel. The voltage standing wave ratios (VSWR) were measured on each antenna element at the end of the cable feed connected to the distribution unit and to the distributor feed cables. The results are listed in table 1, which includes the decoupling and omnidirection of the ground pattern.

The bearing accuracy was measured at the cardinal points to verify that the stacked antenna was radiating a satisfactory VOR signal. The radiated VOR signal was received by a Yagi antenna 40 ft (12.2 m) high at a distance of 500 ft (152.1 m). And after signal amplification by a broadband amplifier (Radiation Devices Company model BBA-1), a diode detector provided the

TABLE 1. INITIAL INSTALLATION TEST RESULTS

Antenna Element	VSWR
Sine 1	1.04
Sine 2	1.07
Sine 3	1.02
Sine 4	1.03
Sine 5	1.07
Reference 1	1.04
Reference 2	1.08
Reference 3	1.02
Reference 4	1.09
Reference 5	1.05
Reference 6	1.06
Cosine 1	1.04
Cosine 2	1.07
Cosine 3	1.05
Cosine 4	1.02
Cosine 5	1.04

Distribution Unit and All Antenna Elements	
Sine	1.1
Reference	1.1
Cosine	1.06

Decoupling Between Antenna Channels	
Sine - Cosine	61 dB
Sine - Reference	52 dB
Cosine - Reference	50 dB

Antenna Ground Radiation Pattern Omnidirectional $\pm$2dB

The amplitude and phase of the individual antenna elements was not measured.

signal to the VOR station monitor. By rotating the stacked antenna, the bearing errors were -3°, 1.25°, -1.5°, and 2° at azimuths of 0°, 90°, 180°, and 270° respectively.

From these errors a quadrantal error (reference 3) was indicated. This type of error is the result of inequality of current from the antenna pairs and/or misphasing between antenna pairs. To correct the error, the contractor's engineer employed the correction indicated in table 2 and five wavelengths of RG 214/U were added to the sine (sideband 2) channel for the initial correction.

TABLE 2. QUADRANTAL ERROR CORRECTION (109 MHz)

Error (Degrees)	Attenuation Sine or Cosine (Decibels)	RG/214U Length (Wavelength)
± 2.5	0.76	5
± 2	0.61	4
± 1.5	0.46	3
± 1.0	0.30	2
± 0.5	0.15	1

NOTE: At 109 MHz one wavelength of RG/214U = 6 feet (1.82 m)

AIRBORNE MEASUREMENTS. The Convair 580 aircraft, N49, with a tail-mounted Dorne and Margolin split-loop antenna was employed in the orbital and radial flights. Calibrated Bendix MN-85FA and Collins 51R-3 receivers supplied the signals for course deviation and field strength recording.

Nulls in the radiation pattern were taken into consideration in selecting orbits employed in the flight tests. Angles where the nulls occurred in the radiation pattern were derived from the equation:

$$\theta = \text{ARC SIN } \frac{(180° \times N)}{a}$$

N = 0, ±1, ±2, ±3 ----
a = antenna height in electrical degrees

Occurrence of nulls for each variable antenna was reduced to the matrix in table 3. Orbits were limited to angles less than 10°. Since ground measurements were referred to the center of the antenna in order to correlate the flight test results with elevation angles used in ground measurements, approximately 5.7° should be added to the elevation angles of the field strength curves obtained in the ground measurements.

TABLE 3. NULL MATRIX OF ANTENNA PAIRS

Variable Antenna	Antenna Height (wavelength)	Null Number 1	2	3	4	5	6	7	8
		(degrees above ground)							
1	3.2	8.9	18.2	27.6	38.1	50.5			
2	4.0	7.2	14.5	22.1	30.1	38.8			
3	4.6	6.2	12.4	18.9	25.5	32.6	40.3		
4	5.3	5.4	10.9	16.5	22.2	28.2	34.5	41.4	
5	6.0	4.7	9.5	14.4	19.3	24.5	29.8	35.4	41.5

At angles greater than 10°, as observed from the matrix, nulls from different variable antennas may occur at the same elevation as evidenced by the example of variable antenna 2 (third null) and variable antenna 4 (fourth null).

ORBITAL FLIGHTS. Orbital flights were accomplished with course guidance provided by extended area instrumentation radar (EAIR). During test flights, (results shown in figures 9, 10, 11, and 12) five wavelengths of RG 214/U were used to provide the attenuation in the sine channel (sideband 2) to compensate for quadrantal error. At elevation angles of 1.47°, 1.7°, 3.06°, and 9.3° the peak-to-peak bearing errors were 3.5°, 2.5°, 3.1°, and 4.5° respectively, as measured with the Bendix MN-85FA receiver.

Corresponding bearing errors measured with the Collins 51R-3 receiver were 4.2°, 2.4°, 2.8°, and 3.0°. The maximum difference between errors measured by the two receivers was 1.5°, and occurs in the 9.3° elevation orbit near the nulls of variable antennas 1 and 5. Bearing errors greater than 4° (±2°) were recorded from both receivers which exceeded specified commissioning tolerances (references 2 and 3).

Orbits completed with five wavelengths of RG 214/U inserted in the antenna's sine channel indicated an excessive correction was made.

The results of orbits made with reduced attenuation, by using less wavelengths of RG 214/U in the sine channel, appear in figures 13, 14, 15, and 16. At an elevation of 3.06° with three and two wavelengths of RG 214/U in the sine channel, the maximum error was the same. However, there were differences in the values measured by the receivers. When the Bendix receiver error was 4.3°, the Collins receiver indicated 3.4° at this elevation. The error was less with the five wavelengths of RG 214/U inserted as evidenced in figure 11. The reduction of the attenuation inserted in the sine channel did not reduce the bearing error to any considerable amount, but from the observation of the curves, the bearing error curves do show a shift from the negative to values in the more positive direction with the attenuation reduction. Basically, the redistribution of the bearing about the zero axis can be achieved by adjustment in the VOR goniometer. Consequently, a method to reduce the bearing error is necessary, and doubt exists whether optimum adjustments as installed were completed by the contractor. Receipt of the antenna for testing was made on the premise that the antenna was tested at 109 MHz and that the line lengths were tailored for proper phase for each antenna bay.

RADIAL FLIGHTS. Inbound and outbound radial flights were made to observe course bends and roughness. Some of the inbound flights are shown in figures 17, 18, and 19. The DME in the VOR site was used for measuring between the aircraft and station (slant range). This means of measurement was used in the radial flight results (figure 17). The EAIR site provided the ground distance markers for radial flight results in figures 18 and 19. The course deviations did not repeat in these plots due to the fact that different reflecting objects affect the courses at different altitudes when over the same location or at similar angles of elevation.

The distance from the station has been converted to elevation angles permitting examination of any large course deviations related to particular angles of elevation that could be attributed to the effects of antenna pair nulls. From the course deviation curves, numerous course bends are evident. The larger deviations will occur at the extremes of the low and high angles of elevation.

An outbound 220° radial at an altitude of 6,500 ft (1981.2 m) was made to determine the maximum distance the radiated signal could be received. When the aircraft was 105 nautical miles (nmi) from the VOR station the "flags" appeared on both receivers.

The vertical plane field strength in figure 20 was obtained by taking the products of the signal strength and slant range at incremental distances or elevation. The distance from the station were converted to angles of elevation. From the polar curve, the maximum value of the major lobe occurred at an elevation of 12°. A portion of the curve was plotted using rectangular coordinates enabling an expanded view of the effects at small angles of elevation.

The "cone of confusion" effects on the azimuth guidance signal as the aircraft flies over the VOR site are shown in figure 21. Signal crossovers are evident in the cone of confusion, and the volume affected is increased at the higher altitudes as noted by the increased distance away from the station before a usable signal is obtained.

Vertical polarization measurements were made by employing a crossed dipole antenna mounted to the movable fixture on the 110 ft (33.5 m) wooden pole. Other equipment used included: a polariscope, a Bendix MN-85FA receiver, and the rectilinear recorders.

The changes in vertical polarization with elevation angle is depicted in figure 22. At the elevation angle below the horizon the polarization is excessive but above the horizon the polarization is within $\pm 2°$.

The field strength measurements of all the antenna sine elements were completed using only the horizontal antenna on the crossed dipole mounted to the 110 ft (33.5 m) pole. The sine elements were used because they faced the pole and a larger signal was directed toward the receiving antenna. Results of these measurements are shown in figures 23 through 38. All combinations of the sine elements were energized permitting a qualitative analysis of the sideband radiation pattern behavior and the contribution of the radiation from the various sideband elements.

The field strength measurements of the reference elements were accomplished in the same way as the sideband measurements. However, all combinations of three reference elements were disabled to observe the effects of the disabled elements on the overall field strength of the reference antenna. The results are depicted in figures 39 through 59. During these measurements, the power-divider connector, normally energizing the element, was terminated with a 50 ohm load. In practice, the malfunction of three reference elements is unlikely, and the results may differ because an element failure will cause an unbalance in the power-distributing network.

GROUND MEASUREMENTS. The ground-bearing measurements were performed by mechanically rotating the Thomson/CSF antenna. Since the antenna is higher than other NAFEC antennas tested, it was necessary to use the existing 110 ft (33.5 m) pole for mounting the receiving antenna. The receiving antenna height was adjusted for measurement of each bay to assure sufficient signal level for proper operation of the calibrated station monitor. Results of these measurements are shown in figures 60 through 64.

OBSTRUCTION TESTS. Flight tests were accomplished by employing different types of ground obstructions in the near field of the antenna. Orbits of 25 nmi at 1,500 ft (457.2 m) (elevation angle 0.57°) were made to observe the effects.

A single number 6 AWG(4.1 mm) wire 30 ft (9.1 m) high, located as shown in figure 65, was used in the first obstruction flight test. In the second test, a 4X4 (to the inch) wire mesh cylinder 9 ft X 9 ft (figure 66) was located 60 ft (18.3 m) away from the antenna at a height of 25 ft (7.6 m).

Another test was made to determine the effects of location on the VOR antenna in relation to a remote center air-ground (RCAG) facility. A VHF circularly polarized (swastika) antenna was mounted at a height of 40 ft (12.2 m) on a portable tower 60 ft (18.3 m) away from the VOR antenna.

The results of the obstruction tests are shown in figure 67 taken from the rectilinear recorder. In figure 67a the normal orbit recording transition is the same as the condition for a single wire since the effects of the wire were not noticeable for any orbit transitions.

Figure 67b shows the scattering effects which are noticeable when the cylinder was used. Detailed analysis of scattering effects from wires and cylinders are covered in reference 4.

The swastika antenna had the most effect on the recording of orbit transitions as noted by the flatness of the curve (figure 67c). Consequently, the location of a VOR with this antenna in close proximity to an RCAG site should not be permitted.

APPLICABILITY CONSIDERATIONS. An antenna used as an integral part of a conventional VOR system must not only be compatible with other system components, but must also fulfill the requirement of providing accurate bearing information.

Granting liberal allowances, the bearing accuracy of the five-bay antenna was marginal in performance. The effects of scattering by obstacles were less with the five-bay antenna compared to conventional VOR antennas (reference 5). This improvement was attributed to the field strength gradient near the horizon. The effects of scattering with nearby obstructions located below the horizon of the five-bay antenna resulted in unsatisfactory performance. Since the factory-tested, five-bay antenna was installed by their representative and released for test, the unsatisfactory performance results must be attributed to design deficiencies or [illegible]nt tolerances. An examination of the theoretical free-space patter[illegible]rge lobes at negative angles in both carrier and sidebands. Th[illegible]e radiation is probably the cause of deteriorated performance i[illegible]ce of nearby obstacles.

Excessive bearing error in each bay may result in self-induced scalloping. Correction of the fault is dependent on the proper adjustment of the bays in order that they be electrically identical. In addition, it is assumed that the manufacturer selected the proper spacing and alignment between the bays. This is done to assure the desired location of the nulls, and therefore minimize bearing error. An attempt was made to correlate the radial test results in figures 17, 18, and 19 with the individual bay error curves shown in figures 60 through 64; however, the course deviations were not in agreement. Some of these discrepancies may be attributed to the attitude of the aircraft, aircraft antenna pattern, and other variables encountered in the flight test.

A monitor is required to assure proper operation of the stacked antenna if commissioned for field use. When excessive bearing error exists, prompt detection of the contributing bay is required. The monitor used in a conventional VOR is inadequate because a single monitor antenna would not detect malfunctions in individual bays.

In reference 6, a gradient of 16.93 dB/6° was obtained from a free-space pattern of a theoretical five-bay antenna. From figure 39 the measured gradient of the Thomson/CSF antenna was 6 dB/6°, and the theoretical pattern shows a gradient of 9 dB/6°. The spacings of the bays in the theoretical antenna were one-half and three-half wavelengths. These spacings cannot be applied to the Thomson/CSF antenna because the size of each bay, including spacers and carrier element, exceeds one-half wavelength.

A computer program was developed from reference 6 for a theoretical analysis of stacked antennas. The Fortran IV program was converted to Basic computer language for the Tektronix Incorporated 4051 computer. The listings are found in appendix A.

Details of the antenna installation are in appendix B. The coaxial cables of the antenna assembly are of continuous lengths inserted in the tube connections of their respective bays, which puts some restraints in the assembly or disassembly of the antenna. Likewise, any heavy icing on the sleeve-like housing may prevent needed repair to any malfunctioning antenna bay.

CONCLUSIONS

Based upon the results of the evaluation of the stacked five-bay antenna, it is concluded that:

1. The bearing error was considered marginal since maximum bearing errors recorded from the Collins and Bendix receivers were 4.2° and 4.5°, respectively, which exceeds the commissioning tolerance of 4° ($\pm$2°).

2. Additional improvements in gradient and sidelobe reduction is required to reduce the undesirable effects on course structure of the scattering from nearby obstacles below the antenna horizon.

RECOMMENDATIONS

It is recommended that:

1. The five-bay antenna not be considered for field use until it is modified to satisfy bearing tolerance, increased gradient, and reduction in sidelobes.

2. An appropriate monitor be provided with any future stacked antenna considered for field use.

3. An improved radome design be implemented allowing easy access to the antenna elements for adjustment or maintenance. Ice formation would immobilize the sleeve-like construction.

REFERENCES

1. Wilkinson, Ernest J., An N-Way Hybrid Power Divider, IRE Transactions on microwave theory and techniques, January 1960.

2. United States Standard Flight Inspection Manual, FAA Handbook OA P8200.1, Section 201.3 VOR Flight Inspection Procedure, Chg 24, June 19, 1973.

3. Maintenance of VHF Omnirange Equipment, FAA Order 6790.4A appendix 2, October 1, 1974.

4. Gruenberg, H. and Hirasawa, K., Effects of Scattering by Obstacles in the Field of VOR/DVOR, Final Report No. FAA-RD-76-21, July 1976.

5. Bell, Wayne E. and Lind, Edward N., Test with Wilcox Slotted-Cyclinder VOR Antenna, Final Report No. FAA-RD-76-30, April 1976.

6. Sengupta, Dipak L., Large Gradient VOR Handbook, Final Report No. FAA-RD-74-22, August 1974.

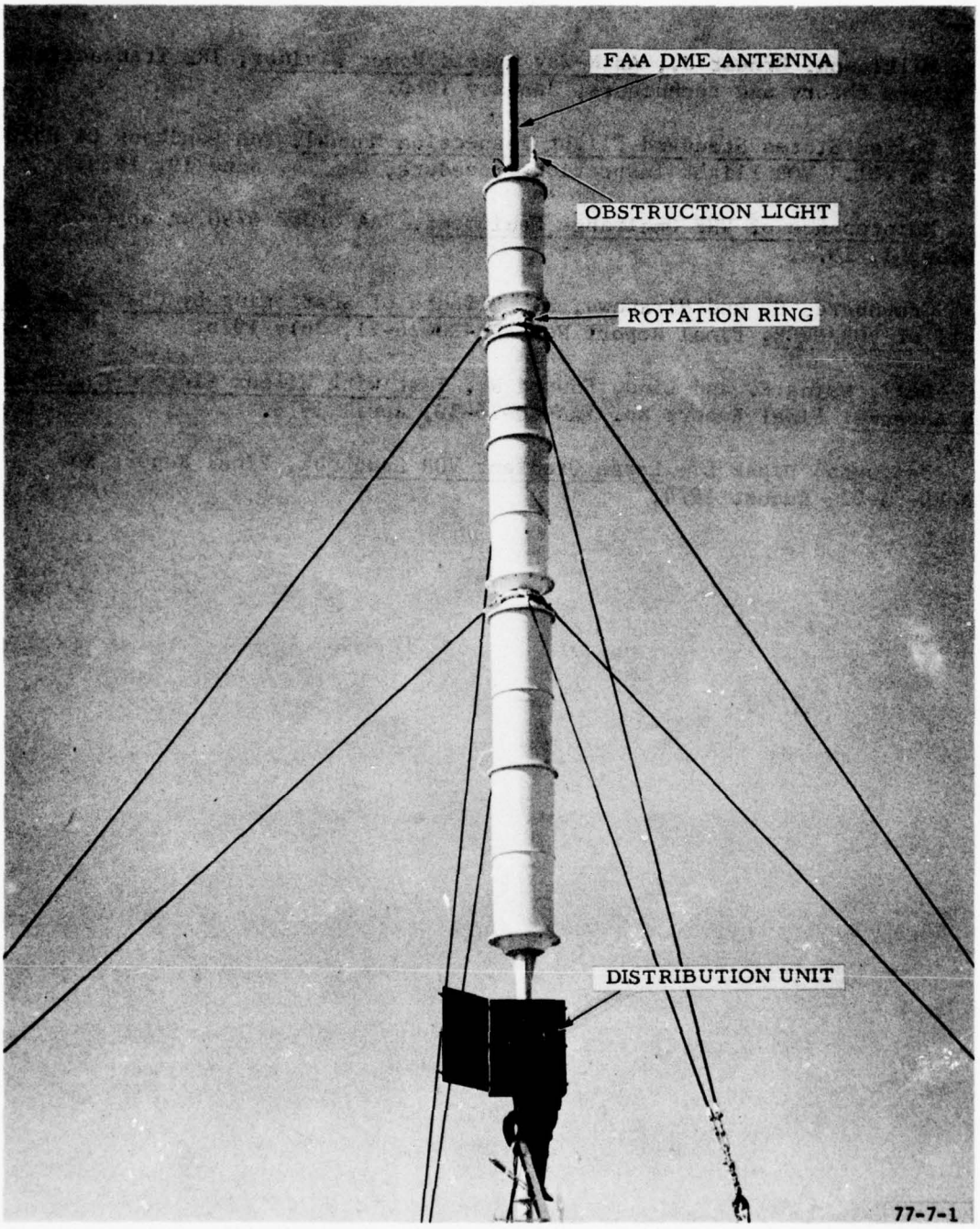


FIGURE 1. THOMSON/CSF FIVE-BAY ANTENNA (WITH RADOME)

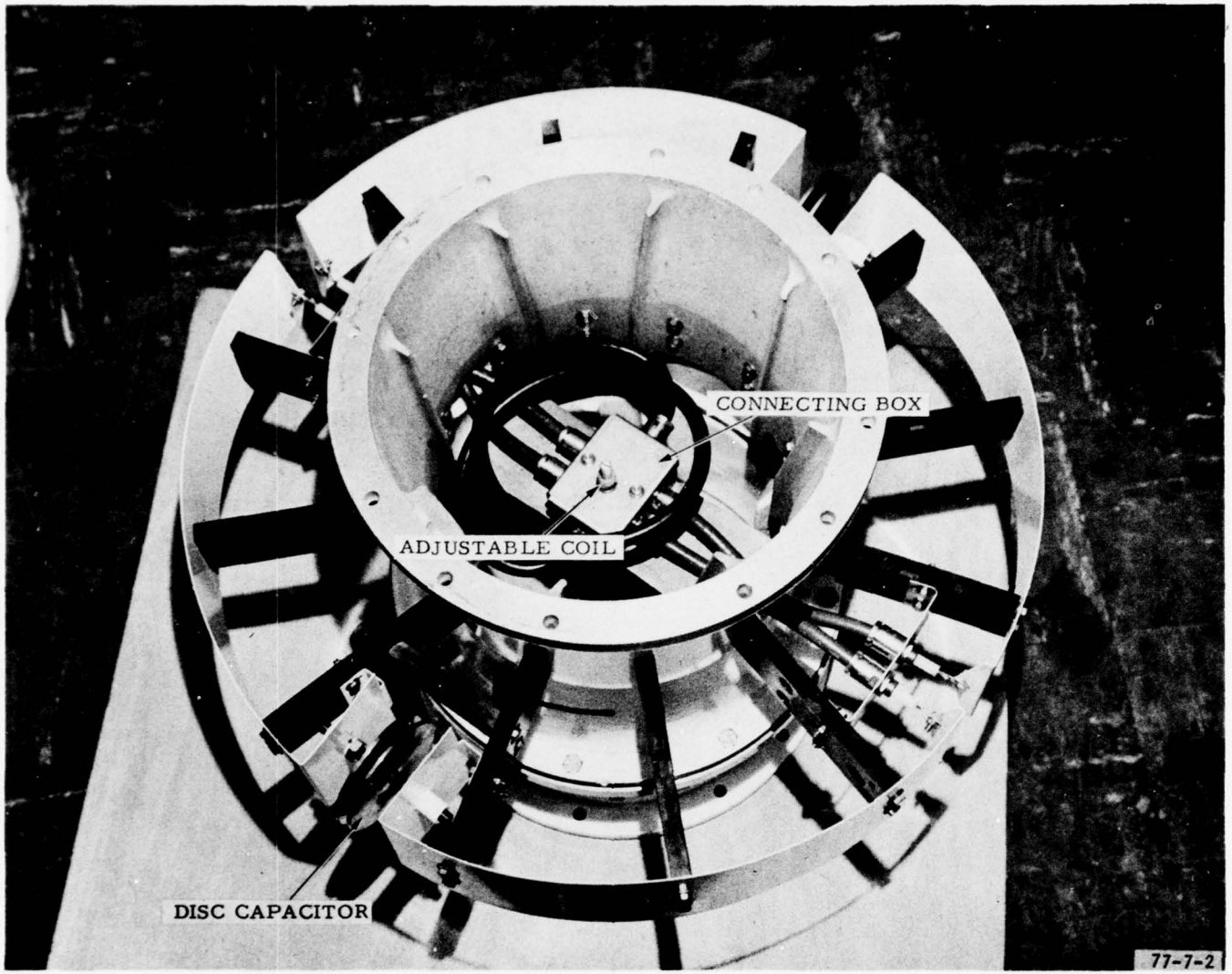


FIGURE 2. REFERENCE (CARRIER) ANTENNA

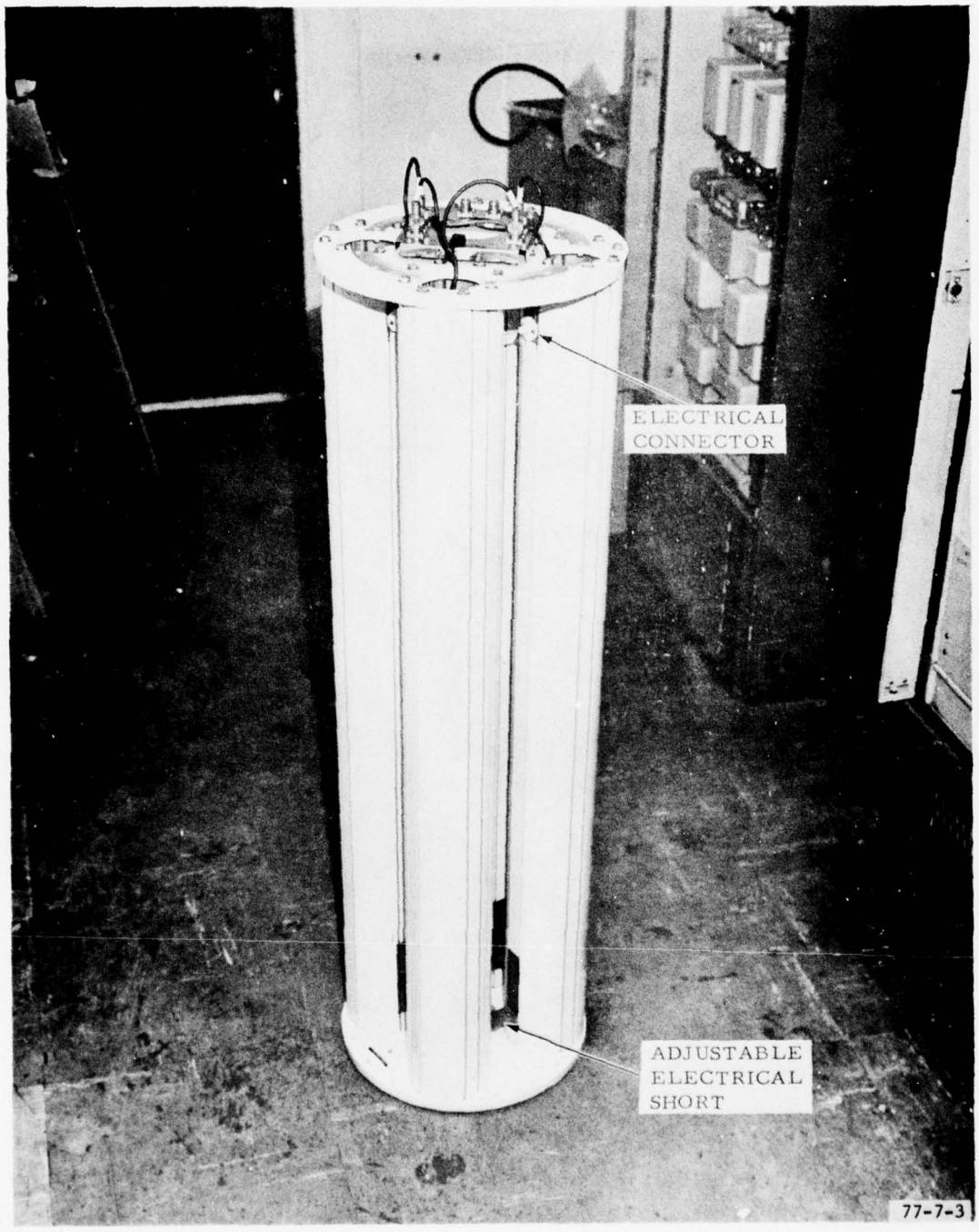


FIGURE 3. VARIABLE (SIDEBAND) ANTENNA

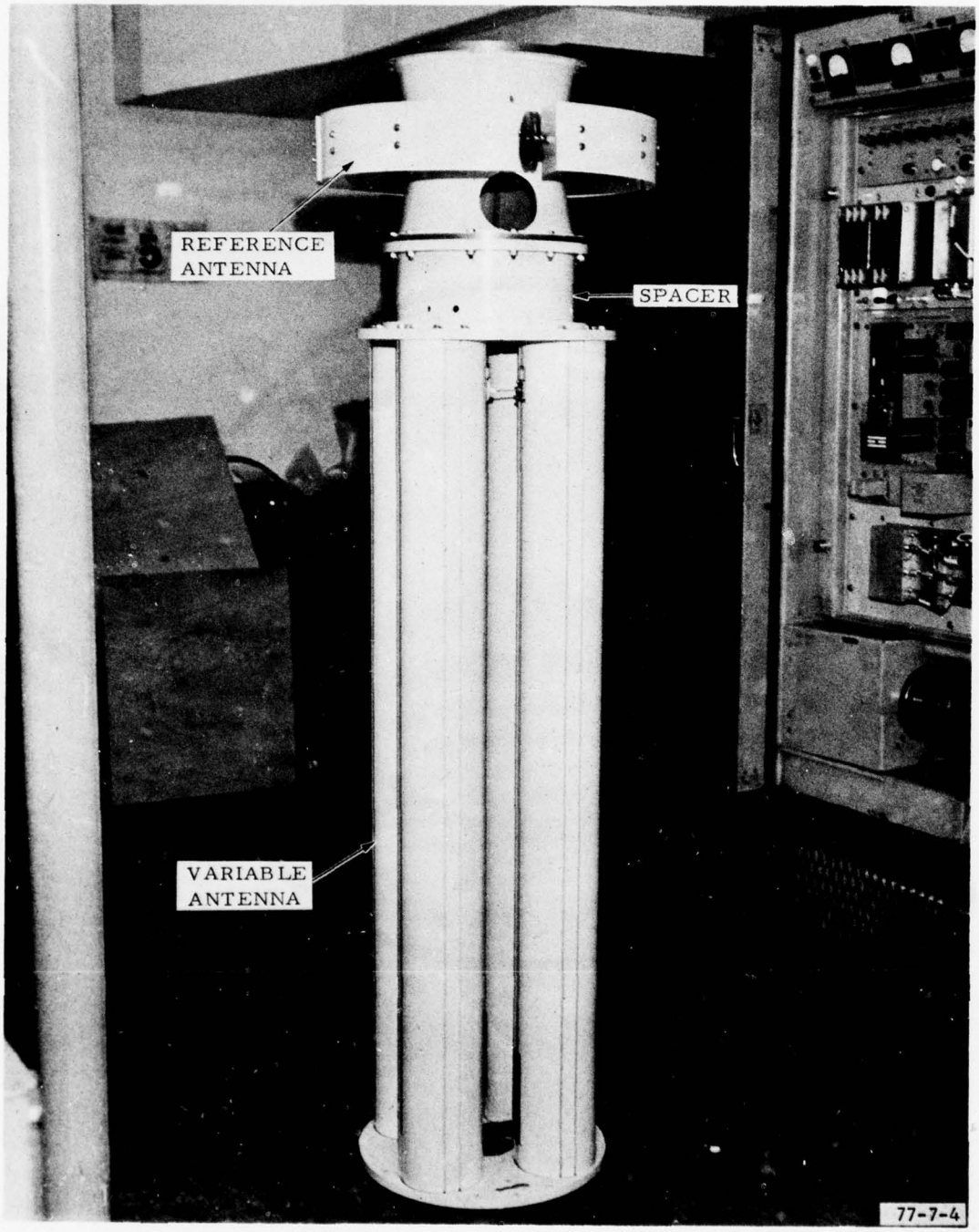


FIGURE 4. ANTENNA BAY ASSEMBLY (PARTIAL)

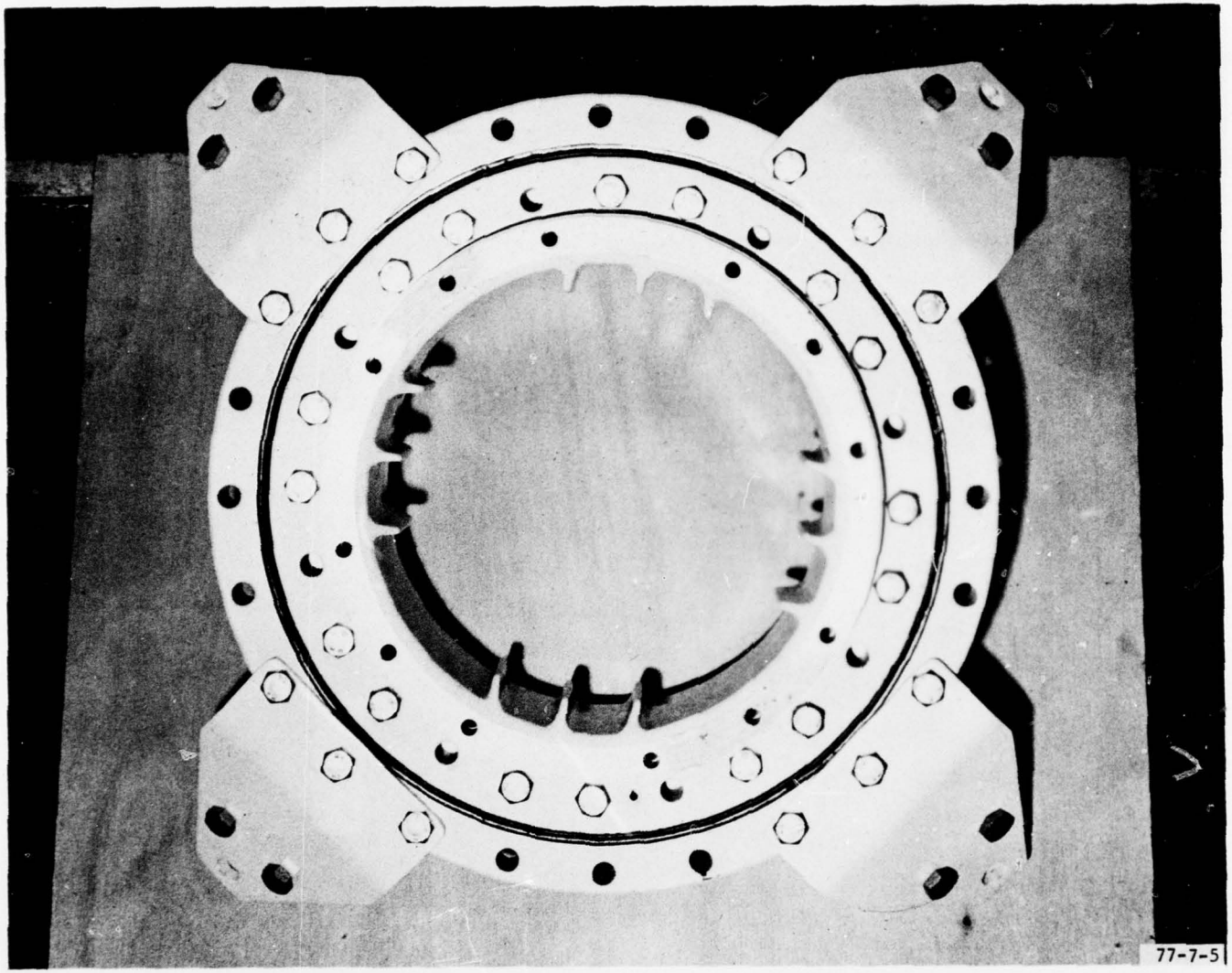


FIGURE 5. ROTATION RING AND GUY ATTACHMENT

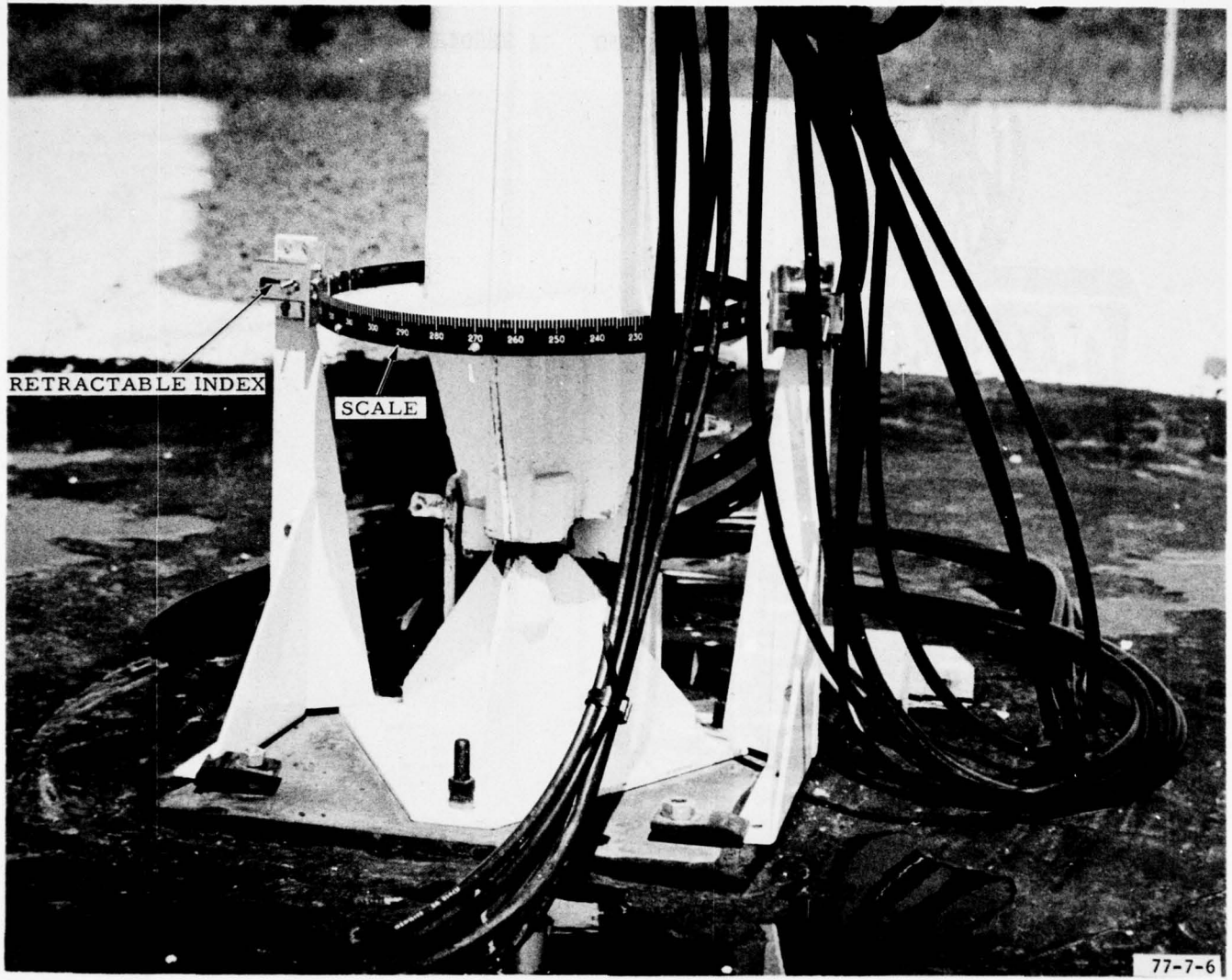


FIGURE 6. ANTENNA STAND WITH SWIVEL BASE

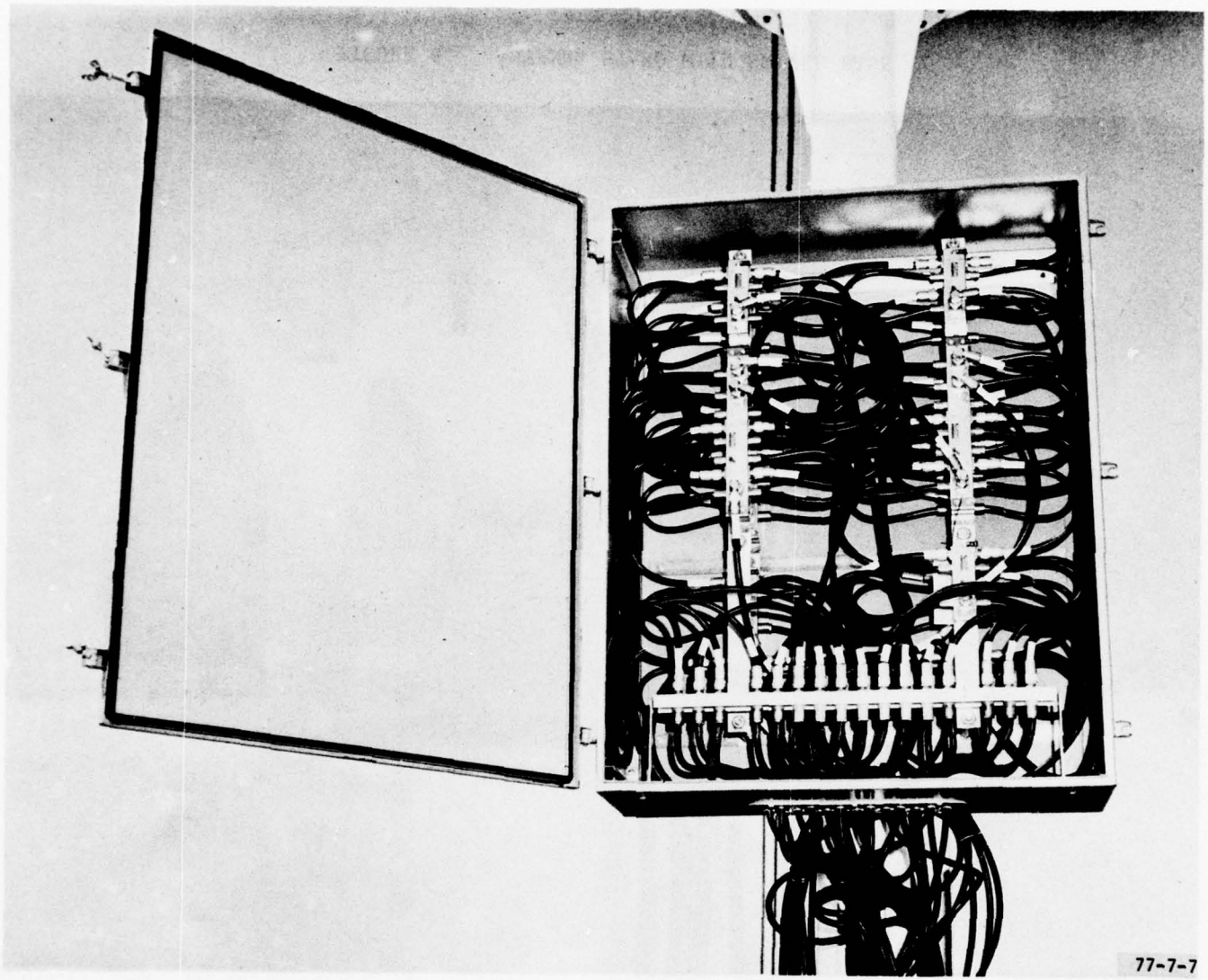


FIGURE 7. DISTRIBUTION UNIT

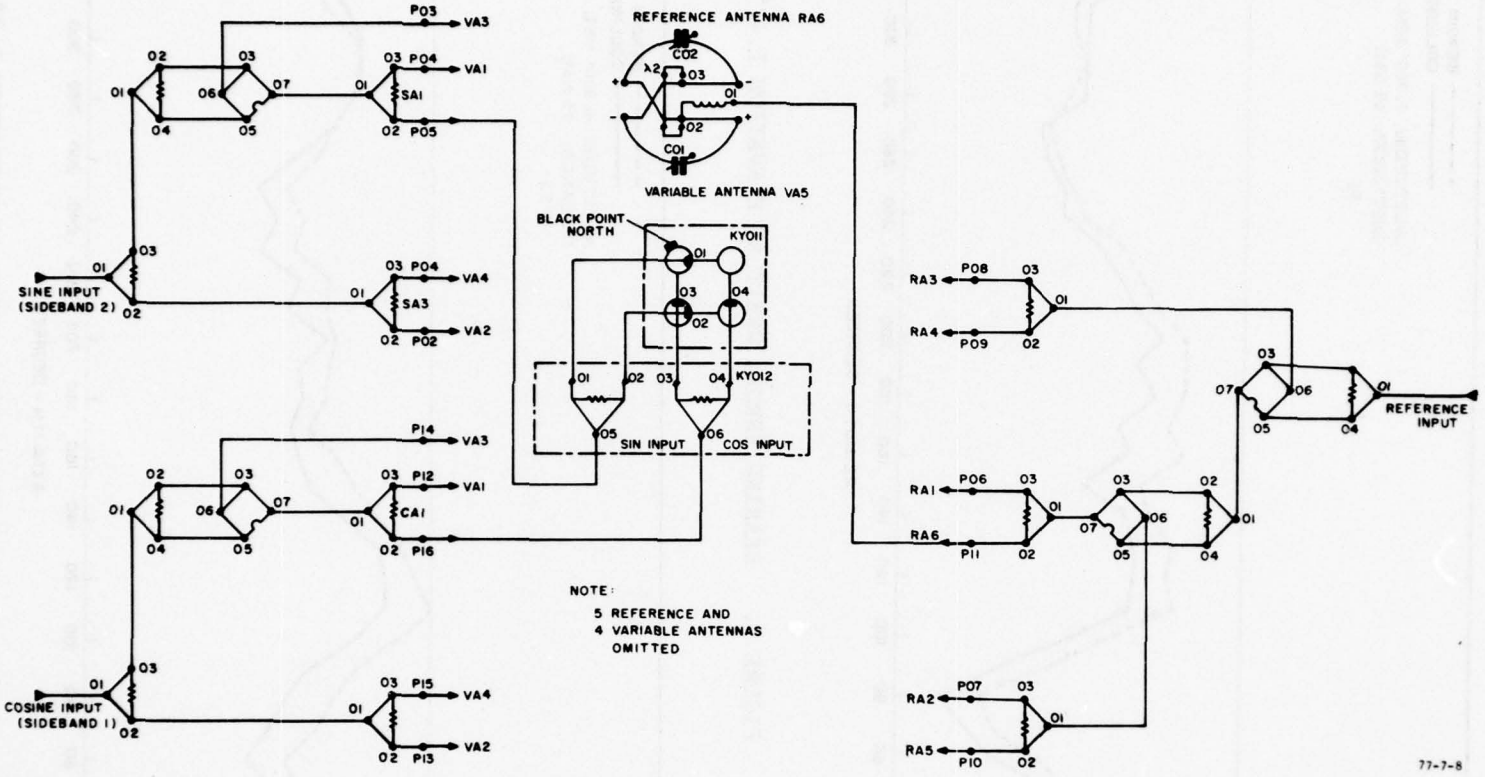


FIGURE 8. THOMSON/CSF ANTENNA (PARTIAL SCHEMATIC)

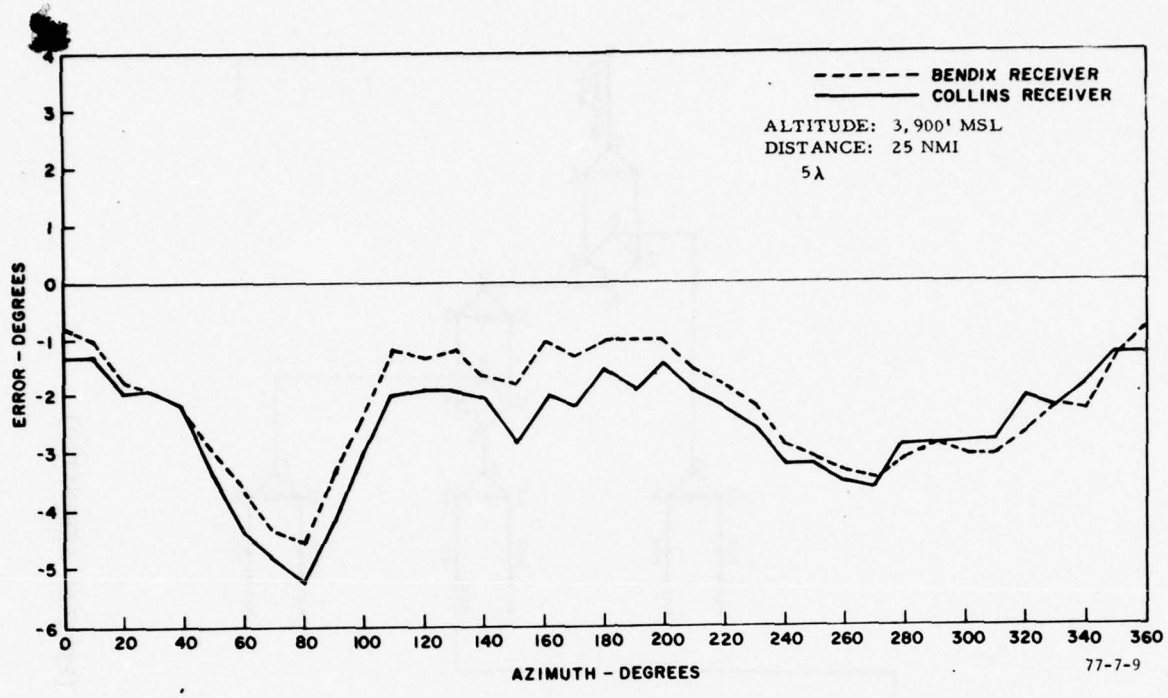


FIGURE 9. BEARING ERROR, ORBIT AT ELEVATION 1.47°

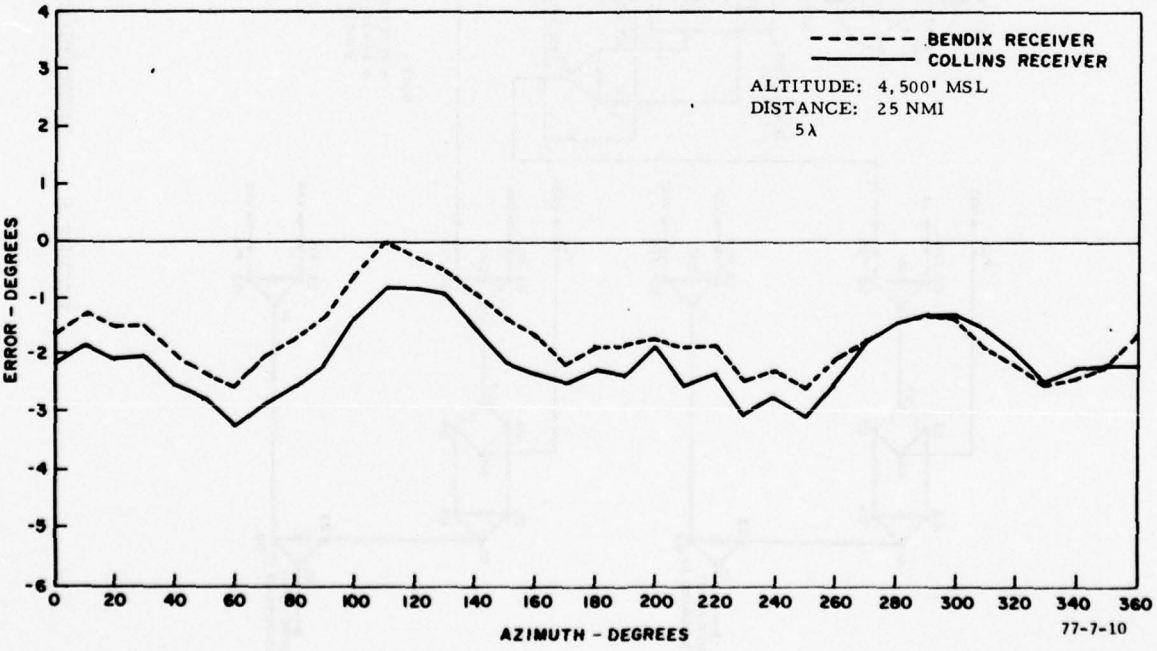


FIGURE 10. BEARING ERROR, ORBIT AT ELEVATION 1.7°

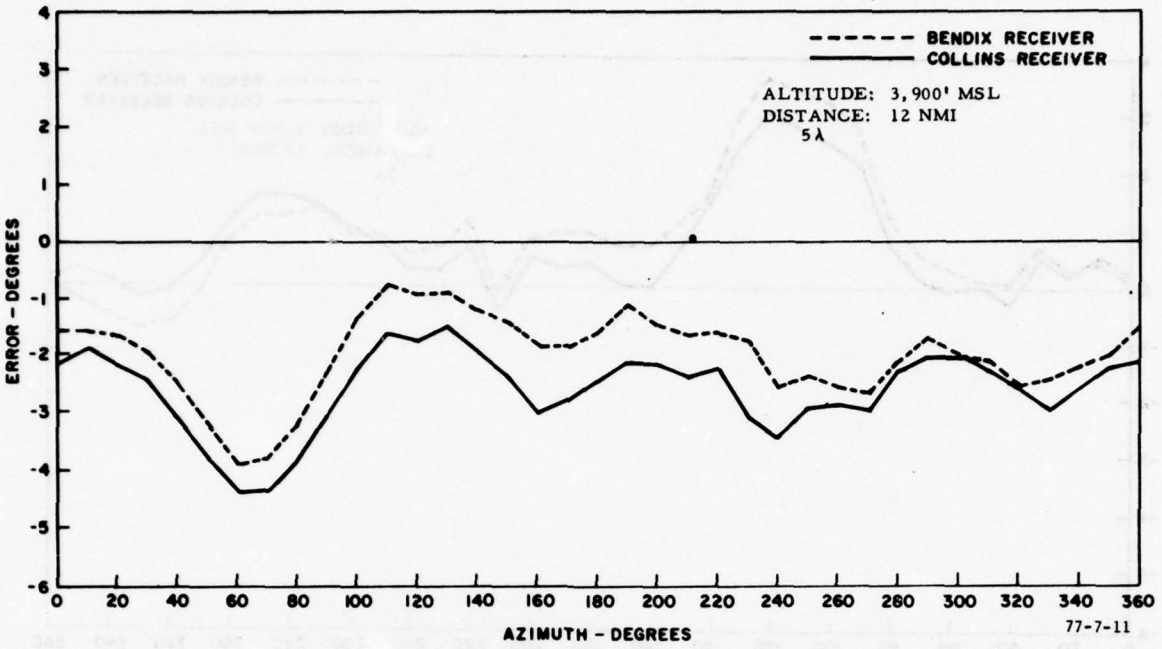


FIGURE 11. BEARING ERROR, ORBIT AT ELEVATION 3.06°

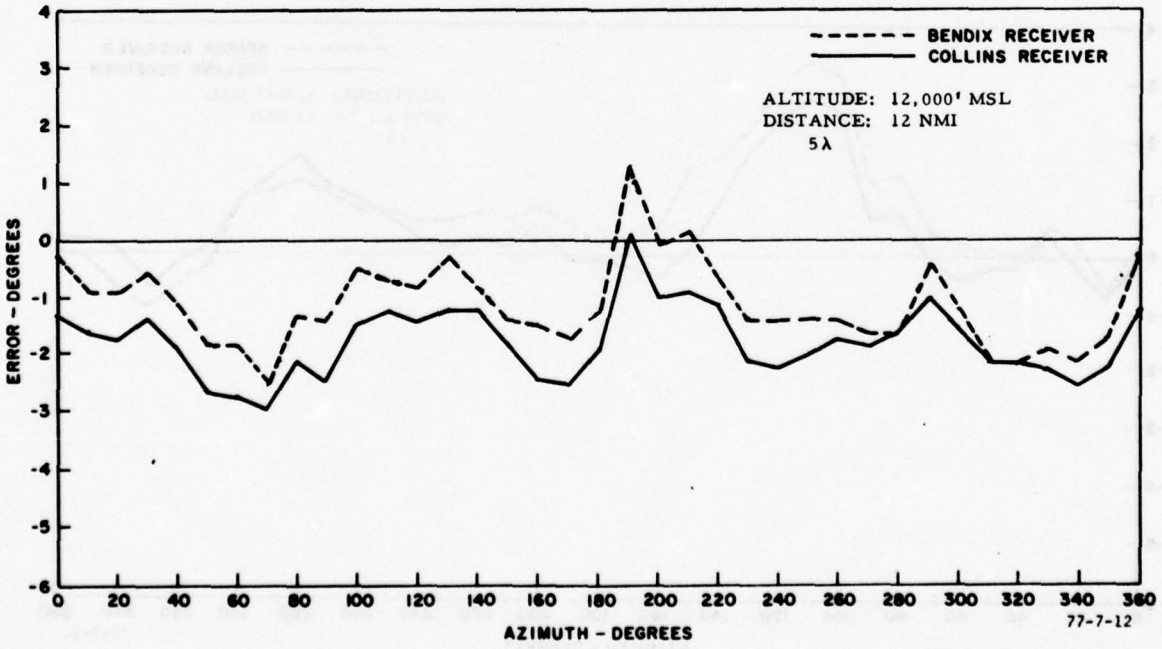


FIGURE 12. BEARING ERROR, ORBIT AT ELEVATION 9.3°

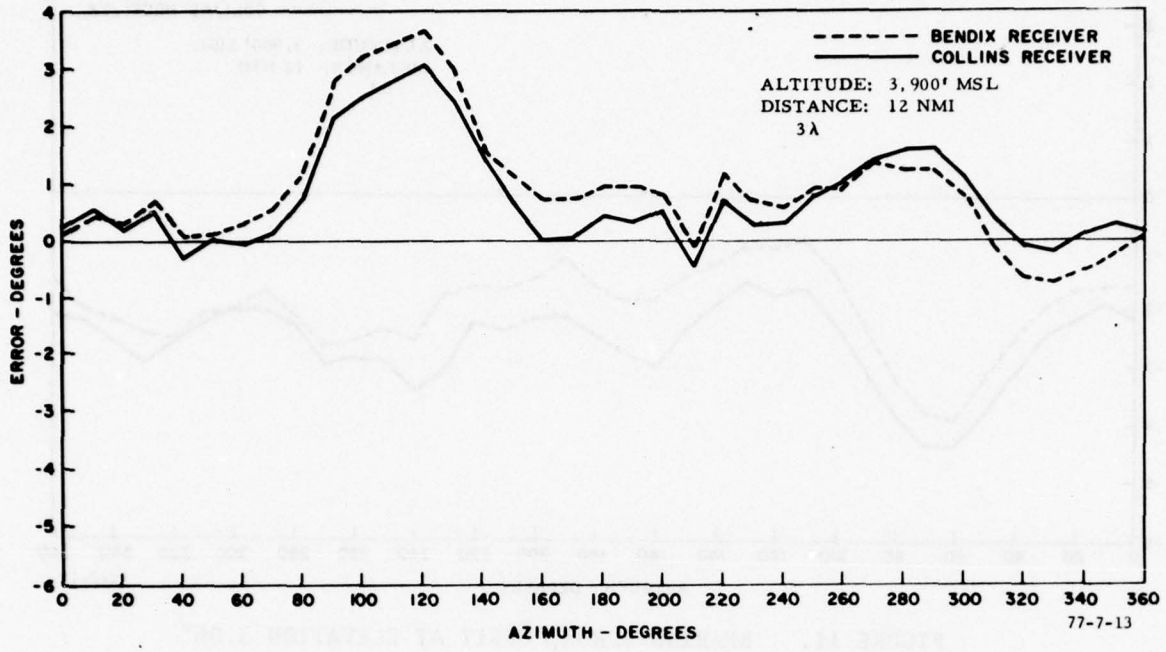


FIGURE 13. BEARING ERROR, ORBIT AT 3.06° (3 WAVELENGTHS)

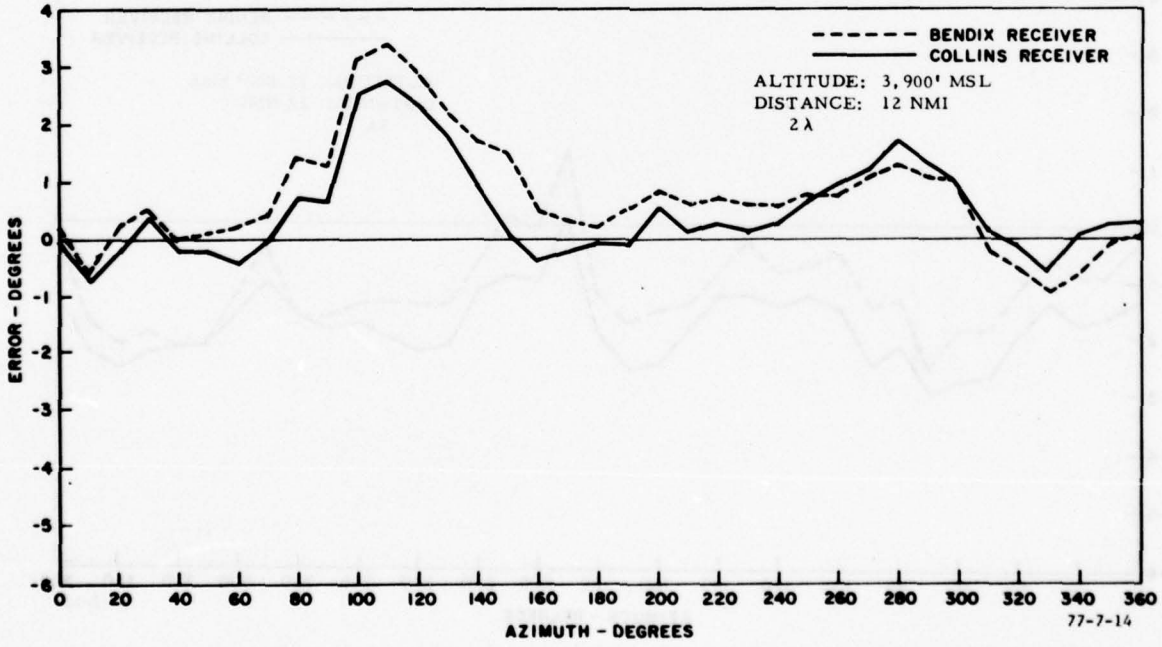


FIGURE 14. BEARING ERROR, ORBIT AT 3.06° (2 WAVELENGTHS)

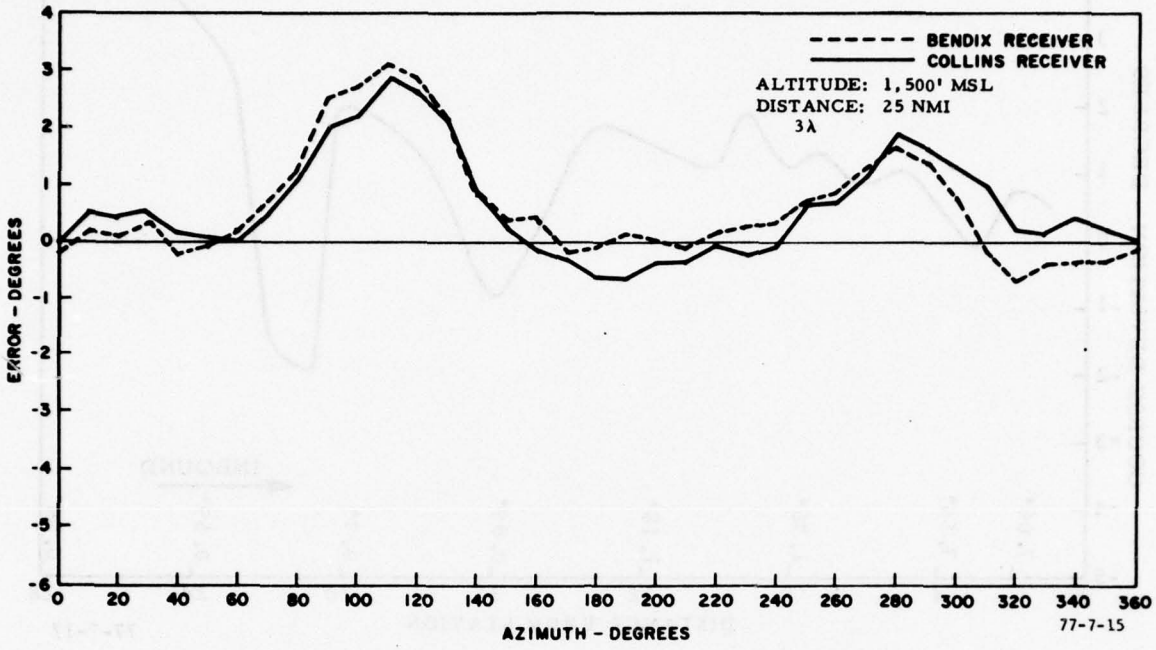


FIGURE 15. BEARING ERROR, ORBIT AT 0.57° (3 WAVELENGTHS)

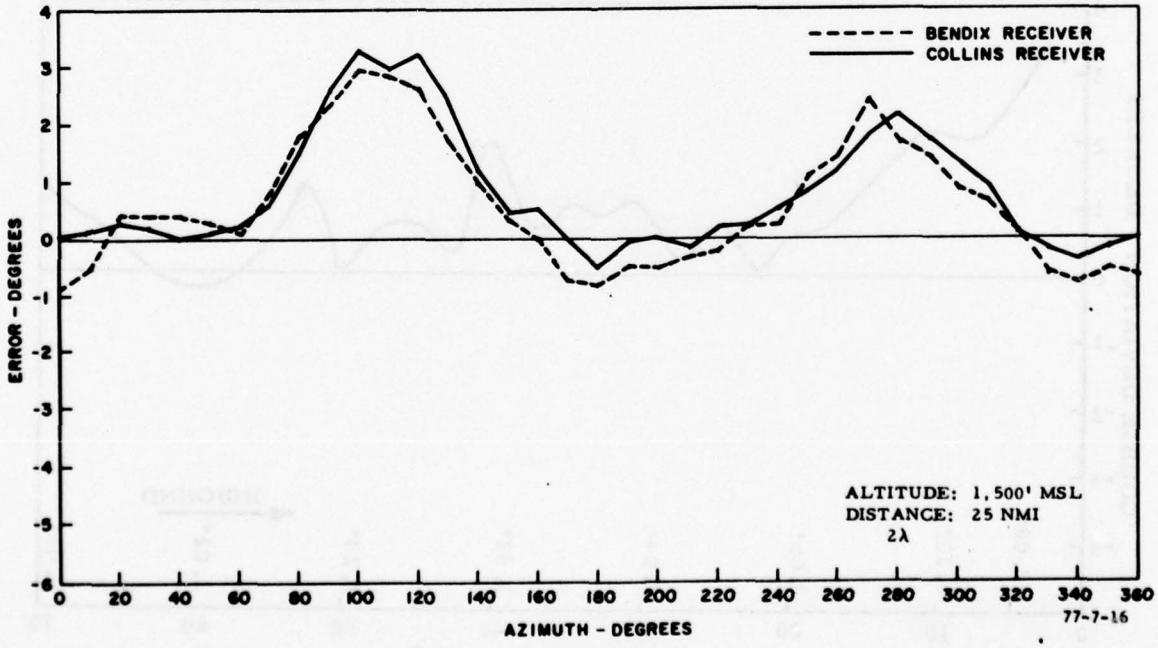


FIGURE 16. BEARING ERROR, ORBIT AT 0.57° (2 WAVELENGTHS)

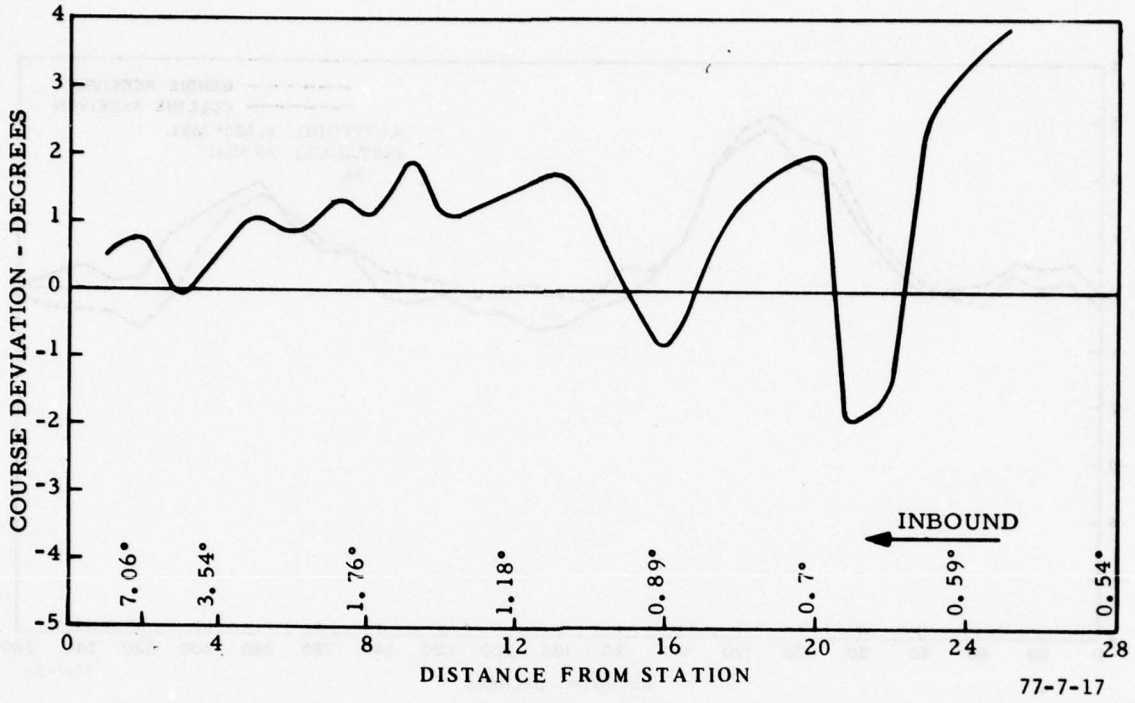


FIGURE 17. INDICATED STATION ERROR, RADIAL 330°, ALTITUDE 1,500 FT. MSL

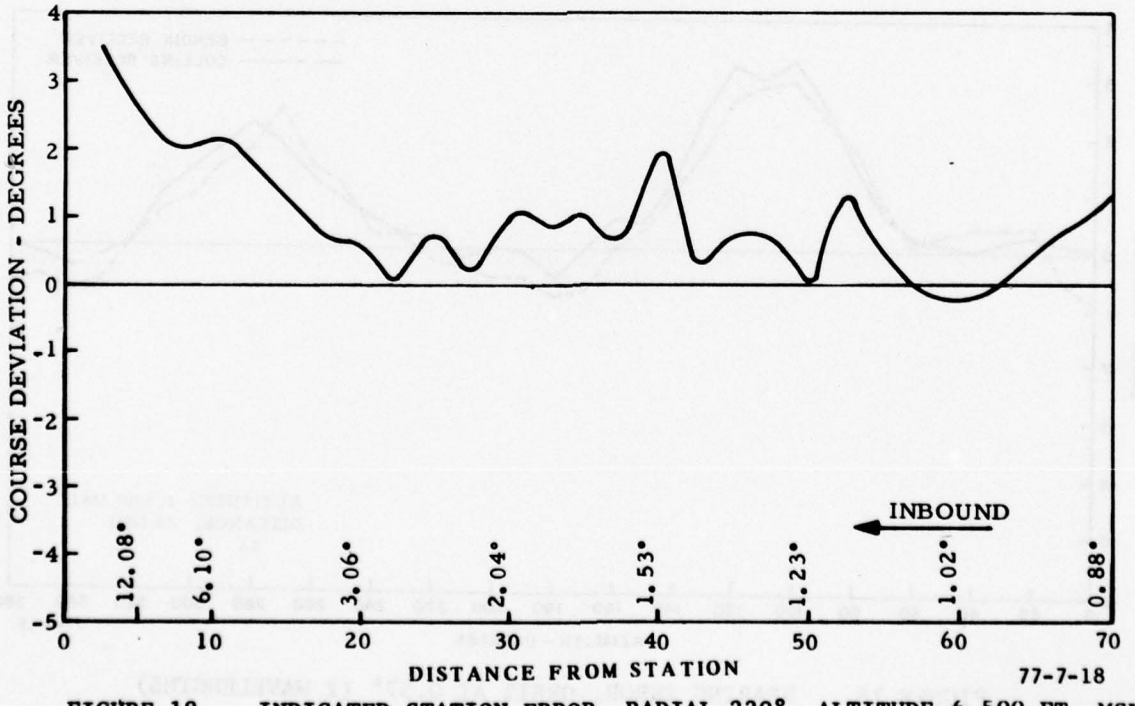


FIGURE 18. INDICATED STATION ERROR, RADIAL 220°, ALTITUDE 6,500 FT. MSL

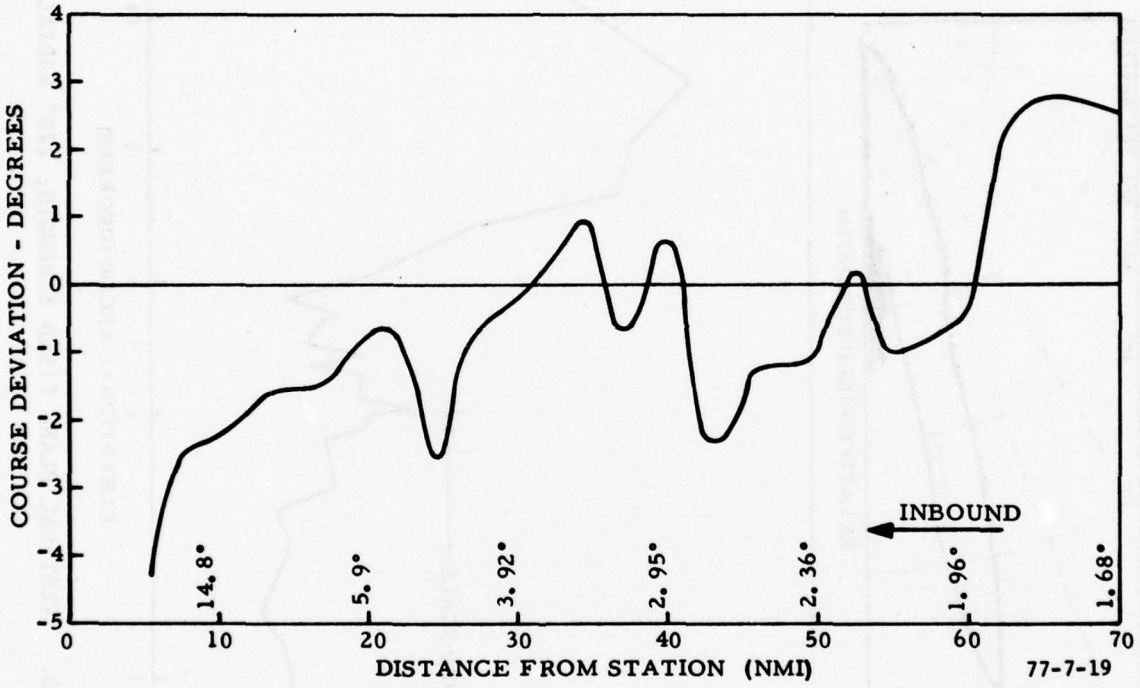


FIGURE 19. INDICATED STATION ERROR, RADIAL 220°, ALTITUDE 12,500 FT. MSL

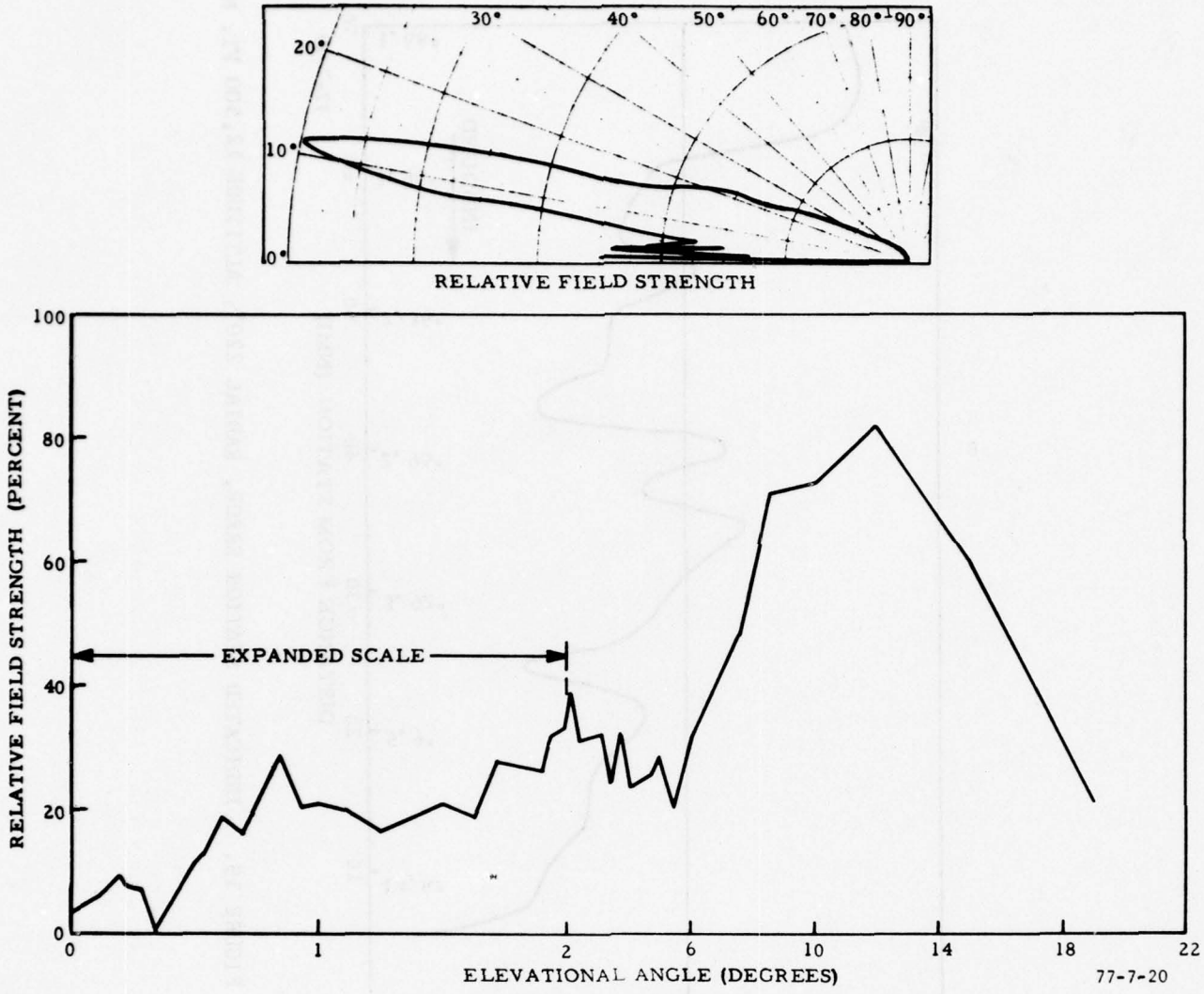


FIGURE 20. VERTICAL PLANE FIELD STRENGTH, 220° RADIAL

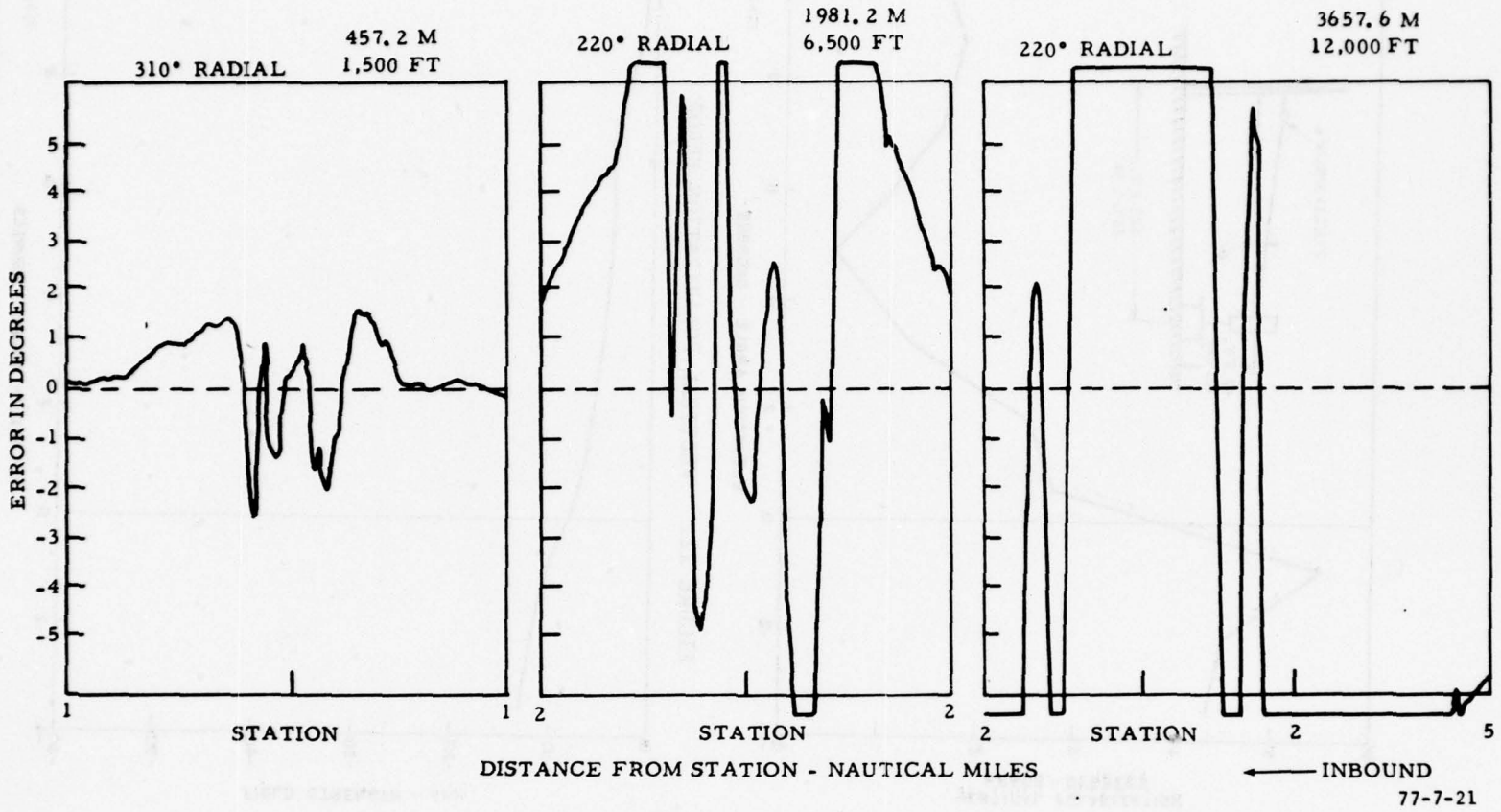


FIGURE 21. CONE OF CONFUSION

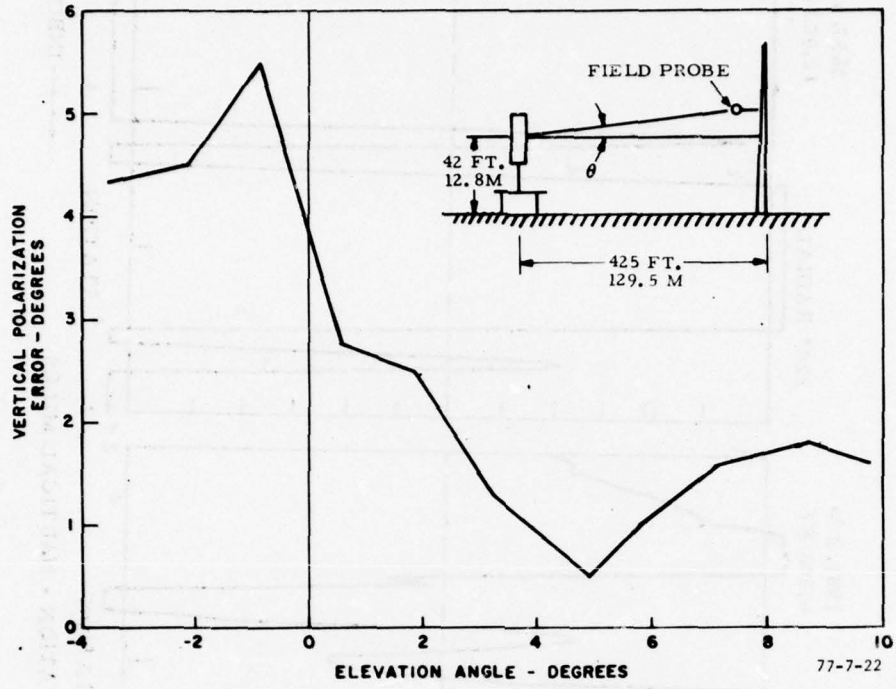


FIGURE 22. VERTICAL POLARIZATION ERROR

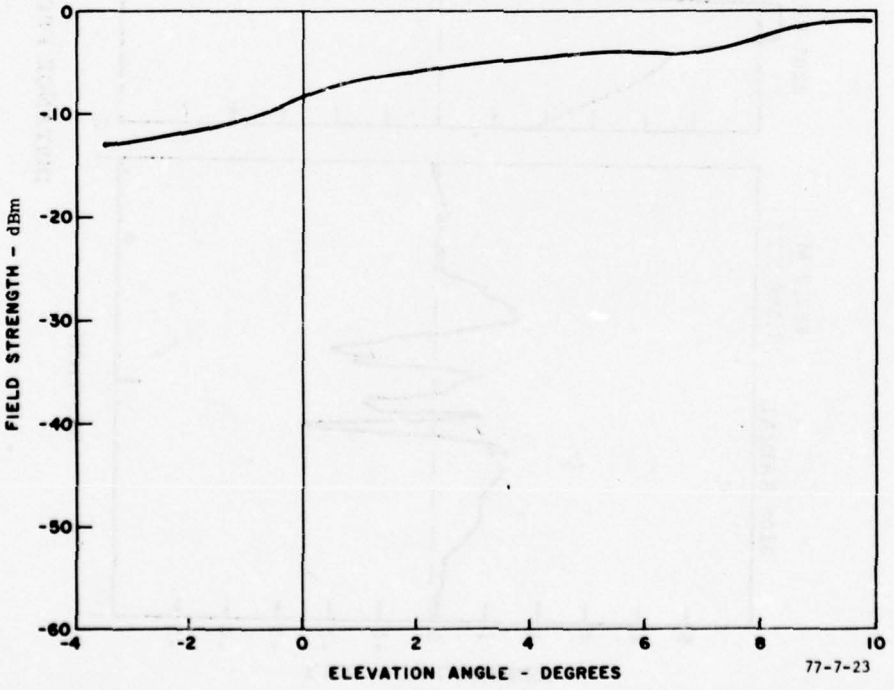


FIGURE 23. FIELD STRENGTH, ALL SINE ELEMENTS ENERGIZED

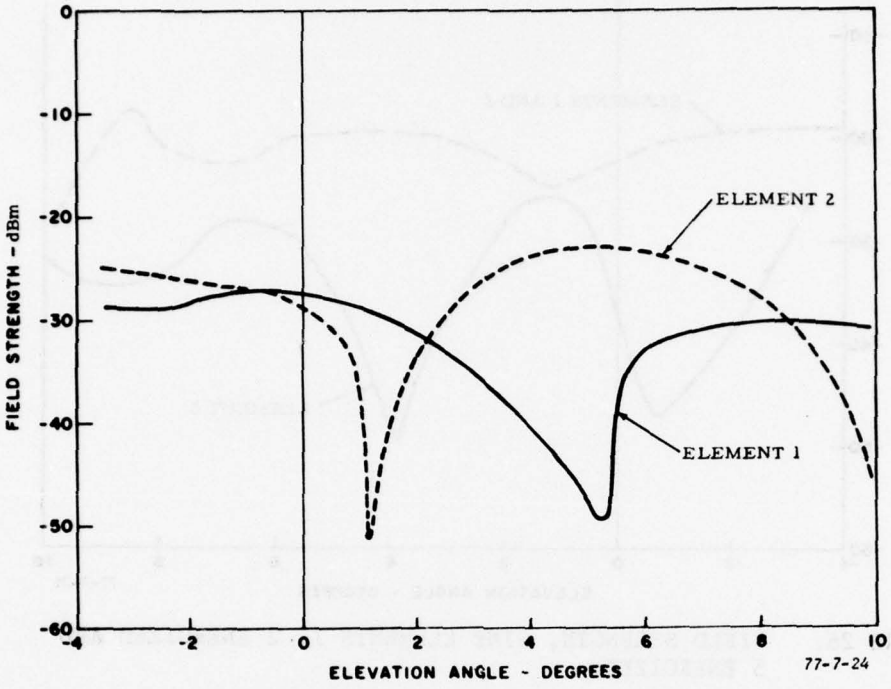


FIGURE 24. FIELD STRENGTH, SINE ELEMENTS 1 ENERGIZED AND 2 ENERGIZED

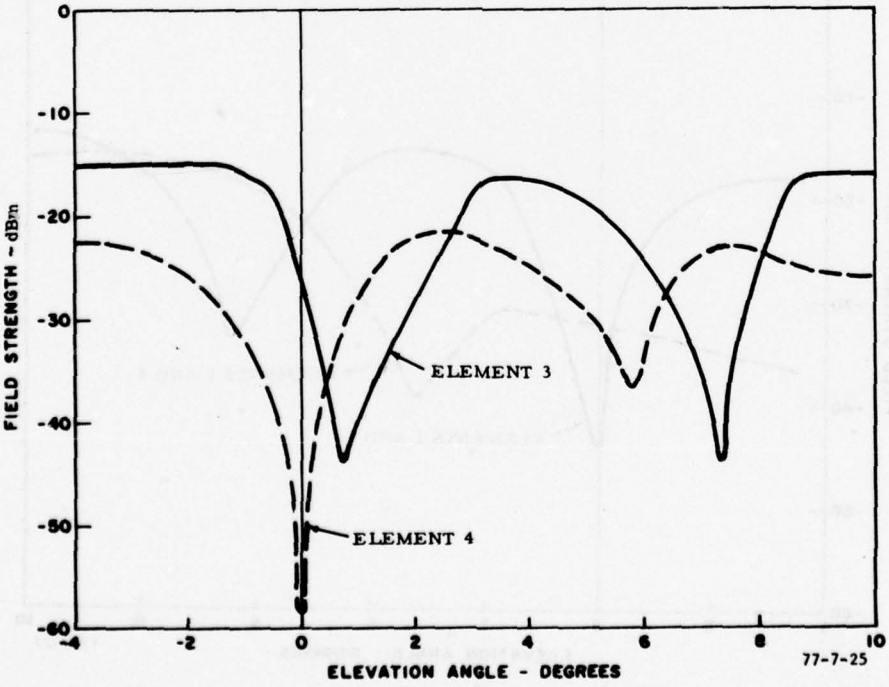


FIGURE 25. FIELD STRENGTH, SINE ELEMENTS 3 ENERGIZED AND 4 ENERGIZED

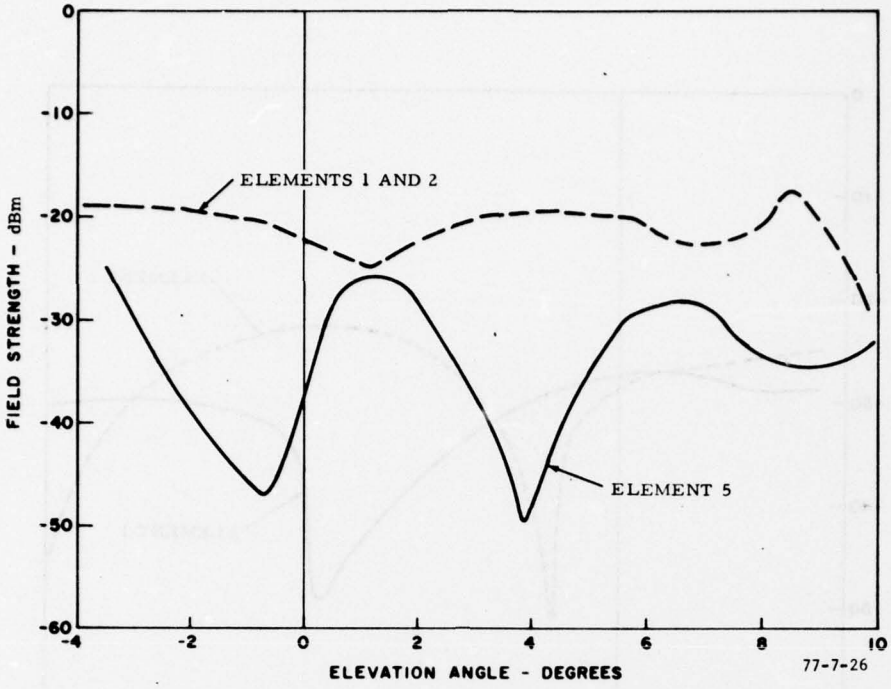


FIGURE 26. FIELD STRENGTH, SINE ELEMENTS 1, 2 ENERGIZED AND 5 ENERGIZED

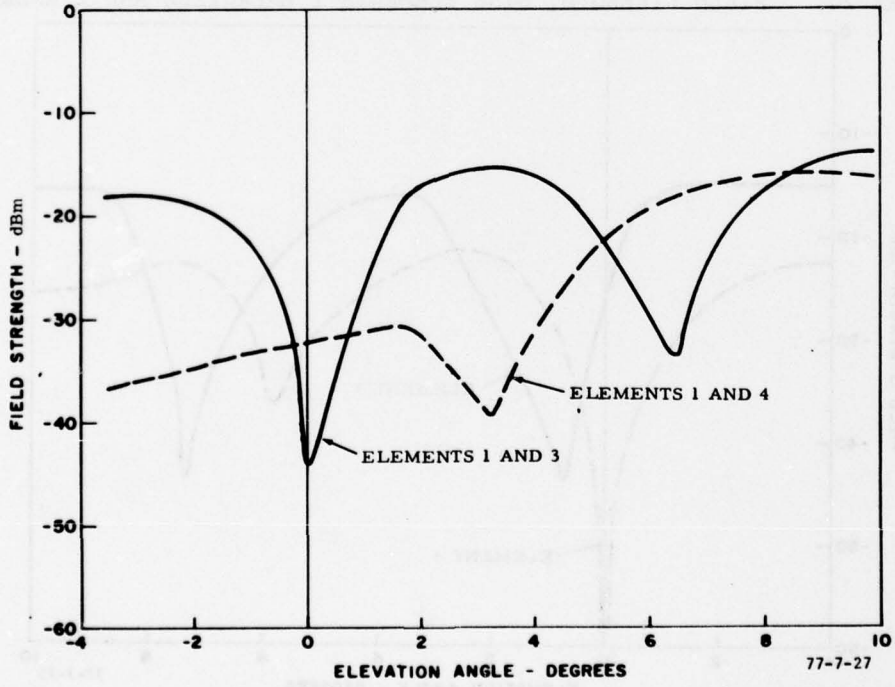


FIGURE 27. FIELD STRENGTH, SINE ELEMENTS 1, 3 ENERGIZED AND 1, 4 ENERGIZED

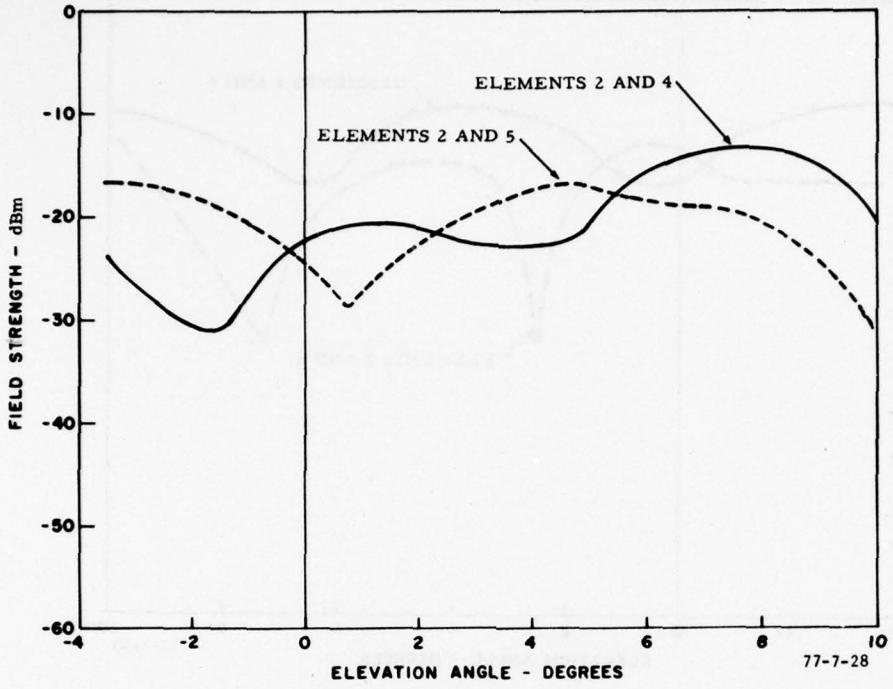


FIGURE 28. FIELD STRENGTH, SINE ELEMENTS 1, 5 ENERGIZED AND 2. 3 ENERGIZED

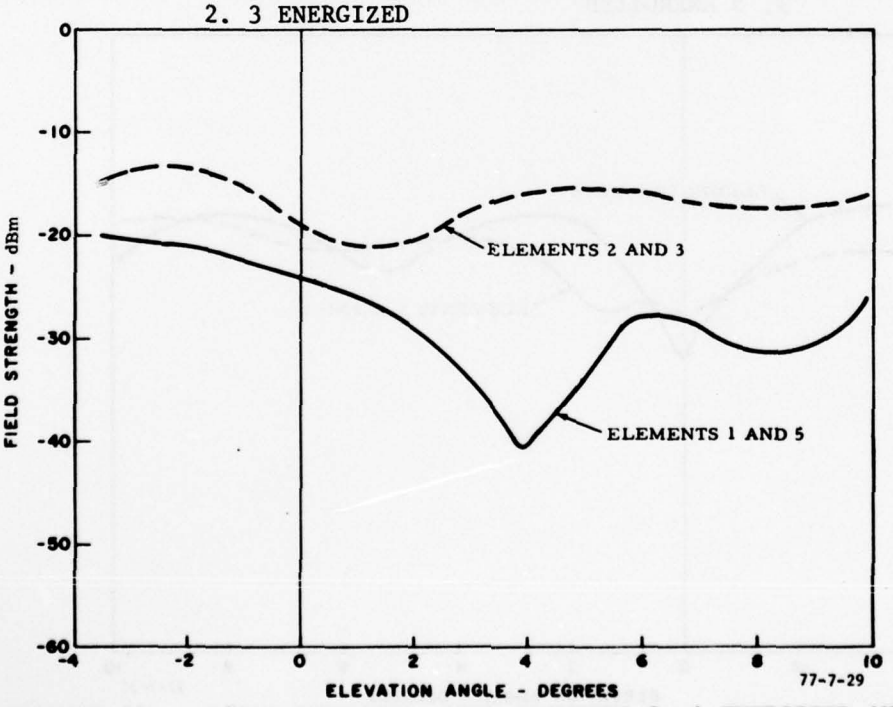


FIGURE 29. FIELD STRENGTH, SINE ELEMENTS 2, 4 ENERGIZED AND 2, 5 ENERGIZED

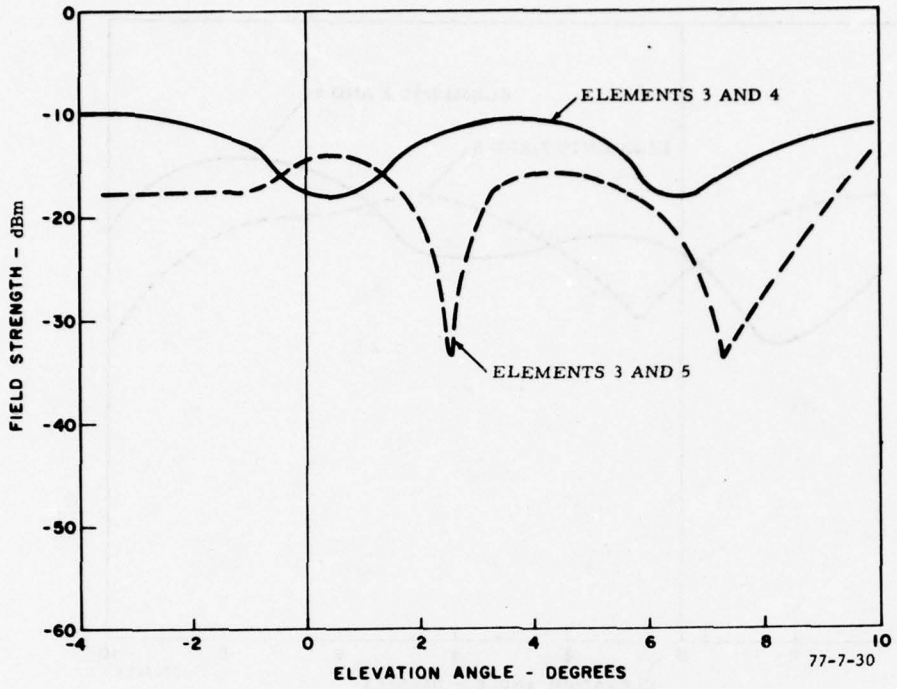


FIGURE 30. FIELD STRENGTH, SINE ELEMENTS 3, 4 ENERGIZED AND 3, 5 ENERGIZED

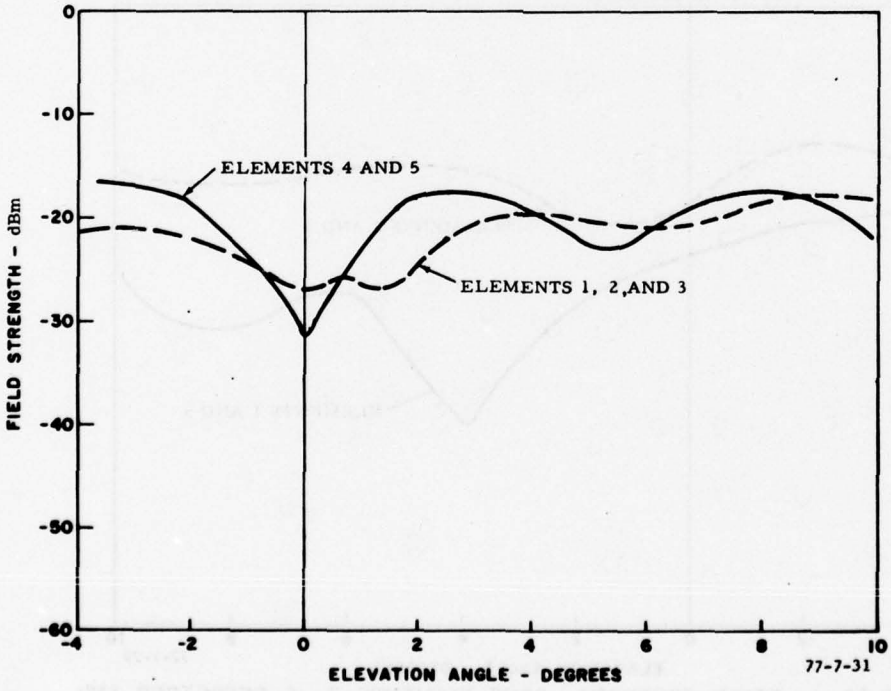


FIGURE 31. FIELD STRENGTH, SINE ELEMENTS 4, 5 ENERGIZED AND 1, 2, 3 ENERGIZED

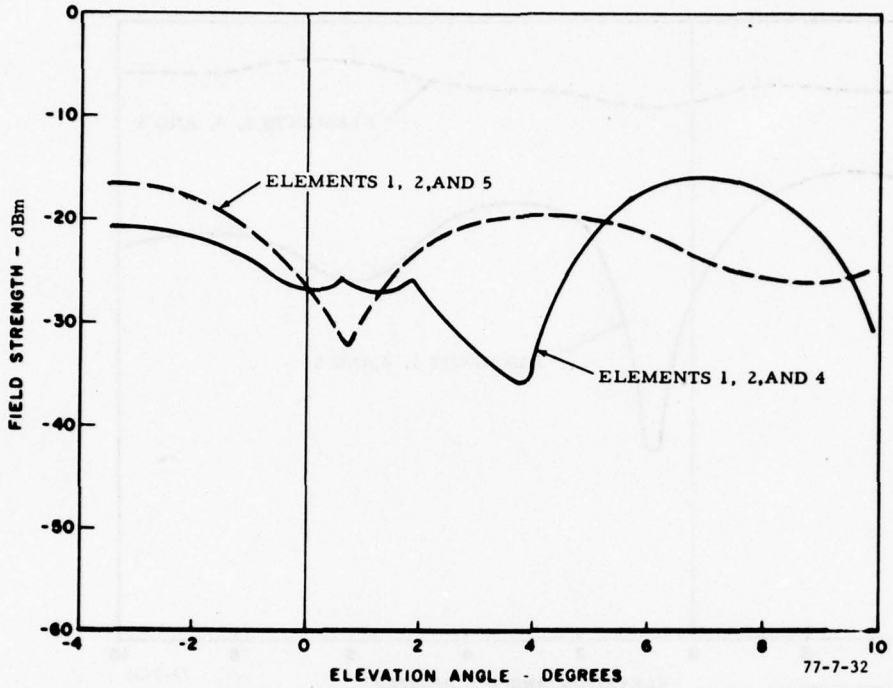


FIGURE 32. FIELD STRENGTH, SINE ELEMENTS 1, 2, 4 ENERGIZED AND 1, 2, 5 ENERGIZED

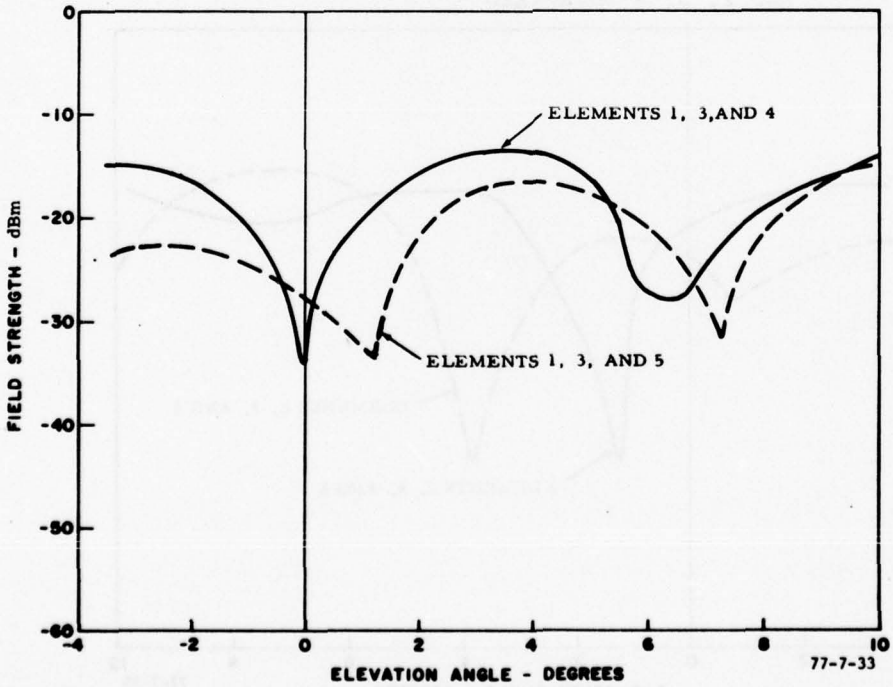


FIGURE 33. FIELD STRENGTH, SINE ELEMENTS 1, 3, 4 ENERGIZED AND 1, 3, 4, 5 ENERGIZED

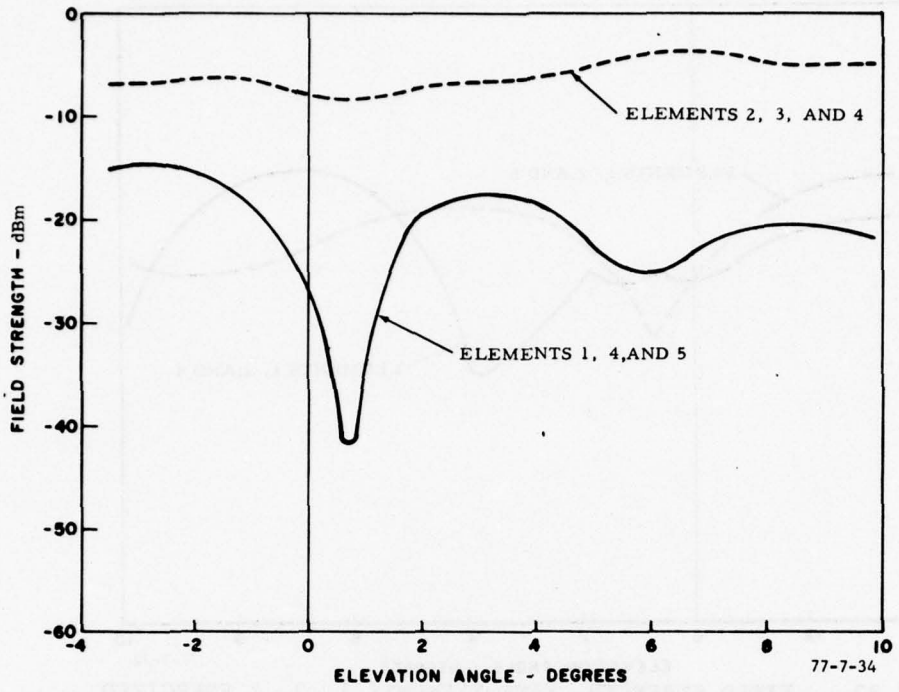


FIGURE 34. FIELD STRENGTH, SINE ELEMENTS 1, 4, 5 ENERGIZED AND 2. 3. 4 ENERGIZED

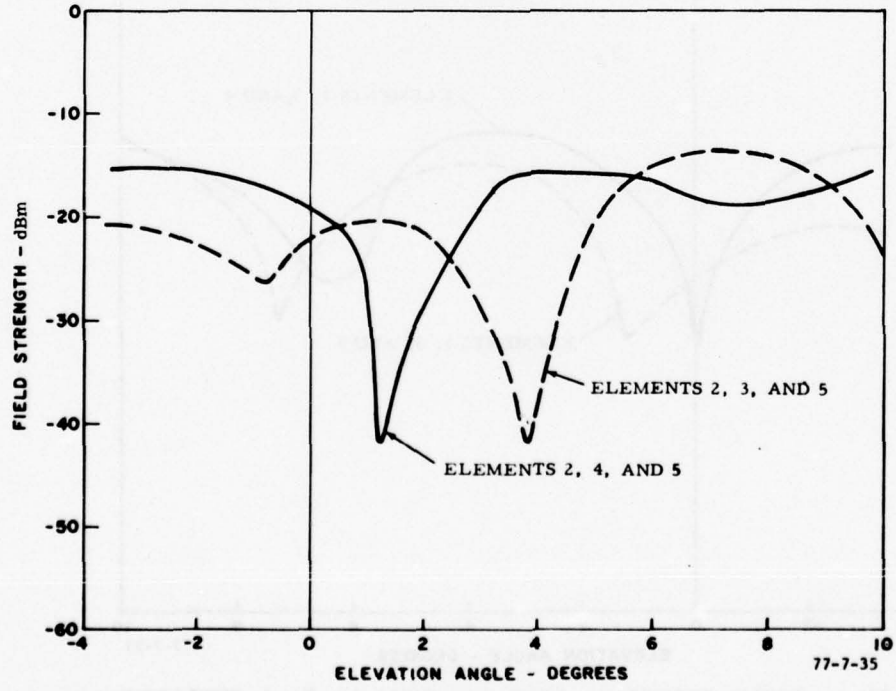


FIGURE 35. FIELD STRENGTH, SINE ELEMENTS 2, 3, 5 ENERGIZED AND 2, 4, 5, ENERGIZED

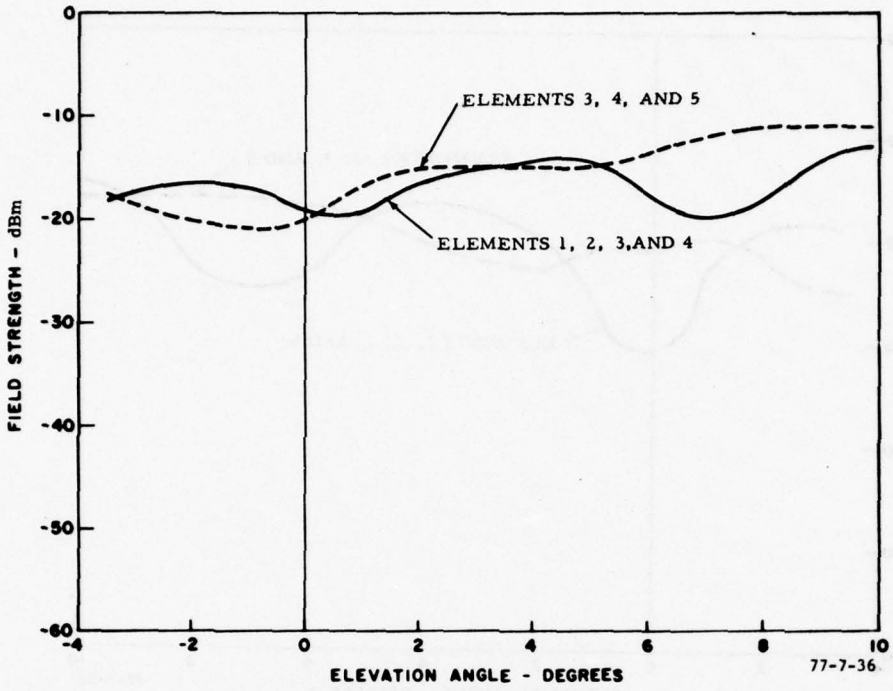


FIGURE 36. FIELD STRENGTH, SINE ELEMENTS 3, 4, 5 ENERGIZED AND 1, 2, 3, 4 ENERGIZED

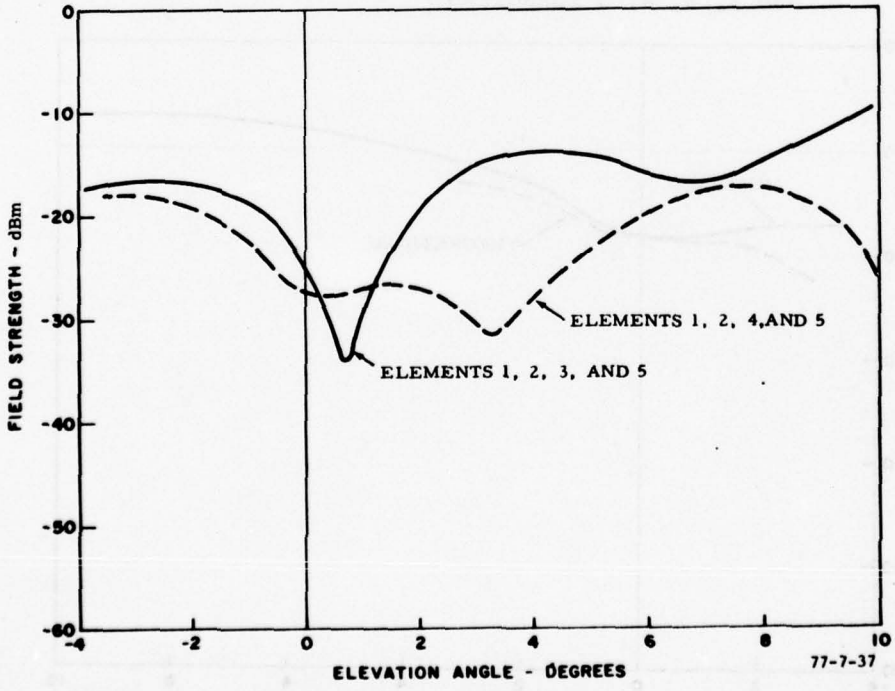


FIGURE 37. FIELD STRENGTH, SINE ELEMENTS 1, 2, 3, 5 ENERGIZED AND 1, 2, 4, 5 ENERGIZED

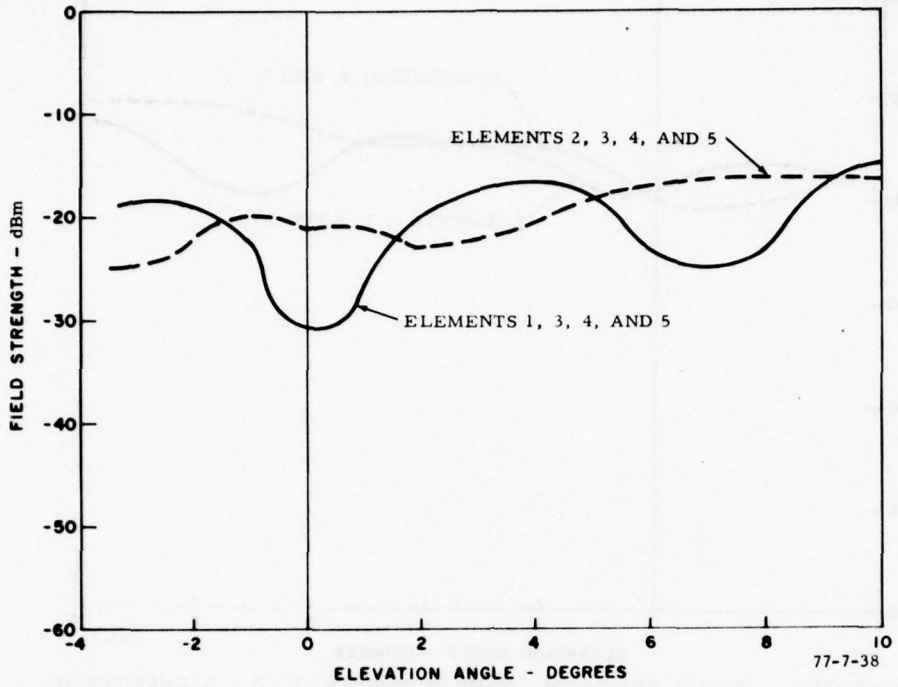


FIGURE 38. FIELD STRENGTH, SINE ELEMENTS 1, 3, 4, 5 ENERGIZED AND 2, 3, 4, 5 ENERGIZED

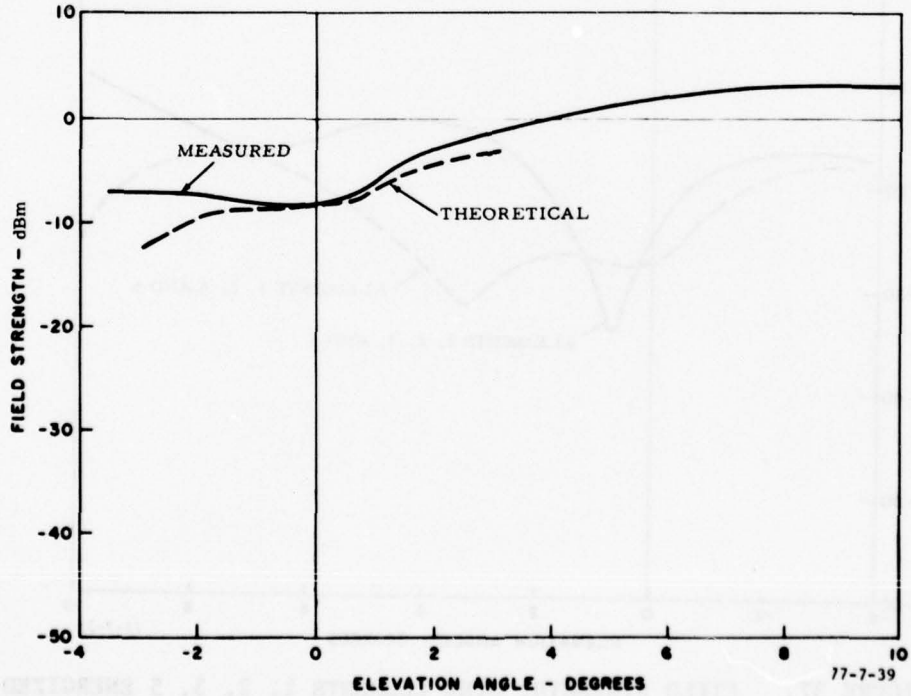


FIGURE 39. FIELD STRENGTH, ALL REFERENCE ELEMENTS ENERGIZED

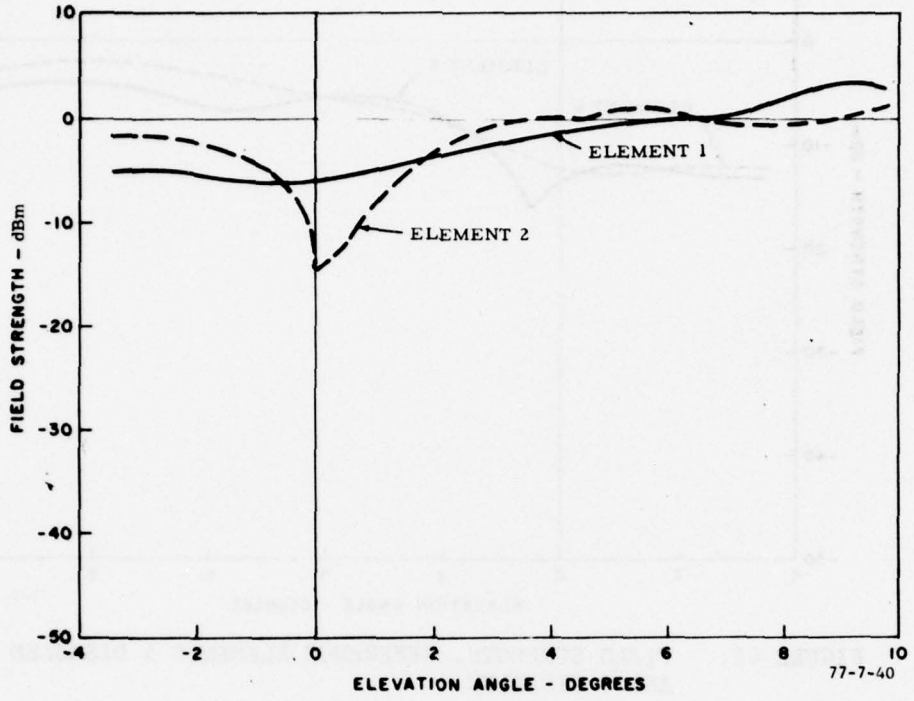


FIGURE 40. FIELD STRENGTH, REFERENCES ELEMENTS 1 DISABLED AND 2 DISABLED

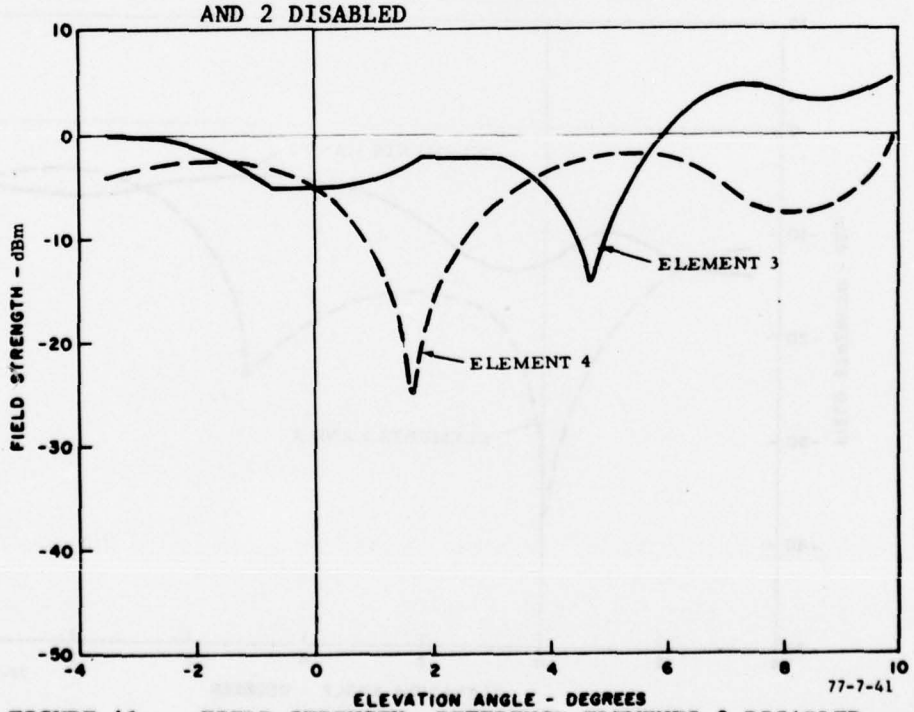


FIGURE 41. FIELD STRENGTH, REFERENCE ELEMENTS 3 DISABLED AND 4 DISABLED

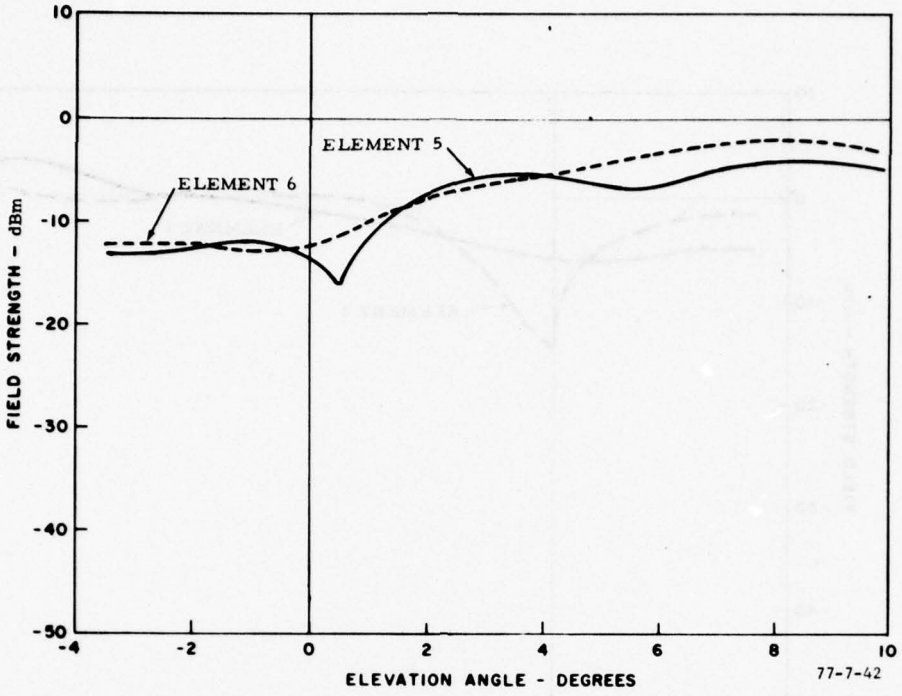


FIGURE 42. FIELD STRENGTH, REFERENCE ELEMENTS 5 DISABLED AND 6 DISABLED

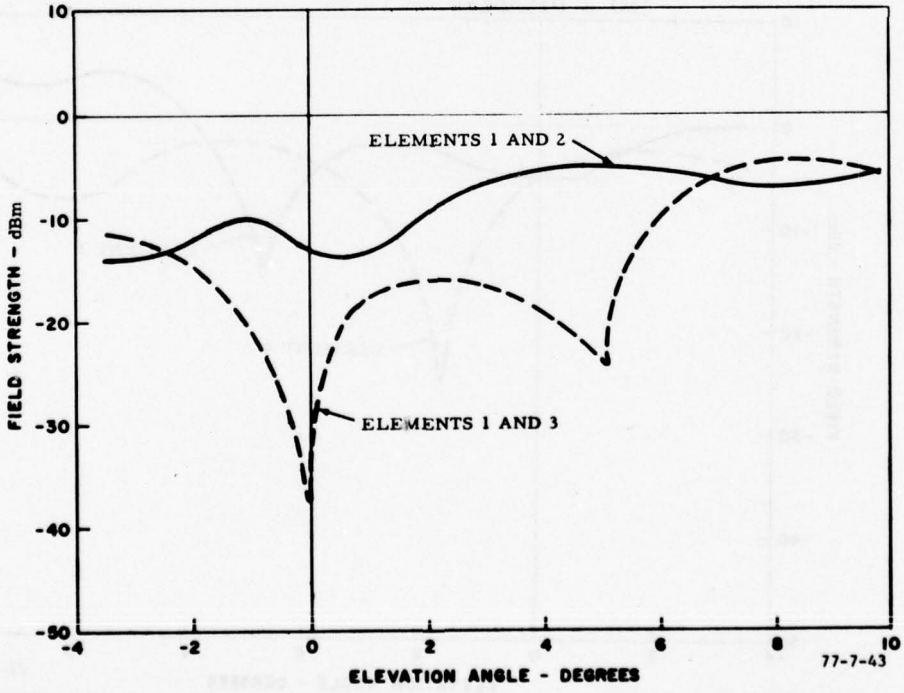


FIGURE 43. FIELD STRENGTH, REFERENCE ELEMENTS 1, 2 DISABLED 1, 3 DISABLED

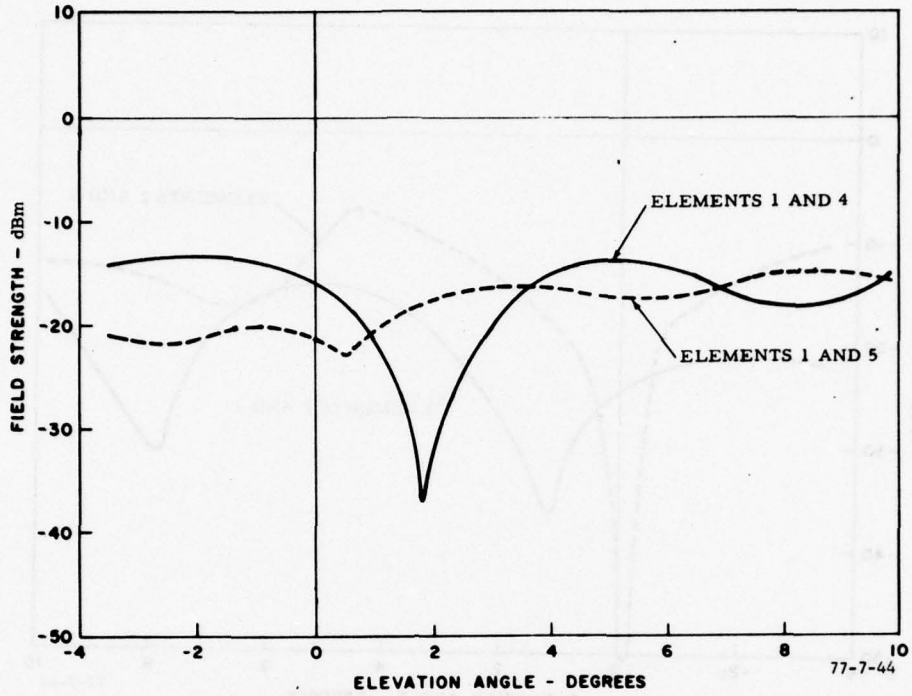


FIGURE 44. FIELD STRENGTH, REFERENCE ELEMENTS 1, 4 DISABLED AND 1. 5 DISABLED

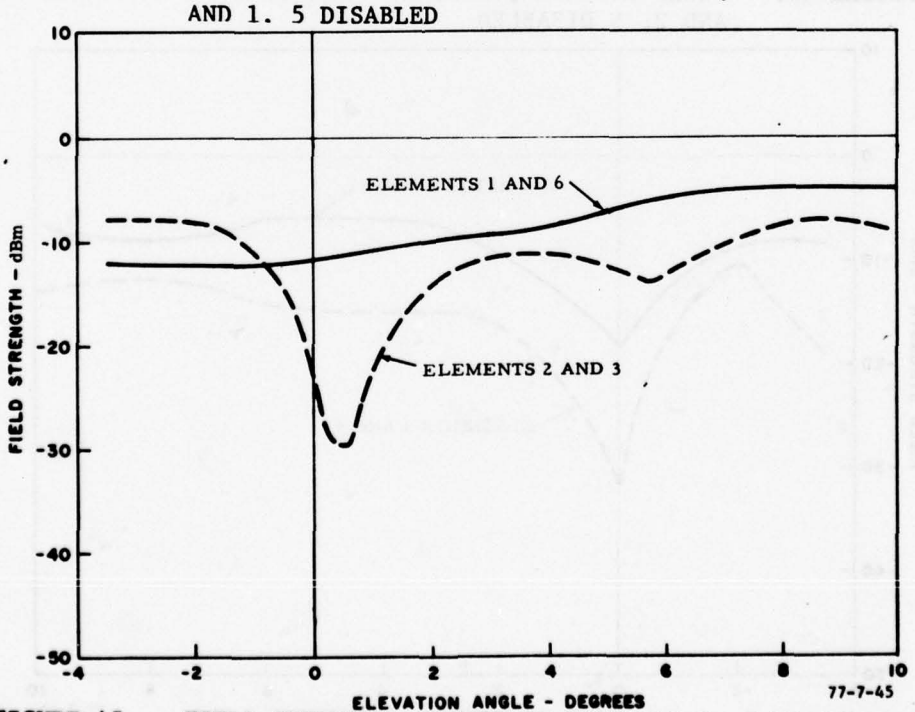


FIGURE 45. FIELD STRENGTH, REFERENCE ELEMENTS 1, 6 DISABLED AND 2, 3 DISABLED

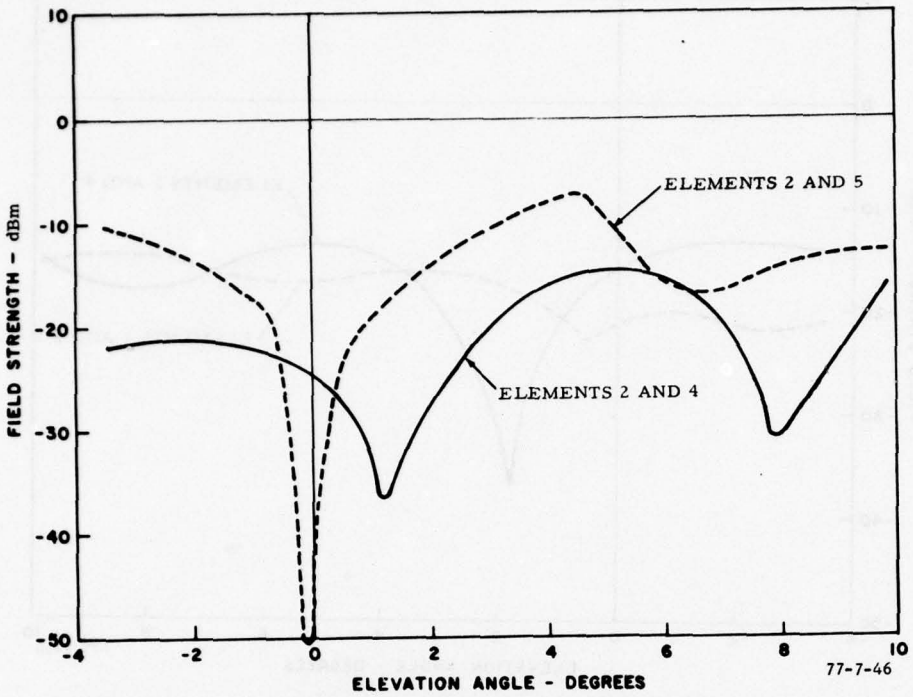


FIGURE 46. FIELD STRENGTH, REFERENCE ELEMENTS 2, 4 DISABLED AND 2, 5 DISABLED

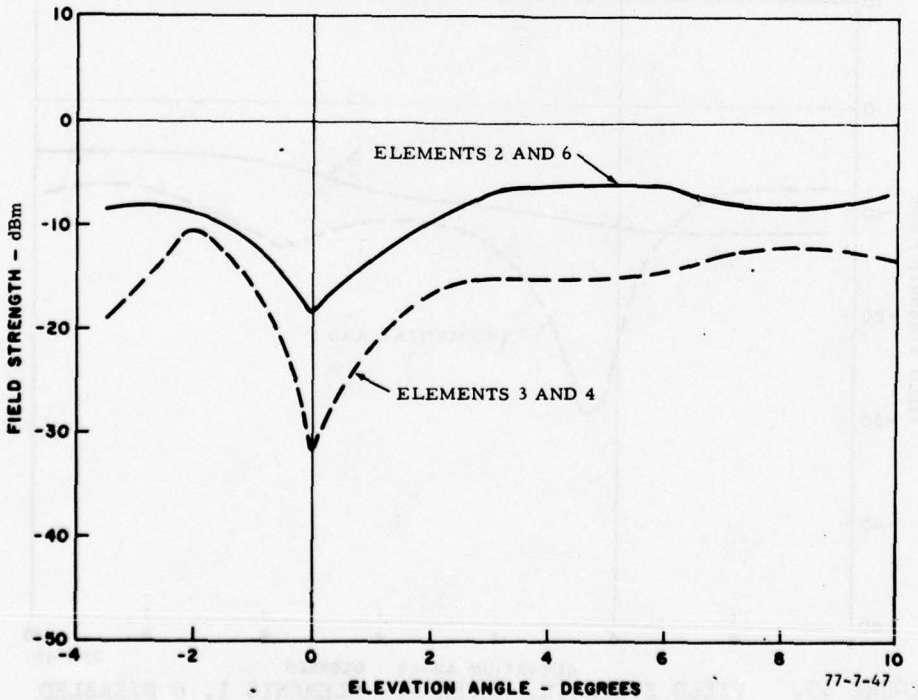


FIGURE 47. FIELD STRENGTH, REFERENCE ELEMENTS 2, 6 DISABLED AND 3, 4 DISABLED

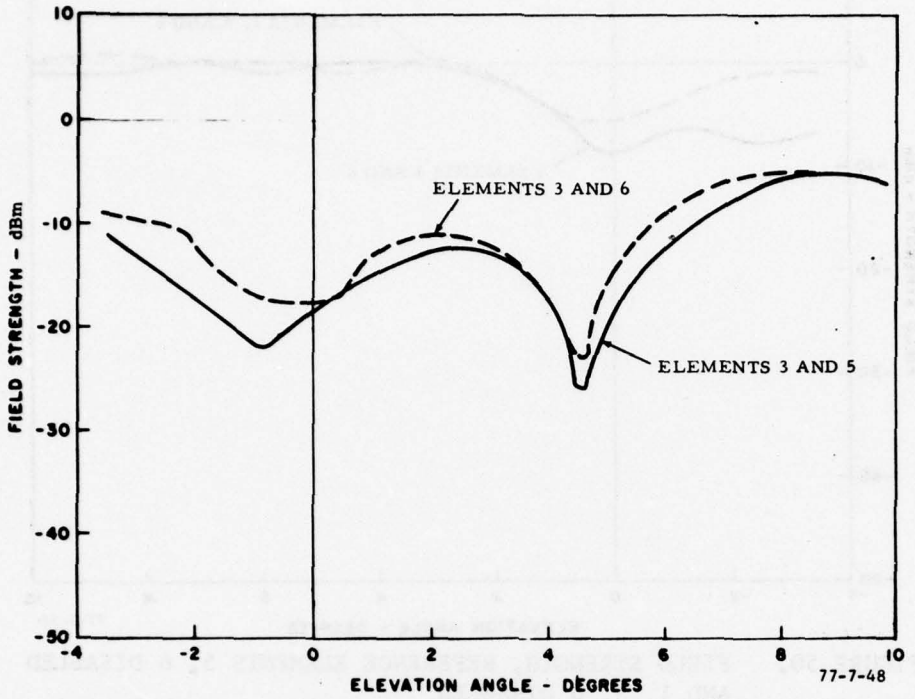


FIGURE 48. FIELD STRENGTH, REFERENCE ELEMENTS 3, 5 DISABLED AND 3, 6 DISABLED

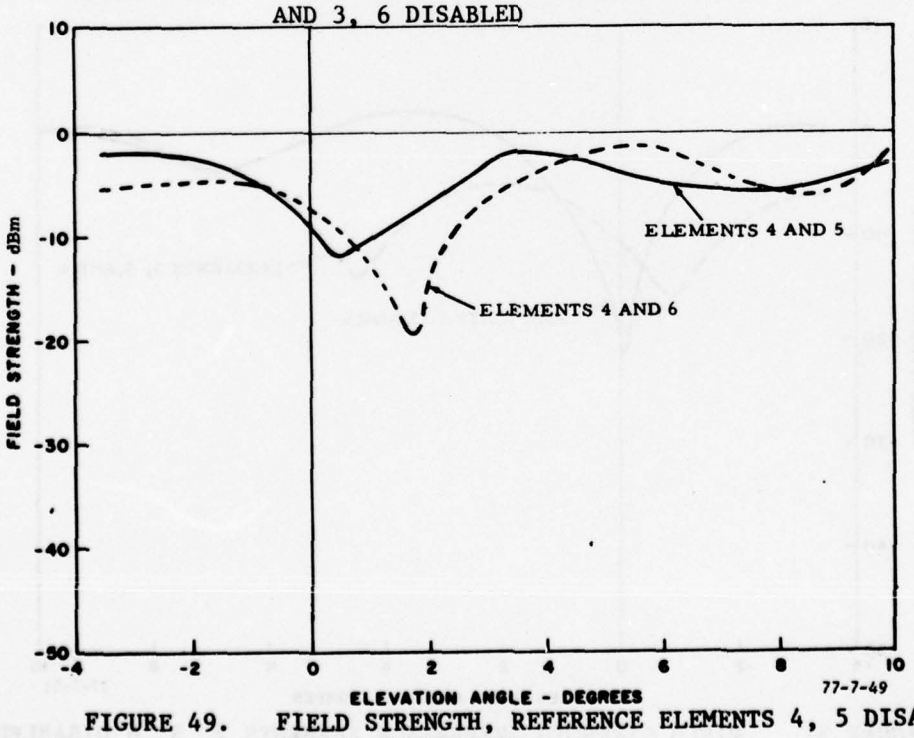


FIGURE 49. FIELD STRENGTH, REFERENCE ELEMENTS 4, 5 DISABLED AND 4, 6 DISABLED

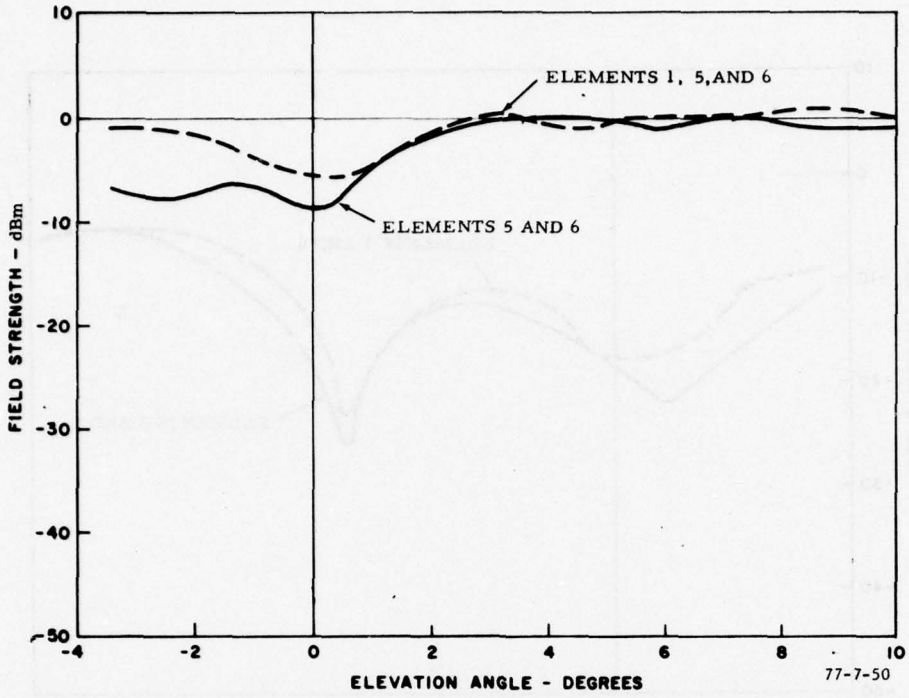


FIGURE 50. FIELD STRENGTH, REFERENCE ELEMENTS 5, 6 DISABLED AND 1, 5, 6 DISABLED

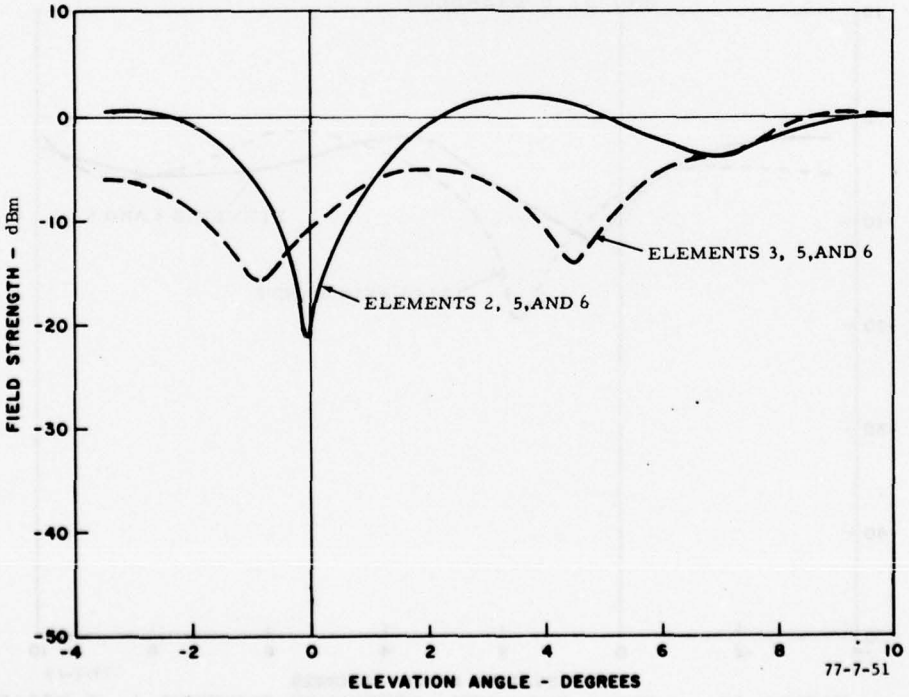


FIGURE 51. FIELD STRENGTH, REFERENCE ELEMENTS 2, 5, 6 DISABLED AND 3, 5, 6 DISABLED

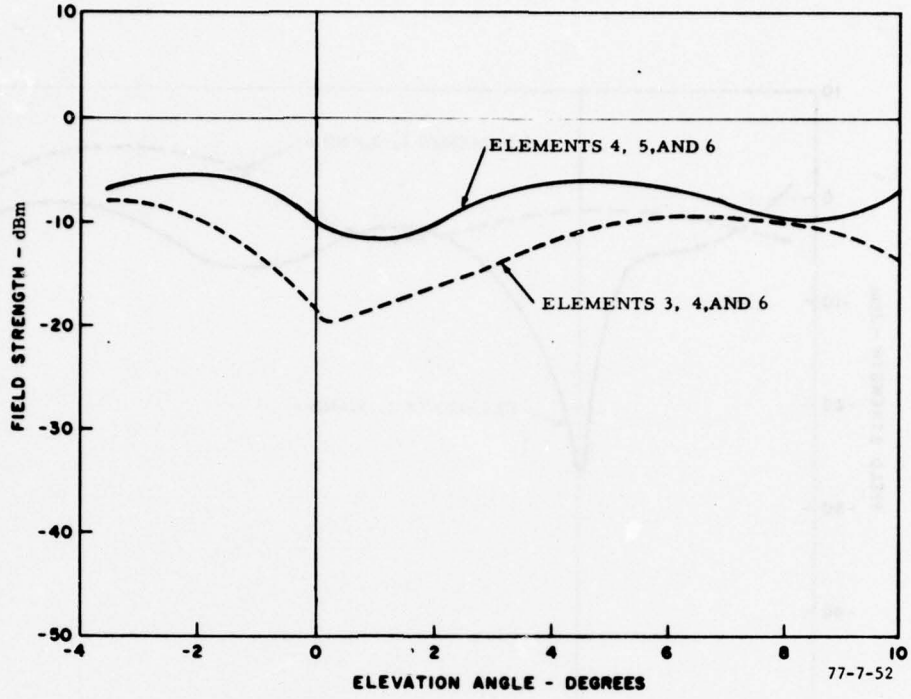


FIGURE 52. FIELD STRENGTH, REFERENCE ELEMENTS 4, 5, 6 DISABLED AND 3, 4, 6 DISABLED

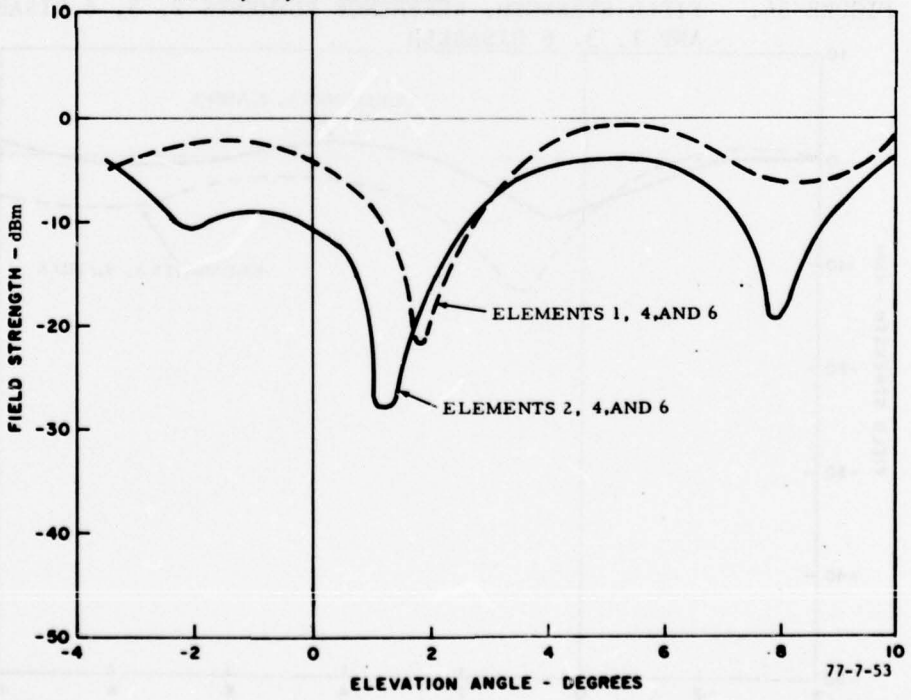


FIGURE 53. FIELD STRENGTH, REFERENCE ELEMENTS 2, 4, 6 DISABLED 1, 4, 6 DISABLED

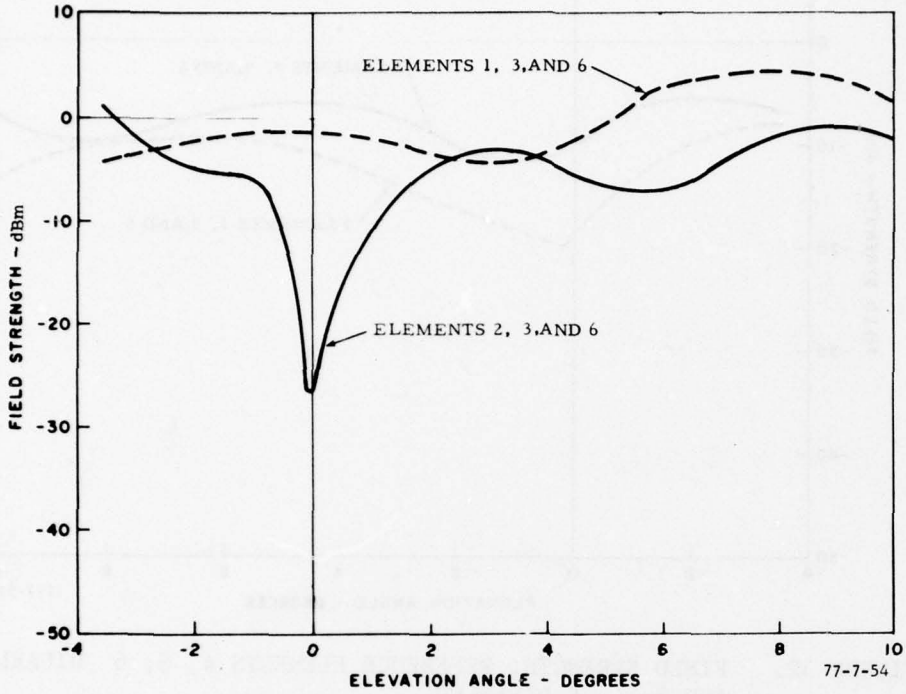


FIGURE 54. FIELD STRENGTH, REFERENCE ELEMENTS 2, 3, 6 DISABLED AND 1, 3, 6 DISABLED

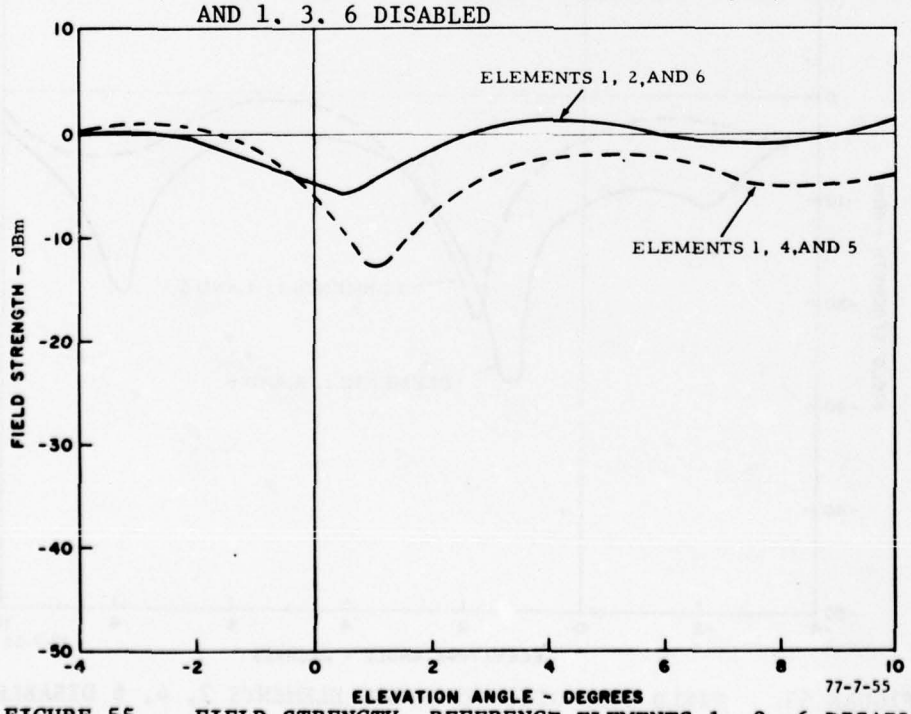


FIGURE 55. FIELD STRENGTH, REFERENCE ELEMENTS 1, 2, 6 DISABLED AND 1, 4, 5 DISABLED

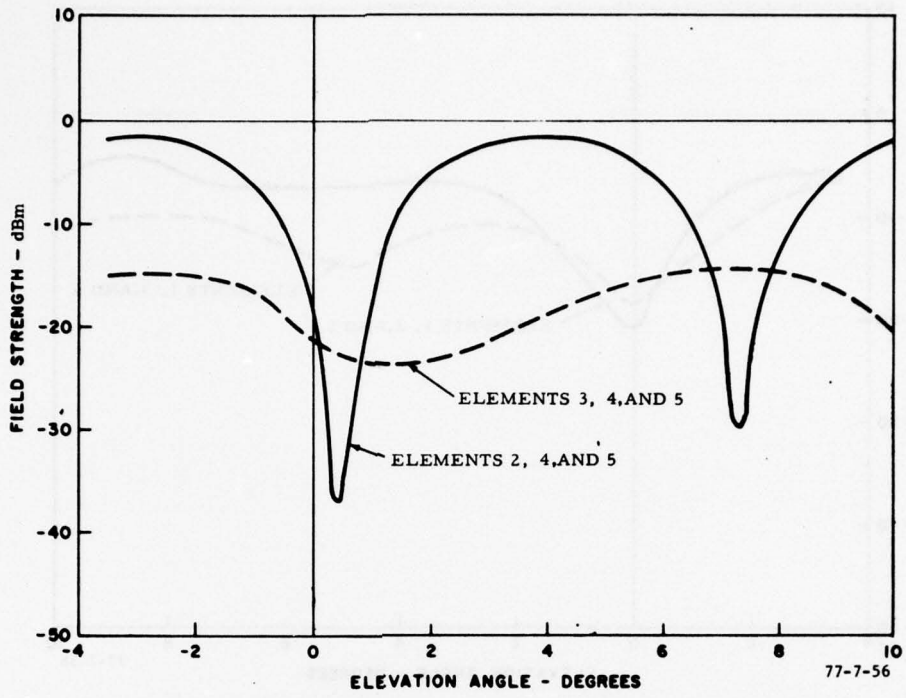


FIGURE 56. FIELD STRENGTH, REFERENCE ELEMENTS 2, 4, 5 DISABLED AND 3, 4, 5 DISABLED

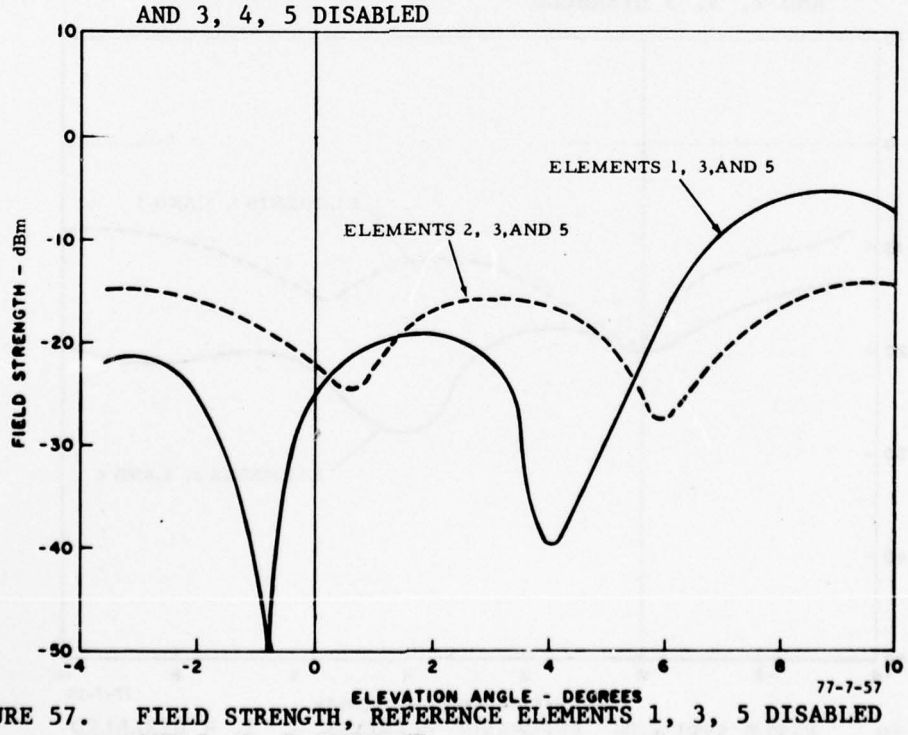


FIGURE 57. FIELD STRENGTH, REFERENCE ELEMENTS 1, 3, 5 DISABLED AND 2, 3, 5 DISABLED

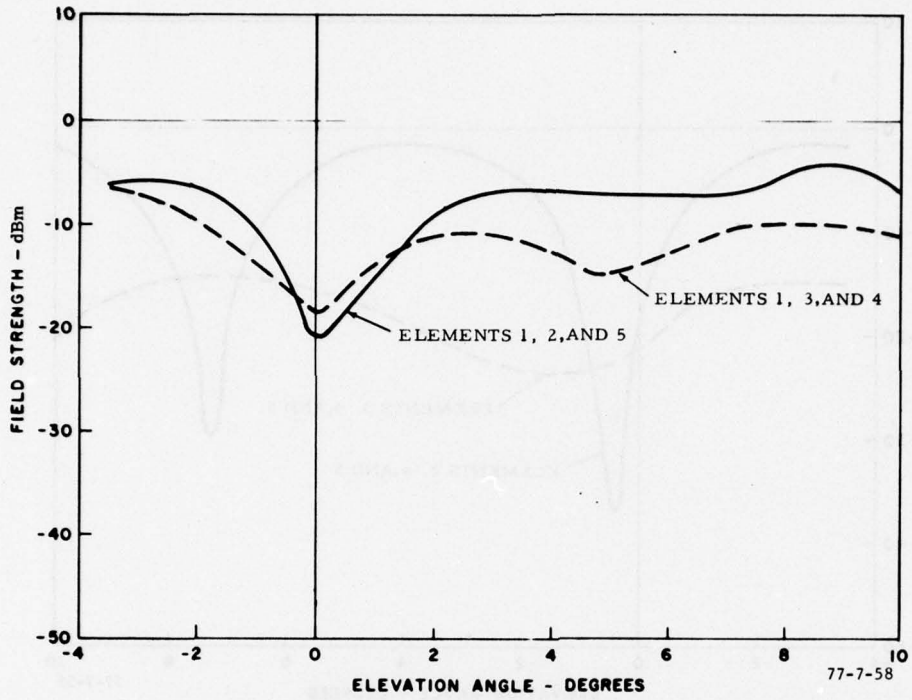


FIGURE 58. FIELD STRENGTH, REFERENCE ELEMENTS 1, 2, 5 DISABLED AND 2, 3, 5 DISABLED

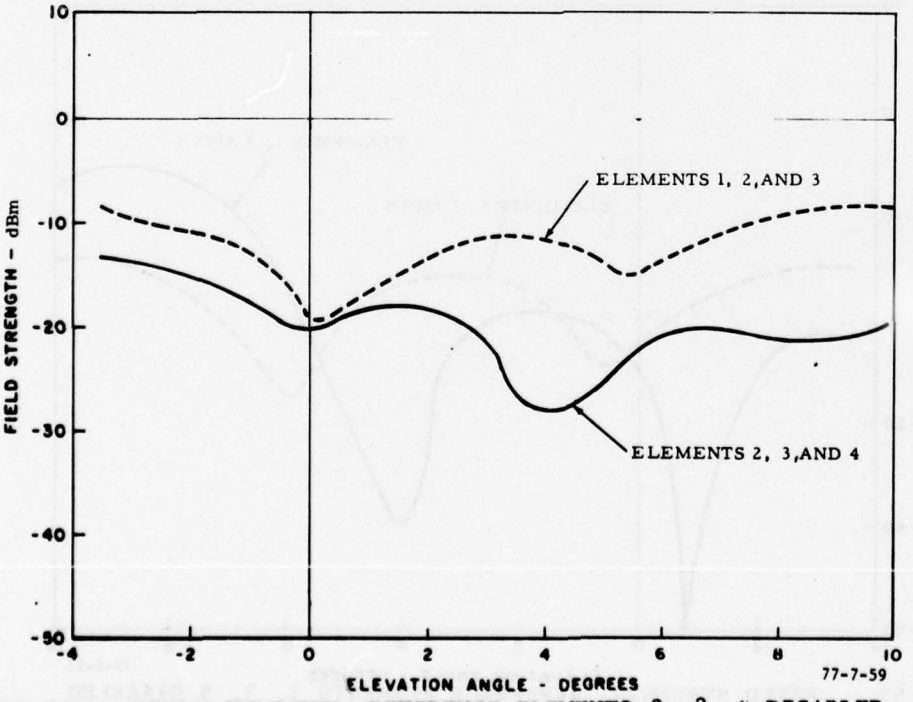


FIGURE 59. FIELD STRENGTH, REFERENCE ELEMENTS 2, 3, 4 DISABLED AND 1, 2, 3 DISABLED

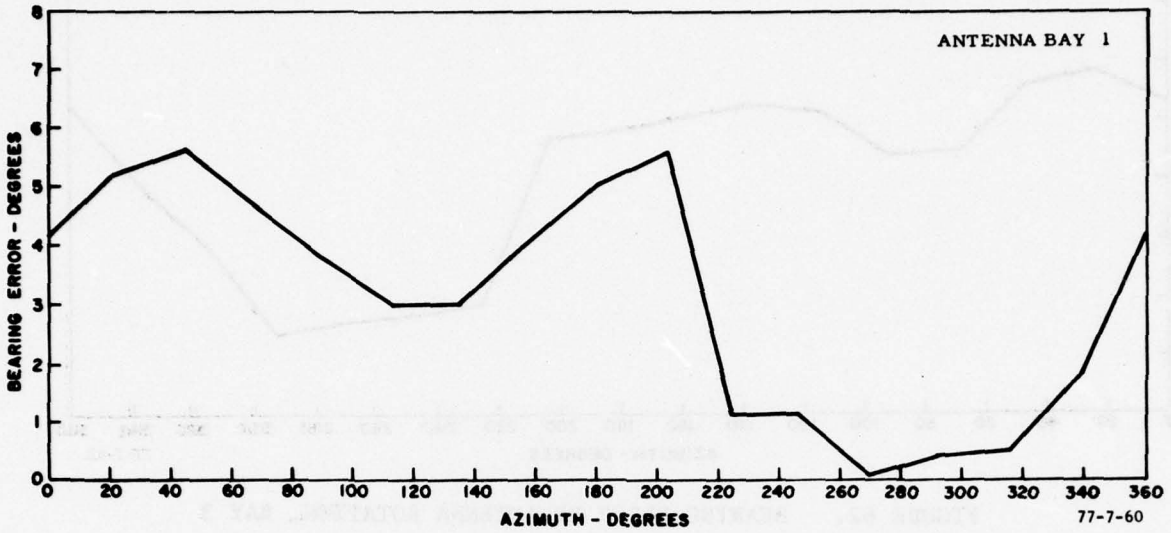


FIGURE 60. BEARING ERROR BY ANTENNA ROTATION, BAY 1

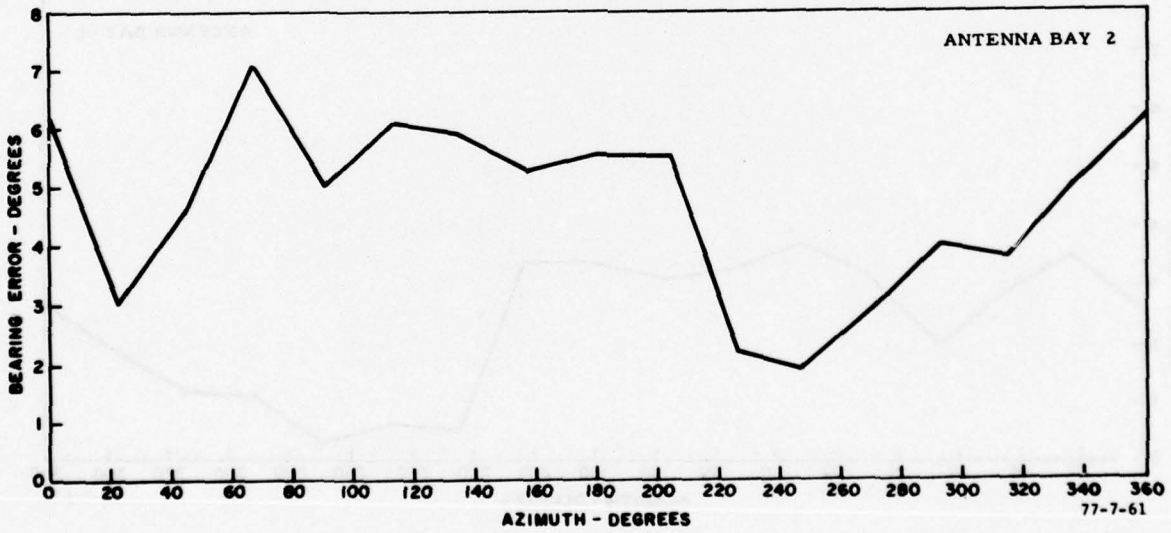


FIGURE 61. BEARING ERROR BY ANTENNA ROTATION, BAY 2

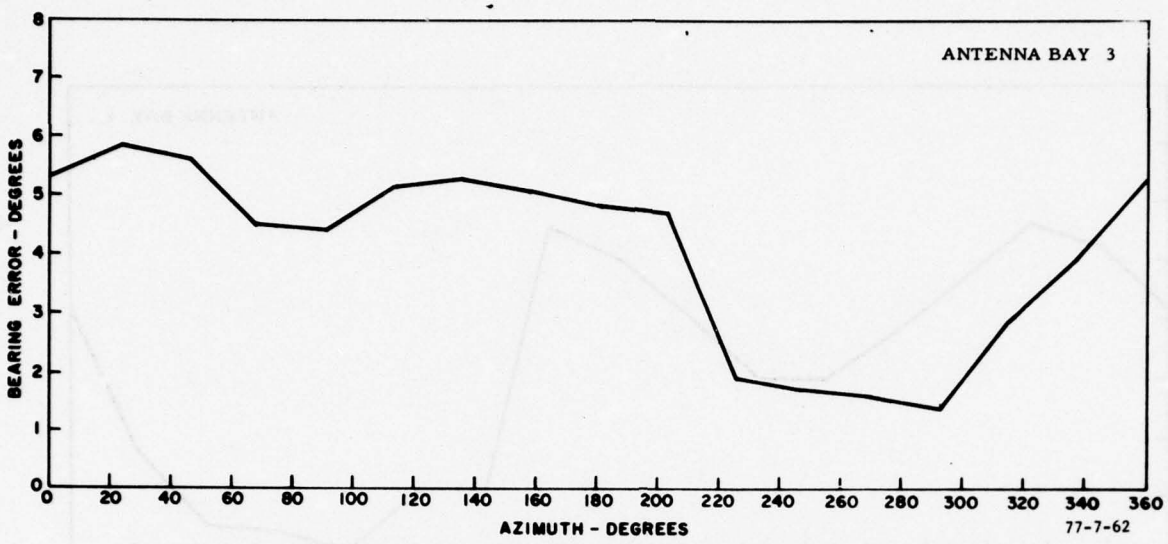


FIGURE 62. BEARING ERROR BY ANTENNA ROTATION, BAY 3

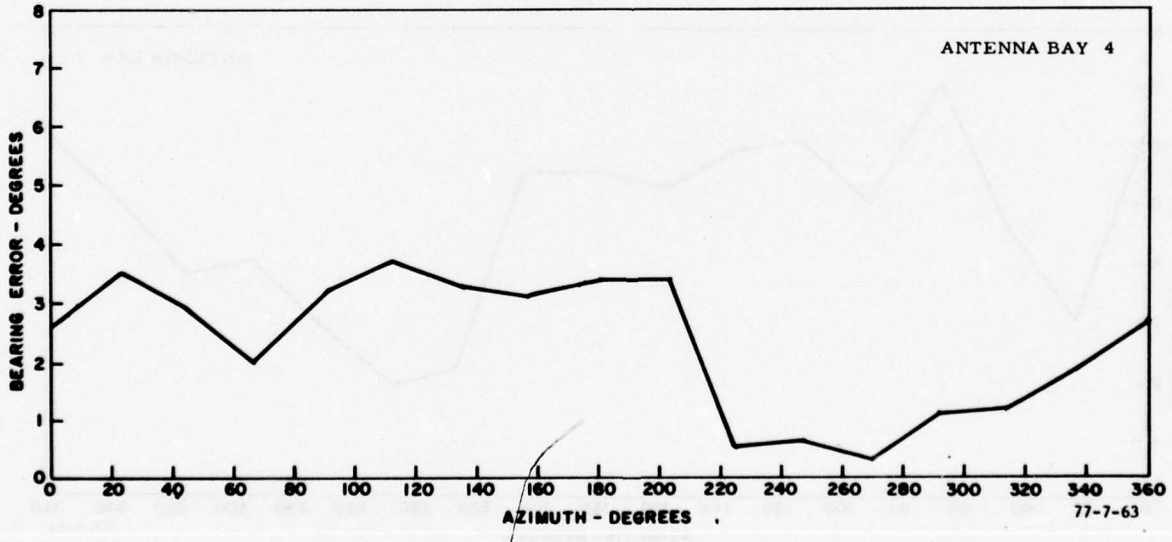


FIGURE 63. BEARING ERROR BY ANTENNA ROTATION, BAY 4

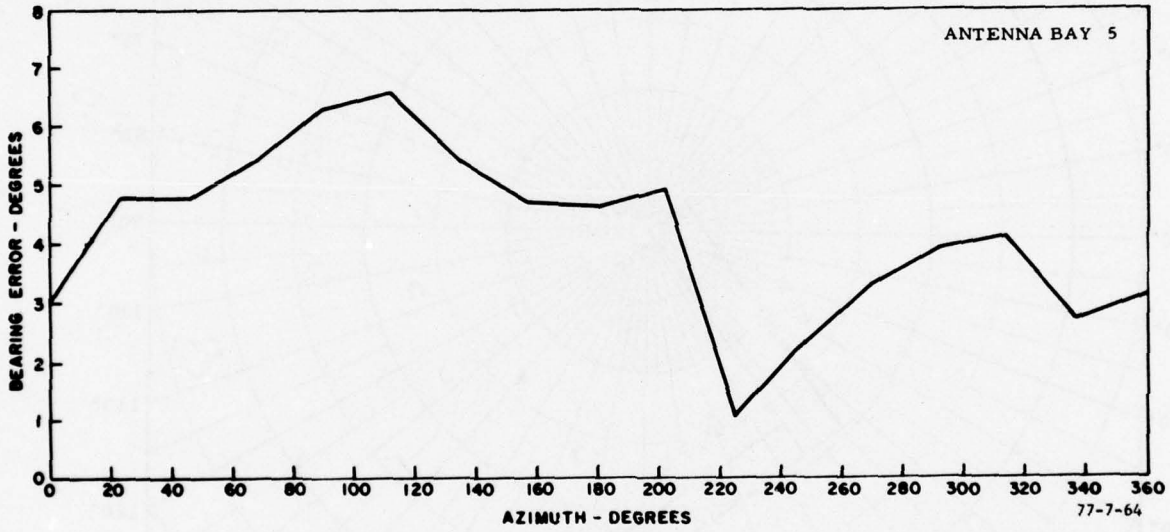


FIGURE 64. BEARING ERROR BY ANTENNA ROTATION, BAY 5

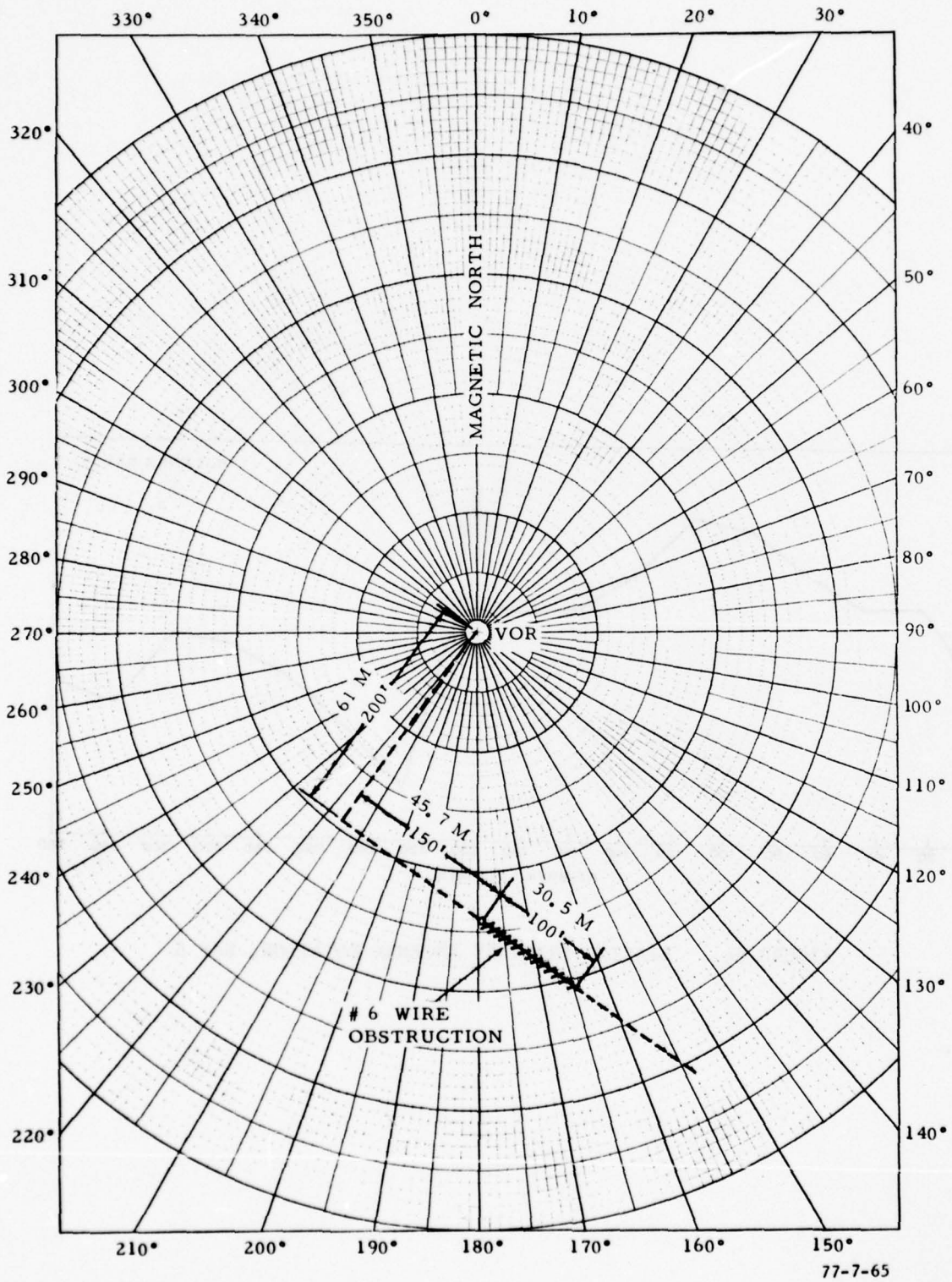


FIGURE 65. WIRE LOCATION

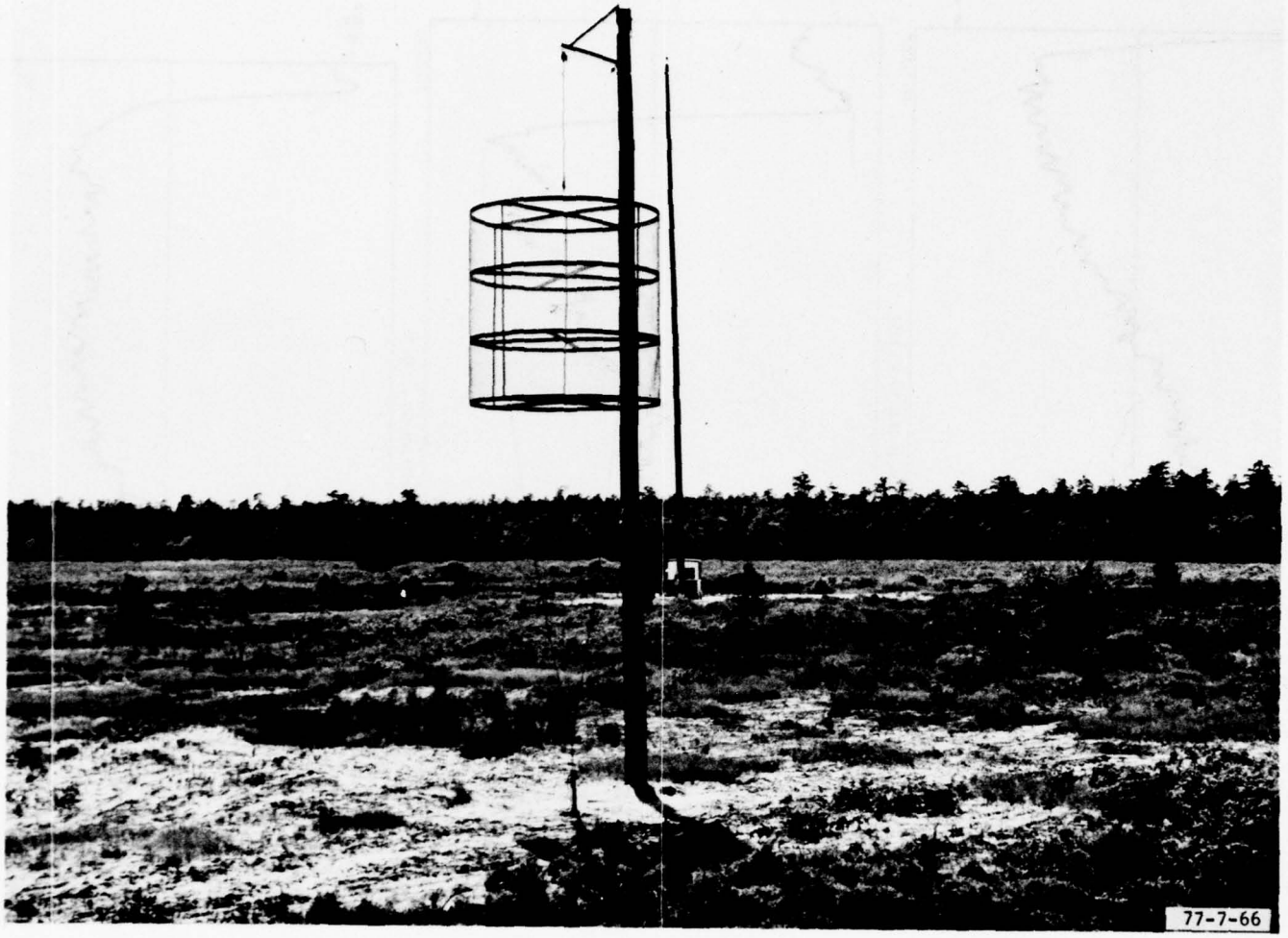


FIGURE 66. WIRE MESH CYLINDER

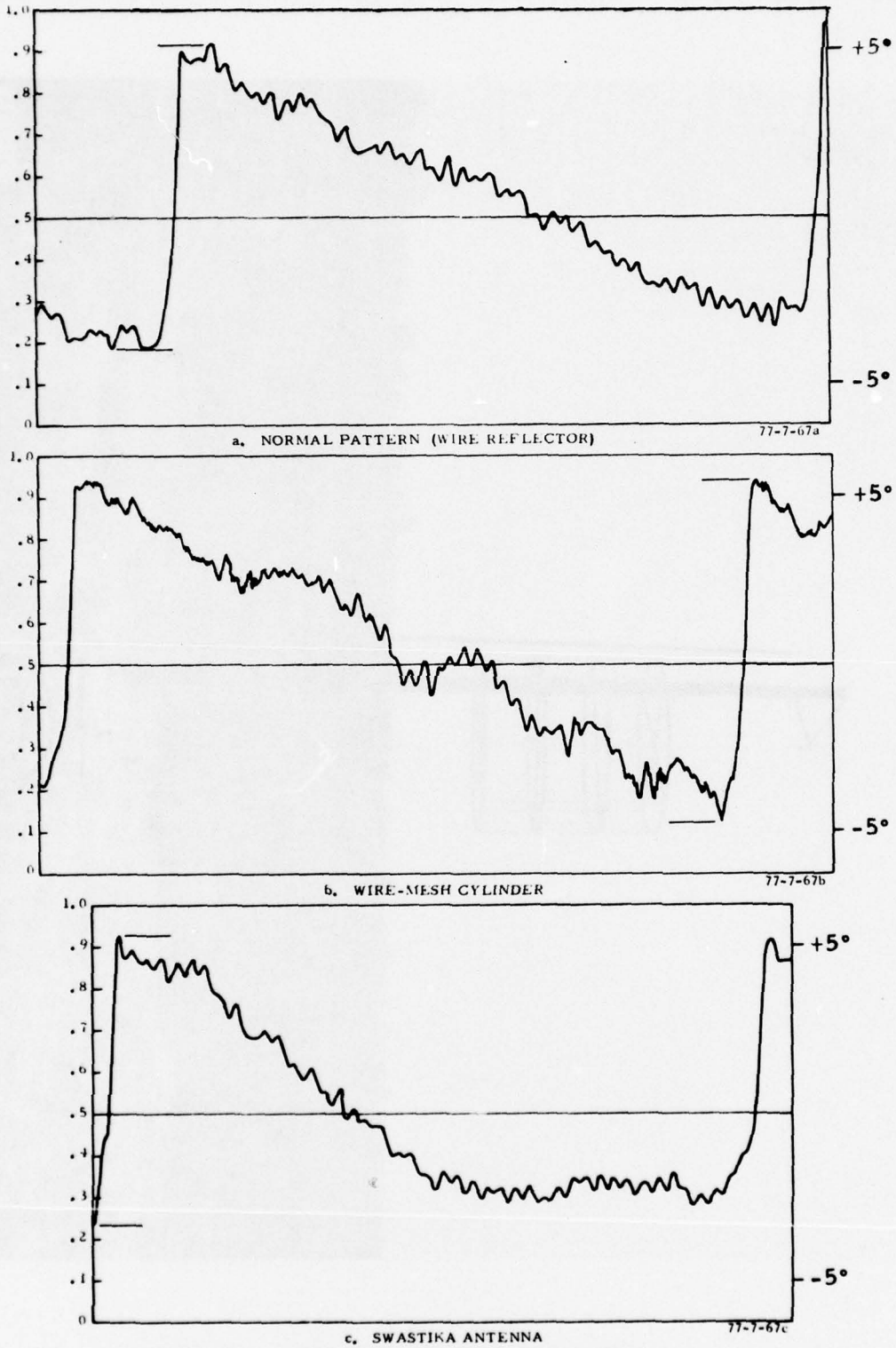


FIGURE 67. OBSTRUCTION TEST RECORDINGS

APPENDIX A

FORTRAN IV PROGRAM LISTING, BASIC PROGRAM LISTING, AND THEORETICAL FREE-SPACE PATTERN

TABLE OF CONTENTS

	Page
FORTRAN IV PROGRAM	A-1
BASIC PROGRAM	A-2

LIST OF ILLUSTRATIONS

Figure		Page
A-1	Computed pattern of Scanwell Five-Bay VOR Antenna	A-6
A-2	Example of Free-Space Carrier Pattern with 35° RF Phasing on Carrier Elements 3 and 4	A-7
A-3	Example of Free-Space Carrier Pattern with 40° RF Phasing on Carrier Elements 3 and 4	A-8

```
FORTRAN IV

0001  1     FORMAT(1X,'INPUT NUMBER OF ANTENNAS',$)
0002  2     FORMAT(1X,'POSITION OF EACH')
0003  3     FORMAT(1X,'AMPLITUDE OF EACH')
0004  4     FORMAT(1X,'PHASE OF EACH')
0005  5     FORMAT(I5)
0006  6     FORMAT(7F10.3)
0007  7     FORMAT(1X,7F10.3)
0008        REAL PI
0009        DIMENSION Z(7),C(7),D(7),V(7),VOLT(181)
0010        DATA WAVE,PI/108.3,3.1416/
0011        TYPE 1
0012        ACCEPT 5,K
0013        TYPE 2
0014        ACCEPT 6,(Z(J),J=1,K)
0015        TYPE 3
0016        ACCEPT 6,(C(J),J=1,K)
0017        DO 20 J=1,K
0018  20    V(J)=50.*C(J)
0019        TYPE 4
0020        ACCEPT 6,(D(J),J=1,K)
0021        DO 22 J=1,K
0022  22    D(J)=D(J)*PI/180.
0023        DO 40 J=1,179
0024        BETA=FLOAT(180-J)
0025        ALPHA=BETA*PI/180.
0026        COSA=COS(ALPHA)
0027        SINA=SIN(ALPHA)
0028        VOLTR=0.
0029        VOLTI=0.
0030        DO 30 I=1,K
0031        VOLTR=VOLTR+COS(2.*PI/WAVE*Z(I)*COSA+D(I))*V(I)
0032        VOLTI=VOLTI+SIN(2.*PI/WAVE*Z(I)*COSA+D(I))*V(I)
0033  30    CONTINUE
0034        VOLT(J)=ABS(SQRT(VOLTR*VOLTR+VOLTI*VOLTI)*SINA)
0035  40    CONTINUE
0036        VOLTA=0.
0037        VOLTM=-100.
0038        DO 45 J=1,179
0039        IF(VOLT(J).GT.VOLTM) VOLTM=VOLT(J)
0041  45    VOLTA=VOLTA+VOLT(J)
0042        VOLTA=VOLTA/179.
0043        GAINA=20.*ALOG10(VOLTA)
0044        DO 47 J=1,179
0045        GAIN=20.*ALOG10(VOLT(J)/VOLTA)
0046        BETA=FLOAT(180-J)
0047  47    TYPE 7,BETA,GAIN
0048        DO 50 J=1,K
0049  50    TYPE 7,Z(J),C(J),V(J),D(J)
0050        STOP
0051        END
```

BEST AVAILABLE COPY

```
LIST
4 RUN 100
100 W1=360
110 X1=PI
120 PRINT "#14, THOMSON/CSF ANTENNA, CHOICE OF TABULATE,"
130 PRINT "GRAPHICS OR BOTH, WITH NEGATIVE ON RIGHT"
140 PRINT
150 PRINT
160 PRINT
170 PRI "DO YOU WANT A TABULATION ONLY? (YES=1), GRAPHICS ONLY?(YES=2)"
180 PRINT "OR BOTH? (YES=3)"
190 INPUT A
200 PRINT "IS THIS FOR CARRIER? (YES=1), OR SIDEBAND? (YES=2)"
210 INPUT P
220 PRINT
230 PRINT "INPUT NUMBER OF ANTENNAS?"
240 INPUT K
250 DELETE Z,C,D,V
260 DIM Z(K),C(K),D(K),V(K)
270 DIM V1(181),B(181),G(181)
280 PRINT "POSITION IN DEGREES"
290 FOR J=1 TO K
300 PRINT "#";J," ";
310 INPUT Z(J)
320 NEXT J
330 PRINT "AMPLITUDE OF EACH"
340 FOR J=1 TO K
350 PRINT "#";J," ";
360 INPUT C(J)
370 NEXT J
380 FOR J=1 TO K
390 V(J)=50*C(J)
400 NEXT J
410 PRINT "PHASE OF EACH"
420 FOR J=1 TO K
```


BEST AVAILABLE COPY

```
430 PRINT "#";J," ";
440 INPUT D(J)
450 NEXT J
460 FOR J=1 TO K
470 D(J)=D(J)*X1/180
480 NEXT J
490 FOR J=1 TO 179
500 B1=180-J
510 A1=B1*X1/180
520 C1=COS(A1)
530 S1=SIN(A1)
540 V2=0
550 V3=0
560 FOR I=1 TO K
570 V2=V2+COS(2*X1/W1*Z(I)*C1+D(I))*V(I)
580 V3=V3+SIN(2*X1/W1*Z(I)*C1+D(I))*V(I)
590 NEXT I
600 V1(J)=ABS(SQR(V2*V2+V3*V3)*S1)
610 NEXT J
620 V4=0
630 V5=-100
640 FOR J=1 TO 179
650 IF V1(J)>V5 THEN 670
660 GO TO 680
670 V5=V1(J)
680 V4=V4+V1(J)
690 NEXT J
700 V4=V4/179
710 G1=20*LGT(V4)
720 IF A=2 THEN 740
730 PRINT "ANG(DEG), GAIN(DB)"
740 FOR J=1 TO 179
750 G(J)=20*LGT(V1(J)/V4)
760 B(J)=180-J
770 IF A=2 THEN 790
```


BEST AVAILABLE COPY

```
780 PRINT B(J),G(J)
790 NEXT J
800 FOR J=1 TO K
810 IF A=2 THEN 830
820 PRINT Z(J);" ";C(J);" ";V(J);" ";D(J)
830 NEXT J
840 IF A=1 THEN 1200
850 PAGE
860 WINDOW -90,90,-50,20
870 VIEWPORT 25,125,15,95
880 FOR X=-90 TO 90 STEP 30
890 AXIS 0,0,X,X
900 MOVE X-8,-54
910 PRINT X*-1
920 NEXT X
930 FOR Y=-50 TO 20 STEP 10
940 AXIS 0,0,X,Y
950 MOVE -105,Y-2
960 PRINT Y
970 NEXT Y
980 MOVE -15,-58
990 PRINT "ELEVATION ANGLE, DEGREES"
1000 MOVE -30,22
1010 GO TO P OF 1020,1040
1020 PRINT "THOMSON/CSF CARRIER PATTERN"
1030 GO TO 1050
1040 PRINT "THOMSON/CSF SIDEBAND PATTERN"
1050 C$="GAIN IN DB"
1060 MOVE -115,-10
1070 FOR I=1 TO LEN(C$)
1080 B$=SEG(C$,I,1)
1090 PRINT B$;"HJ";
1100 NEXT I
1110 WINDOW 0,180,-50,20
1120 FOR I=179 TO 1 STEP -1
```


BEST AVAILABLE COPY

BEST AVAILABLE COPY

```
1130 G5=G(I)
1140 IF I=179 THEN 1160
1150 GO TO 1180
1160 MOVE B(I),G5
1170 GO TO 1190
1180 DRAW B(I),G5
1190 NEXT I
1200 END
```

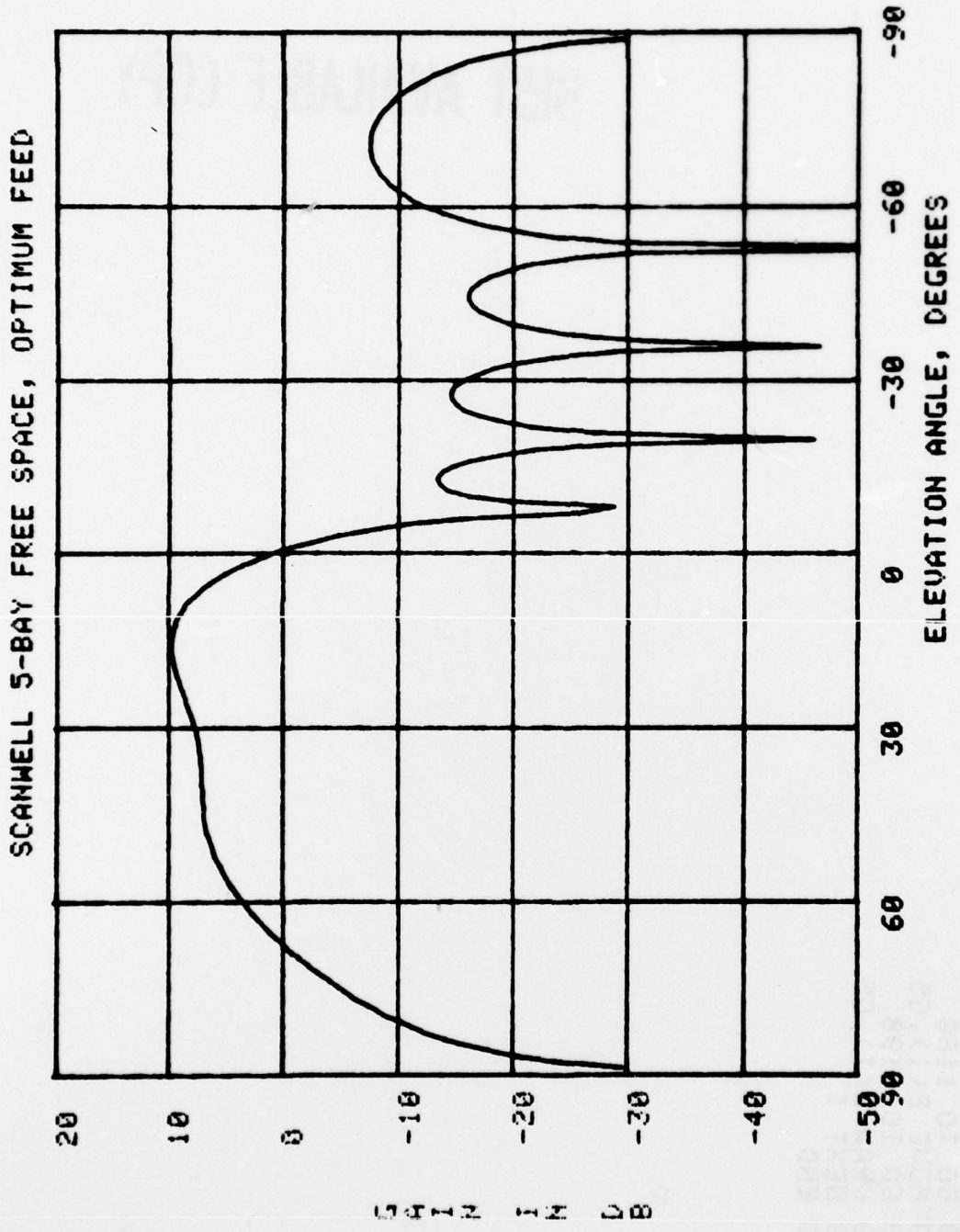


FIGURE A-1. COMPUTED PATTERN OF SCANWELL FIVE-BAY VOR ANTENNA

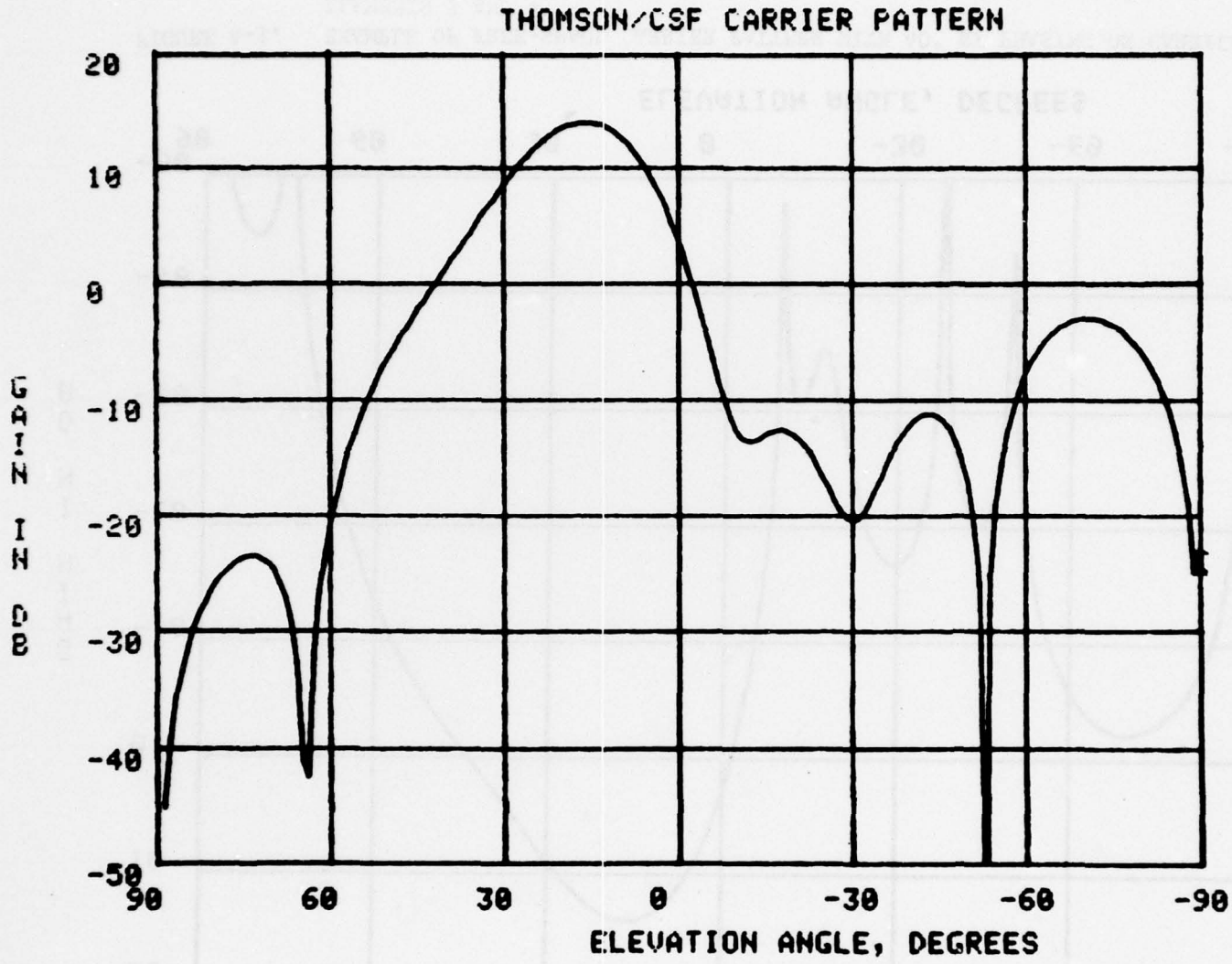


FIGURE A-2. EXAMPLE OF FREE-SPACE CARRIER PATTERN WITH 35° RF PHASING ON CARRIER ELEMENTS 3 AND 4

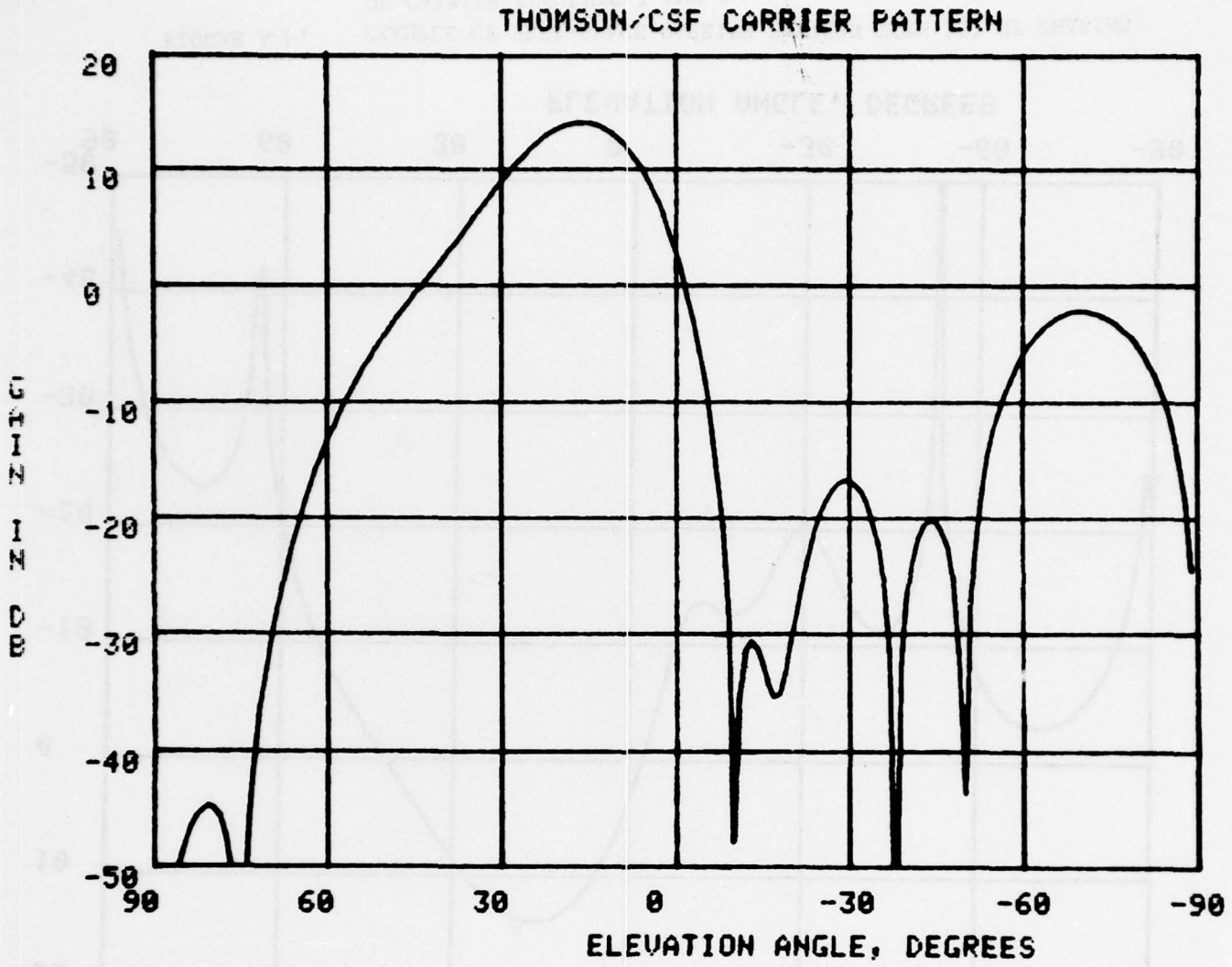


FIGURE A-3. EXAMPLE OF FREE-SPACE CARRIER PATTERN WITH 40° RF PHASING ON CARRIER ELEMENTS 3 AND 4

APPENDIX B

DETAILS OF ANTENNA INSTALLATION

LIST OF ILLUSTRATIONS

Figure		Page
B-1	VORTAC Antenna Housing Removed and Concrete Pouring for Guy Anchoring Pads	B-1
B-2	Preparing Roof for Antenna Installation after VORTAC Housing Removal	B-2
B-3	Assembling the Antenna	B-3
B-4	Hoisting the Antenna for Roof Installation	B-4

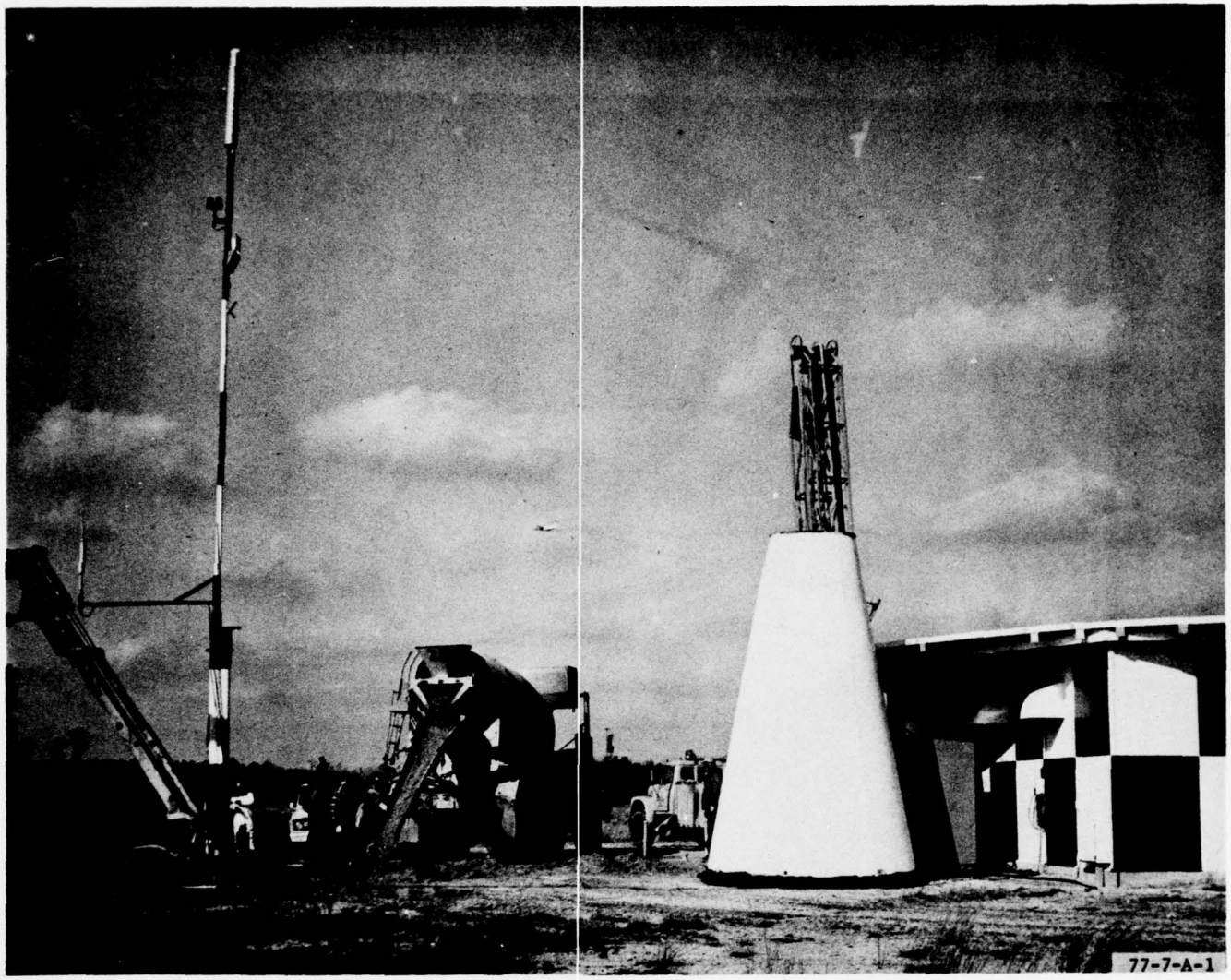


FIGURE B-1. VORTAC ANTENNA HOUSING REMOVED AND CONCRETE POURING FOR GUY ANCHORING PADS



FIGURE B-2 PREPARING ROOF FOR ANTENNA INSTALLATION AFTER VORTAC HOUSING REMOVAL

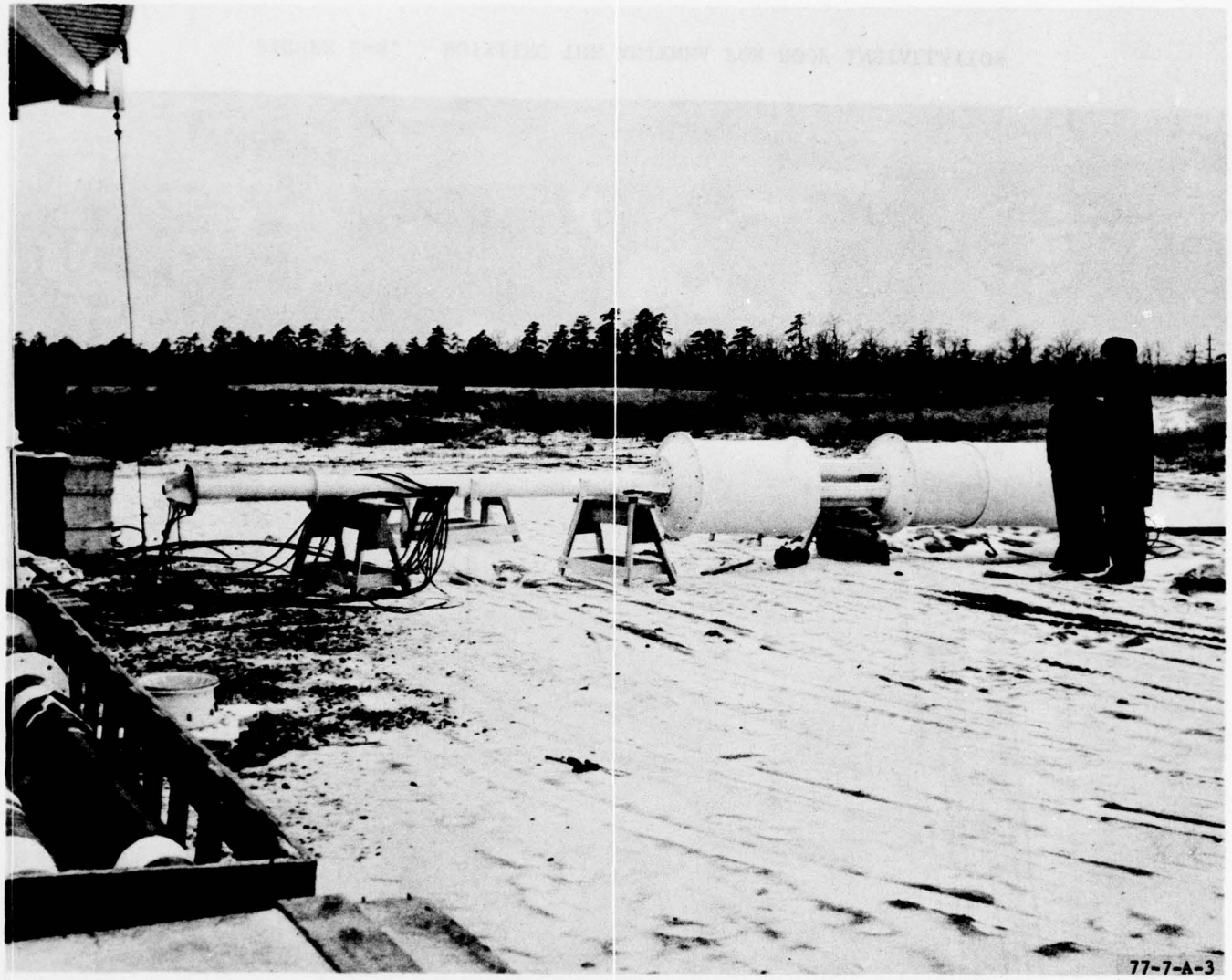


FIGURE B-3. ASSEMBLING THE ANTENNA

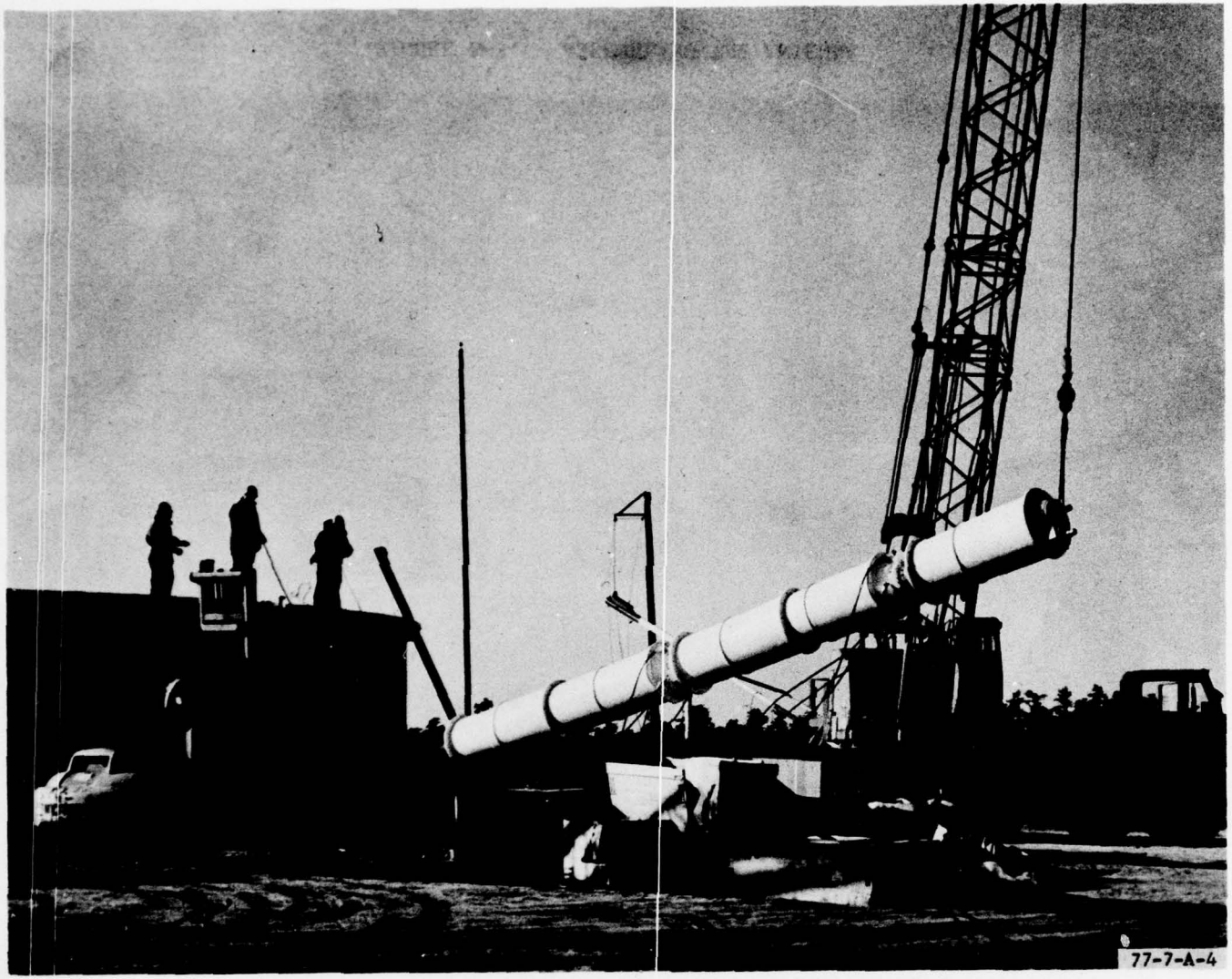


FIGURE B-4. HOISTING THE ANTENNA FOR ROOF INSTALLATION